Chiral Organolanthanides Designed for Asymmetric Catalysis. Synthesis, Characterization, and Configurational Interconversions of Chiral, C_1-Symmetric Organolanthanide Halides, Amides, and Hydrocarbyls

Michael A. Giardello,† Vincent P. Conticello,† Laurent Brard,† Michal Sabat,† Arnold L. Rheingold,‡ Charlotte L. Stern,† and Tobin J. Marks*,†

Contribution from the Departments of Chemistry, Northwestern University, Evanston, Illinois 60208-3113, and University of Delaware, Newark, Delaware 19716

Received February 17, 1994®

Abstract: This contribution describes the synthesis, structural systematics, absolute configurations, and structural interconversions of a series of C_1-symmetric lanthanide chloro, hydrocarbyl, and amide complexes/precatalysts based on chiral chelating $Me_2Si(\eta^5\text{-}Me_4C_5)(\eta^5\text{-}C_5H_3R^*)^{2-}$ ligands $[Me_2SiCp''(R^*Cp)]^{2-}$, where R* = (+)-neomenthyl, (−)-menthyl, and (−)-phenylmenthyl. The ligands are prepared in three steps from known chiral cyclopentadienes. Metalation of the chiral dienes followed by condensation with $Me_4C_5Si(CH_3)_2Cl$ and *in situ* lithiation provides the dianions in nearly quantitative yield. Transmetalation of the lithiated ligands with anhydrous lanthanide trichlorides followed by ambient temperature ether workup provides $Me_2SiCp''(R^*Cp)LnCl_2Li(OEt_2)_2$ complexes in high yield. For (*R*)-Me_2-$SiCp''$[(+)-neomenthylCp]$Lu(\mu\text{-}Cl)_2Li(OEt_2)_2$: space group $P2_12_12_1$; a = 12.240(2), b = 12.876(2), and c = 24.387(5) Å (24 °C); Z = 4; R(F) = 0.0509. As established by NMR and circular dichroism, the diastereomerically pure chloro complexes can be epimerized in appropriate donor solvents to afford mixtures of (*R*)- and (*S*)-configurational isomers with the isomer ratio dependent on solvent, R*, and lanthanide ion. *Selective epimerization* allows enrichment in either antipode with diastereomerically pure complexes obtained in a single recrystallization. Li^+ sequestering crown ethers inhibit epimerization. The temperature dependence of the (*R*) ⇌ (*S*) equilibrium constant in THF yields ΔH = 1.7 ± 0.3 kcal/mol and ΔS = 3.6 ± 0.8 eu for Me_2SiCp''[(+)-neomenthylCp]$Lu(\mu\text{-}Cl)_2Li(OEt_2)_2$ and ΔH = 4.8 ± 0.5 kcal/mol and ΔS = 13.4 ± 0.5 eu for Me_2SiCp''[(−)-menthylCp]$Sm(\mu\text{-}Cl)_2Li(OEt_2)_2$. The mechanism is proposed to involve reversible ring detachment to an intermediate LiCpR* complex. Alkylation or amidation with $ME(SiMe_3)_2$ (M = Li or K, E = CH; M = Na or K, E = N) yields the corresponding chiral hydrocarbyls and amides in high yield. For (*R*/*S*)-Me_2SiCp''[(+)-neomenthylCp]$YCH(SiMe_3)_2$: space group $P2_1$; a = 19.178(4), b = 8.736(1), and c = 21.391(5) Å; β = 97.62(2); Z = 4; R(F) = 0.071. For (*R*)-Me_2SiCp''[(−)-menthylCp]$SmCH(SiMe_3)_2$: space group $P1$; a = 8.993(3), b = 12.738(2), and c = 16.549(4) Å; α = 86.04(2)°; β = 82.81(2)°, γ = 72.91(2)°; Z = 2; R(F) = 0.026. For (*R*)-Me_2SiCp''[(−)-menthylCp]$YCH(SiMe_3)_2$; space group $P2_1$; a = 12.319(3), b = 15.707(4), and c = 18.693(5) Å; β = 91.59(2)°; Z = 4; R(F) = 0.054. For (*S*)-Me_2SiCp''[(+)-neomenthylCp]$SmN(SiMe_3)_2$: space group $P2_1$; a = 9.122(2), b = 10.112(3), and c = 18.478(3) Å; β = 90.58(2)°; Z = 2; R(F) = 0.029. For (*S*)-Me_2-$SiCp''$[(−)-menthylCp]$SmN(SiMe_3)_2$: space group $P2_12_12_1$; a = 10.217(3), b = 19.103(6), and c = 19.456(7) Å; Z = 4; R(F) = 0.044. For (*R*)-Me_2SiCp''[(−)-menthylCp]$YN(SiMe_3)_2$: space group $P1$; a = 8.937(3), b = 12.397(6), and c = 16.673(7) Å; α = 85.53(2)°, β = 82.17(2)°, γ = 74.78(2)°; Z = 2; R(F) = 0.065. The preferred planar chiral configurations of these complexes can be largely understood on the basis of significant, crystallographically identifiable, nonbonded interactions between R* and the remainder of the molecule. The hydrocarbyl and amide complexes are configurationally stable in toluene at 60 °C for many hours but undergo facile epimerization in the presence of primary alkyl amines, presumably via reversible Cp protonation/detachment. The hydrocarbyl complexes undergo rapid hydrogenolysis at ambient temperature, with retention of configuration, to yield the corresponding hydrides.

Introduction

The efficient, stereoselective synthesis of chiral molecules poses a formidable challenge for traditional synthetic methodology. However, chiral transition metal complexes with appropriately engineered ligation spheres can effect asymmetric catalytic transformations with high efficiency and stereoselectivity.[1] A common feature of these structures is the presence of an asymmetric metal–ligand template capable of selectively interacting with a particular enantiotopic face or atom of prochiral substrates. Organolanthanide hydrides $(Cp'_2LnH)_2$[2,3] and $(Me_2SiCp''_2LnH)_2$[4] (Cp' = η^5-Me_5C_5, Cp'' = η^5-Me_4C_5) effectively and selectively catalyze a variety of olefin transformations including hydrogenation,[5] oligomerization/polymerization,[2a,b,3,4,6] isomerization,[7] hydroamination,[8] hydrosilylation,[9] hydrophosphination,[10] hydroboration,[11] and reductive cyclization.[12] The favorable characteristics associated with these complexes—extremely rapid kinetics, large turnover capacity, and tunability with lanthanide ionic radius and ancillary ligation—raise the question of whether appropriate coordination environments can be devised to effect lanthanide-centered asymmetric catalytic transformations.

To date, most synthetic strategies for metallocene asymmetric catalysts have employed C_2-*symmetric* $(CpR^*)_2MCl_2$ structures[13]

† Northwestern University.
‡ University of Delaware.
® Abstract published in *Advance ACS Abstracts*, September 1, 1994.

(1) For leading references in asymmetric homogeneous catalysis, see: (a) Noyori, R. *Asymmetric Catalysis in Organic Synthesis*; Wiley: New York, 1994. (b) Parshall, G. W.; Ittel, S. D. *Homogeneous Catalysisn*, 2nd ed.; Wiley: New York, 1992; Chapters 2, 3, and 6. (c) *Chem. Rev.* **1992**, *92*, 739–1140. This entire issue is dedicated to enantioselective synthesis. (d) Pfaltz, A. *Acc. Chem. Res.* **1993**, *26*, 339–345. (e) Noyori, R. *Chem. Soc. Rev.* **1989**, *18*, 187–208. (f) Scott, J. W. *Top. Stereochem.* **1989**, *19*, 209–225. (g) Brunner, H. *Synthesis* **1988**, 645–654. (h) Bosnich, B. *Asymmetric Catalysis*; NATO ASI Series E 103; Martinus Nijhoff Publishers: Dordrecht, 1986. (i) *Asymmetric Synthesis*; Morrison, J. D., Ed.; Academic Press: New York, 1985; Vol. 5.

0002-7863/94/1516-10212$04.50/0

or elegant linked *ansa*-metallocenes.[14] However, the formation and necessary separation of undesired *meso* isomers[15] (**A**) significantly complicate the latter chemistry. Furthermore, subsequent optical resolution of the two metal-based enantiomers (**B**) is required to obtain homochiral catalysts.[16] To date, the

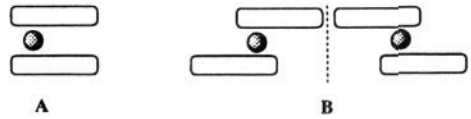

effectiveness of these catalysts in asymmetric transformations has been impressively demonstrated in stereoregular α-olefin polymerization.[17] Such group 4 complexes also show considerable promise in multicomponent catalysts for the asymmetric hydrogenation of nonfunctionalized or lightly-functionalized ketimines and olefins,[18] although the exact molecular nature of the catalysts awaits elucidation.

A rational strategy for asymmetric organolanthanide catalysts requires the construction of suitable asymmetric metal–ligand templates which satisfy three key criteria: (i) preservation of the favorable stereoelectronic characteristics of Cp'_2LnR catalysts,[2,3] (ii) configurational stability of the metal–ligand array, and (iii) separability of metal-centered stereoisomers. We investigate here a design strategy (**C**, **D**) for such systems which offers the

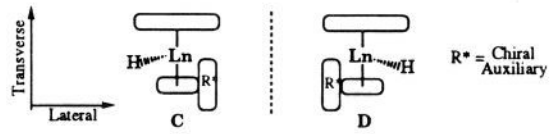

possibility of resolvable, enantiomerically-related, chiral organolanthanide centers with cyclopentadienyl ligation capable, via lateral and transverse shape discrimination, of selectively differentiating between opposite enantiofaces of prochiral substrates. This approach builds upon well-developed ring-linked permethylcyclopentadienyl ($Me_2SiCp''_2LnR$[2b] and $Me_2SiCp''CpLnR$) chemistry.[19] Modification of these ligand systems by incorporating a chiral auxiliary affords C_1-symmetric organolanthanide complexes (**E**, **F**) which address the delineated criteria. A wide

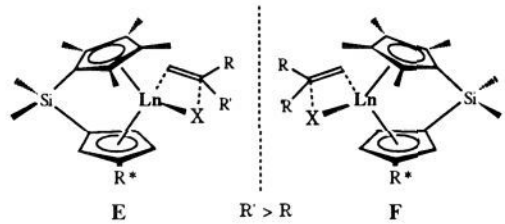

and structurally diverse variety of R* substituents are readily available from the natural chiral pool; this substituent should limit the approach of substrate to the distal face of the metal center, providing lateral discrimination, while also ensuring

(2) (a) Mauermann, H.; Marks, T. J. *Organometallics* **1985**, *4*, 200–202. (b) Jeske, G.; Lauke, H.; Mauermann, H.; Swepston, P. N.; Schumann, H.; Marks, T. J. *J. Am. Chem. Soc.* **1985**, *107*, 8091–8103. (c) den Haan, K. H.; de Boer, J. L.; Teuben, J. H.; Spek, A. L.; Kajic-Prodic, B.; Hays, G. R.; Huis, R. *Organometallics* **1986**, *5*, 1726–1733. (d) Watson, P. L.; Parshall, G. W. *Acc. Chem. Res.* **1985**, *18*, 51–55. (e) Heeres, H. J.; Renkema, J.; Booji, M.; Meetsma, A.; Teuben, J. H. *Organometallics* **1988**, *7*, 2495–2502.

(3) For related Cp'_2ScR complexes, see: (a) Thompson, M. E.; Bercaw, J. E. *Pure Appl. Chem.* **1984**, *56*, 1–11. (b) Burger, B. J.; Thompson, M. E.; Cotter, D. W.; Bercaw, J. E. *J. Am. Chem. Soc.* **1990**, *112*, 1566–1577.

(4) (a) Jeske, G.; Schock, L. E.; Swepston, P. N.; Schumann, H.; Marks, T. J. *J. Am. Chem. Soc.* **1985**, *107*, 8103–8110. (b) Heeres, H. Ph.D. Thesis, University of Gröningen, Gröningen, The Netherlands, 1990.

(5) (a) Jeske, G.; Lauke, H.; Mauermann, H.; Schumann, H.; Marks, T. J. *J. Am. Chem. Soc.* **1985**, *107*, 8111–8118. (b) Evans, W. J.; Bloom, I.; Hunter, W. E.; Atwood, J. L. *J. Am. Chem. Soc.* **1983**, *105*, 1401–1403. (c) Molander, G. A.; Hoberg, J. O. *J. Org. Chem.* **1992**, *57*, 3266–3268.

(6) (a) Watson, P. L.; Herskovitz, T. *ACS Symp. Ser.* **1983**, *212*, 459–479. (b) Watson, P. L. *J. Am. Chem. Soc.* **1982**, *104*, 337–339. (c) Watson, P. L.; Roe, D. C. *J. Am. Chem. Soc.* **1982**, *104*, 6471–6473.

(7) $(Cp'_2LnH)_2$ and $(Me_2SiCp''_2NdH)_2$ catalyze the isomerization of (*E*)-*N*,*N*-dimethyl-3-phenyl-2-butenylamine to (*E*)-*N*,*N*-dimethyl-3-phenyl-1-butenylamine at 80 °C in C_6D_6 (Conticello, V. P.; Giardello, M. A.; Eisen, M.; Marks, T. J., unpublished results). For related Rh-catalyzed isomerizations of allylamines to enamines, see: (a) Tani, K.; Yamagata, T.; Otsuka, S.; Akutagawa, S.; Kumobayashi, H.; Taketomi, T.; Takaya, H.; Miyashita, A.; Noyori, R. *J. Chem. Soc., Chem. Commun.* **1982**, 600–601. (b) Tani, K.; Yamagata, T.; Akutagawa, S.; Kumobayashi, H.; Taketomi, T.; Takaya, H.; Miyashita, H.; Noyori, R.; Otsuka, S. *J. Am. Chem. Soc.* **1984**, *106*, 5208–5217.

(8) (a) Gagné, M. R.; Marks, T. J. *J. Am. Chem. Soc.* **1989**, *111*, 4108–4109. (b) Gagné, M. R.; Nolan, S. P.; Marks, T. J. *Organometallics* **1990**, *9*, 1716–1718. (c) Gagné, M. R.; Stern, C.; Marks, T. J. *J. Am. Chem. Soc.* **1992**, *114*, 275–294.

(9) (a) Sakakura, T.; Lautenschlager, H.; Tanaka, M. *J. Chem. Soc., Chem. Commun.* **1991**, 40–41. (b) Takahashi, T.; Hasegawa, M.; Suzuki, N.; Saburi, M.; Rousset, C. J.; Fanwick, P. E.; Negishi, E. *J. Am. Chem. Soc.* **1991**, *113*, 8564–8566. (c) Molander, G. A.; Julius, M. *J. Org. Chem.* **1992**, *57*, 6347–6351.

(10) Giardello, M. A.; King, W. A.; Nolan, S. P.; Porchia, M.; Sishta, C.; Marks, T. J. In *Energetics of Organometallic Species*; Martinho Simoes, J. A., Ed.; Kluwer: Dordrecht, 1992; pp 35–51.

(11) Harrison, K. N.; Marks, T. J. *J. Am. Chem. Soc.* **1992**, *114*, 9220–9221.

(12) Molander, G. A.; Hoberg, J. O. *J. Am. Chem. Soc.* **1992**, *114*, 3123–3125.

(13) (a) Halterman, R. L. *Chem. Rev.* **1992**, *92*, 965–994 and references therein. (b) Moriarty, K. J.; Rogers, R. D.; Paquette, L. A. *Organometallics* **1989**, *8*, 1512–1517. (c) Paquette, L. A.; Moriarty, K. J.; Rogers, R. D. *Organometallics* **1989**, *8*, 1506–1511. (d) Paquette, L. A.; Moriarty, K. J.; McKinney, J. A.; Rogers, R. D. *Organometallics* **1989**, *8*, 1707–1713. (e) Halterman, R. L.; Vollhardt, K. P. C. *Organometallics* **1988**, *7*, 883–892. (f) Halterman, R. L.; Vollhardt, K. P. C.; Welker, M. E.; Bläser, D.; Boese, R. *J. Am. Chem. Soc.* **1987**, *109*, 8105–8107. (g) Paquette, L. A.; McKinney, J. A.; McLaughlin, M. L.; Rheingold, A. L. *Tetrahedron Lett.* **1986**, *27*, 5599–5602. (h) Halterman, R. L.; Vollhardt, K. P. C. *Tetrahedron Lett.* **1986**, *27*, 1461–1464. (i) Couturier, S.; Tainturier, G.; Gautheron, B. *J. Organomet. Chem.* **1980**, *195*, 291–306. (j) Dormond, A.; El Bouadili, A.; Moise, C. *Tetrahedron Lett.* **1983**, *24*, 3087–3089. (k) Le Blanc, J. C.; Moise, C.; Tirouflet, J. *J. Organomet. Chem.* **1978**, *148*, 171–178. (l) Cesarotti, E.; Kagan, H. B.; Goddard, R.; Kruger, C. *J. Organomet. Chem.* **1978**, *162*, 297–309. (m) Le Blanc, J. C.; Moise, C. *J. Organomet. Chem.* **1976**, *120*, 65–71.

(14) (a) Röll, W.; Brintzinger, H. H.; Rieger, B.; Zolk, R. *Angew. Chem., Int. Ed. Engl.* **1990**, *29*, 279–280. (b) Burger, P.; Hund, H.-U.; Evertz, K.; Brintzinger, H. H. *J. Organomet. Chem.* **1989**, *370*–153–161. (c) Wiesenfeldt, H.; Reinmuth, A.; Barsties, E.; Evertz, K.; Brintzinger, H. H. *J. Organomet. Chem.* **1989**, *369*, 359–370. (d) Gutmann, S.; Burger, P.; Hund, H. U.; Hofmann, J.; Brinzinger, H. H. *J. Organomet. Chem.* **1989**, *369*, 343–357. (e) Ewen, J. A.; Haspeslagh, L.; Atwood, J. L.; Zhang, H. *J. Am. Chem. Soc.* **1987**, *109*, 6544–6545. (f) Röll, W.; Zsolnai, L.; Hüttner, G.; Brintzinger, H. H. *J. Organomet. Chem.* **1987**, *322*, 65–70. (g) Wild, F. R. W. P.; Wasiucionek, M.; Hüttner, G.; Brintzinger, H. H. *J. Organomet. Chem.* **1985**, *288*, 63–67. (h) Schwemlein, H.; Brintzinger, H. H. *J. Organomet. Chem.* **1983**, *254*, 69–73.

(15) (a) Rheingold, A. L.; Robinson, N. P.; Whelan, J.; Bosnich, B. *Organometallics* **1992**, *11*, 1869–1876. (b) Collins, S.; Hong, Y.; Ramachandran, R.; Taylor, N. J. *Organometallics* **1991**, *10*, 2349–2356. (c) Collins, S.; Gauthier, W. J.; Holden, D. A.; Kuntz, B. A.; Taylor, N. J.; Ward, D. G. *Organometallics* **1991**, *10*, 2061–2068. (d) Wild, F. R. W. P.; Wasiucionek, M.; Hüttner, G.; Brintzinger, H. H. *J. Organomet. Chem.* **1985**, *228*, 63–67. (e) Gutmann, S.; Burger, P.; Hund, H. U.; Hofmann, J.; Brintzinger, H. H. *J. Organomet. Chem.* **1989**, *369*, 343–357. (f) Wiesenfeldt, H.; Reinmuth, A.; Barsties, E.; Evertz, K.; Brintzinger, H. H. *J. Organomet. Chem.* **1989**, *369*, 359–370. (g) Collins, S.; Hong, Y.; Taylor, N. J. *Organometallics* **1990**, *9*, 2695–2703.

(16) (a) Wild, F. R. W. P.; Zsolnai, L.; Hüttner, G.; Brintzinger, H. H. *J. Organomet. Chem.* **1982**, *232*, 233–247. (b) Schäfer, A.; Karl, E.; Zsolnai, L.; Hüttner, G.; Brintzinger, H. H. *J. Organomet. Chem.* **1987**, *328*, 87–99.

(17) (a) Ewen, J. A. *J. Am. Chem. Soc.* **1984**, *106*, 6355–6364. (b) Kaminsky, W.; Külper, K.; Brintzinger, H. H.; Wild, F. R. W. P. *Angew. Chem., Int. Ed. Engl.* **1989**, *24*, 507–508. (c) Kaminsky, W.; Külper, K.; Niedoba, S. *Makromol. Chem., Macromol. Symp.* **1986**, *3*, 377–387. (d) Erker, G.; Nolte, R.; Tsay, Y.; Kruger, C. *Angew. Chem., Int. Ed. Engl.* **1989**, *28*, 628–629. (e) Röll, W.; Brintzinger, H. H.; Rieger, B.; Zolk, R. *Angew. Chem., Int. Ed. Engl.* **1990**, *29*, 279–280. (f) Erker, G.; Nolte, R.; Aul, R.; Wilker, S.; Kruger, C.; Noe, R. *J. Am. Chem. Soc.* **1991**, *113*, 7594–7602. (g) Ewen, J. A.; Haspeslagh, L.; Atwood, J. L.; Zhang, H. *J. Am. Chem. Soc.* **1987**, *109*, 6544–6545. (h) Rieger, B.; Mu, X.; Mallin, D. T.; Rausch, M. D.; Chien, J. C. W. *Macromolecules* **1990**, *23*, 3559–3568. (i) Rieger, B. *J. Organomet. Chem.* **1992**, *428*, C33–C36. (j) Kaminsky, W.; Külper, K.; Niedoba, S. *Makromol. Chem., Macromol. Symp.* **1986**, *3*, 377–387.

(18) (a) Broene, R. D.; Buchwald, S. L. *J. Am. Chem. Soc.* **1993**, *115*, 12569–12570. (b) Willoughby, C. A.; Buchwald, S. L. *J. Am. Chem. Soc.* **1992**, *114*, 7562–7564. (c) Halterman, R. L.; Vollhardt, K. P. C.; Welker, M. E.; Blaser, D.; Boese, R. *J. Am. Chem. Soc.* **1987**, *109*, 8105–8114.

(19) Stern, D.; Sabat, M.; Marks, T. J. *J. Am. Chem. Soc.* **1990**, *112*, 9558–9575.

the formation of diastereomeric, hence potentially separable, complexes. Selective steric interactions between the CpMe and CpH groups (on opposite faces) and the different substituent groups (R, R') of a prochiral substrate (transverse discrimination) thus constitute the envisioned basis for the enantioselection. It will be seen that the homochiral auxiliaries (R*) (1*S*,2*S*,5*R*)-*trans*-5-methyl-*cis*-2-(2-propyl)cyclohexyl) ((+)-neomenthyl), (1*R*,2*S*,5*R*)-*cis*-5-methyl-*trans*-2-(2-propyl)cyclohexyl ((−)-menthyl), and (1*R*,2*S*,5*R*)-*cis*-5-methyl-*trans*-2-(2-phenyl-2-propyl)-cyclohexyl ((−)-phenylmenthyl) are readily incorporated into these ligands. The known absolute configurations of the chiral auxiliaries provide additional support for configurational assignments made by X-ray diffraction and circular dichroism. A full account of the synthesis, characterization, structures, configurational stability, and reactivity of the chloro, hydrocarbyl, and amide complexes of this ligand system is presented herein. The results represent the first detailed investigation of chiral organolanthanide complexes and provide an important knowledge base regarding stereoselective synthesis, configurational stability, and reactivity. A companion contribution[20] discusses the kinetics and mechanism of several enantioselective/stereoselective catalytic transformations mediated by these chiral structures.

Experimental Section

Materials and Methods. All manipulations of air-sensitive materials were performed with the rigorous exclusion of oxygen and moisture in flame-dried Schlenk-type glassware on a dual manifold Schlenk line, interfaced to a high-vacuum (10^{-6} Torr) line, or in a nitrogen-filled Vacuum Atmospheres glovebox with a high-capacity recirculator (<2 ppm O_2). Argon (Matheson, prepurified) and dihydrogen (Linde) were purified by passage through a MnO/SiO_2[21] oxygen-removal column and a Davison 4 Å molecular sieve column. Ether solvents (tetrahydrofuran, ethyl ether, and 1,2-dimethoxyethane) were predried over KOH and distilled under nitrogen from sodium benzophenone ketyl. Hydrocarbon solvents (toluene, pentane, and heptane) were distilled under nitrogen from Na/K alloy. All solvents for vacuum line manipulations were stored *in vacuo* over Na/K alloy in resealable bulbs. Deuterated solvents were obtained from Cambridge Isotope Laboratories (all 99 atom % D) and were degassed and dried over Na/K alloy. Heptane and diethyl ether (Aldrich, HPLC grade) for circular dichroism spectroscopy were degassed, dried over Na/K alloy, and vacuum-transferred immediately before sample preparation. Sodium hydride (Aldrich, 97%) was used as received.

Anhydrous lanthanide trichlorides were prepared from the corresponding sesquioxides Ln_2O_3 (Cerac, Ln = La, Nd, Sm, Y, Lu) and ammonium chloride.[22] Chlorodimethyl(2,3,4,5-tetramethylcyclopenta-2,4-dien-1-yl)silane ($Me_2Si(CpH)Cl$) was prepared as described previously[19] from 1,2,3,4-tetramethylcyclopentadiene[23] and dichlorodimethylsilane. (1*S*,2*S*,5*R*)-1-Cyclopentadienyl-*trans*-5-methyl-*cis*-2-(propyl)-cyclohexane ([(+)-neomenthylCp]H) was prepared in a modification of the literature procedure[13k,24] from (1*R*,2*S*,5*R*)-*cis*-5-methyl-*trans*-2-(2-propyl)cyclohexanol *p*-toluenesulfonate and freshly prepared cyclopentadienylsodium in THF (7 days reflux, 58% yield, 1–3 mole scale). (1*R*,2*S*,5*R*)-1-Cyclopentadienyl-*cis*-5-methyl-*trans*-2-(2-phenyl-2-propyl)cyclohexane was prepared according to the method of Halterman et al.[13d,25] and was stored under argon at −35 °C. The solid lithium reagents $LiCH_2SiMe_3$,[26] $LiCH(SiMe)_3)_2$,[27] $Li(2\text{-}C_6H_4CH_2NMe_2)$,[28] and $Li(CH_2)_7$-PMe_2[29] were prepared according to literature methods. Sodium bis(trimethylsilyl)amide (Aldrich) was recrystallized from toluene/pentane under nitrogen. Potassium bis(trimethylsilyl)amide was synthesized from KH and bis(trimethylsilyl)amine[30] and was recrystallized from toluene/pentane. Both amidating reagents were sublimed prior to use. $Hg[CH(SiMe_3)_2]_2$ was prepared from $LiCH(SiMe_3)_2$ and sublimed $HgCl_2$[31] and was sublimed and stored under argon. Propylamine (Aldrich) was predried over KOH, freeze–pump–thaw degassed, and dried over Na/K alloy. 12-Crown-4 (Aldrich) was degassed and dried over Na/K alloy.

Physical and Analytical Measurements. NMR spectra were recorded on either Varian VXR 300 (FT, 300 MHz, ^1H; 75 MHz, ^{13}C) or Varian XL-400 (FT, 400 MHz, ^1H; 100 MHz, ^{13}C; 162 MHz, ^{31}P) instruments. ^1H and ^{13}C chemical shifts are referenced to internal solvent resonances and reported relative to TMS. ^{31}P NMR shifts are referenced to external 85% H_3PO_4. NMR experiments on air-sensitive samples were conducted in either Teflon valve-sealed tubes (J. Young) or in screw-capped tubes fitted with septa (Wilmad). Circular dichroism spectra were recorded on a Jasco J-500 spectrophotometer equipped with a JASCO DP-500/AT software package (Version 1.2). Samples were prepared in 1 mm or 10 mm path length cylindrical quartz cuvettes (Hellma Cells) equipped with Teflon needle valves. Solvent blanks were recorded under identical conditions, and the base line was subtracted from the experimental spectrum. Molecular ellipticities [θ] are reported relative to absorption maxima in units of deg·cm^2·dmol^{-1}. Optical activities were measured at 26 °C with an Optical Activity Ltd. AA-100 polarimeter (±0.001°) using a 0.5 dm quartz cell. Concentrations reported with specific rotations are in units of g·(100 cm^3)$^{-1}$. Elemental analyses were performed by Oneida Research Service, Inc., Whitesboro, NY.

KCH(SiMe$_3$)$_2$. This reagent was prepared from potassium sand (1.75 g, 0.0448 mol) and sublimed $Hg[CH(SiMe_3)_2]_2$ (5.69 g, 0.011 mol) in methylcyclohexane (55 mL) in a manner analogous to the preparation of KCH_2SiMe_3.[32] A colorless microcrystalline solid (2.92 g, 67%) was isolated and recrystallized from cold (−78 °C) diethyl ether.

^1H NMR (Et_2O-d_{10}): δ −0.15 (18H), −2.19 (1H). ^{13}C NMR (Et_2O-d_{10}): δ 7.2, 5.8.

[(−)-MenthylCp]H. An efficient, large-scale, one-pot synthesis of this compound was developed as a modified literature procedure.[13k] (+)-Neomenthol (89.3 g, 0.57 mol, degassed) was syringed into a 2 L flask under argon flush followed by THF (300 mL), and the solution was cooled to −20 °C. *N*-Butyllithium (356 mL, 0.57 mol, 1.6 M in hexanes) was then added dropwise over 30 min, and the solution was subsequently stirred for 30 min. *p*-Toluenesulfonyl chloride (116 g, 0.60 mol) was dissolved in THF (300 mL) and added to the solution over the course of 1 h, while the mixture was maintained at −20 °C. The solution was then stirred for 8 h, warmed to −5 °C, and stirred for an additional 1 h. NaCp (60.0 g, 0.68 mol) dissolved in THF (300 mL) was added dropwise to the reaction mixture, while the temperature was maintained at −5 °C. The mixture was allowed to stir for 10 h at −5 °C, warmed to ambient temperature, and stirred for an additional 6 h. The reaction was then quenched by the addition of water (400 mL), and the mixture was added to a separatory funnel. The organics were separated from the aqueous phase, which was then extracted with Et_2O (3 × 150 mL). The combined organics were dried over sodium sulfate and filtered, and all volatiles were removed from the filtrate by rotary evaporation. The resulting dark oil was purified by vacuum distillation. Yield after two distillations based on (+)-neomenthol: 75 g, 0.367 mol, 64%.

Na[(+)-neomenthylCp] (2a). A 1 L Schlenk flask with a Teflon inlet valve was charged with NaH (4.45 g, 0.185 mol). Under Ar flush, THF (600 mL) and freshly distilled, degassed [(+)-neomenthylCp]H (35.0 g, 0.171 mol) were successively syringed into the reaction flask. A condenser was then attached to the reaction flask, and the stirred gray suspension was heated to gentle reflux. Evolution of hydrogen became evident at ca. 40 °C. Reflux was maintained for 12 h until the evolution of H_2 had ceased. The mixture was then cooled to ambient temperature, and the excess NaH was removed via filtration through a predried Celite pad. The filter cake was washed three times with THF (50 mL). The clear, amber filtrate was concentrated *in vacuo* until a colorless solid precipitated. The mixture was warmed to redissolve the precipitate. Pentane (450 mL) was added via syringe carefully to crystallize the product. The colorless solid was isolated via filtration, rinsed with pentane (3 × 50

(20) Giardello, M. A.; Conticello, V. P.; Brard, L.; Gagné, M.; Marks, T. J. *J. Am. Chem. Soc.*, following paper in this issue.
(21) (a) Moeseler, R.; Horvath, B.; Lindenau, D.; Horvath, E. G.; Krauss, H. L. *Z. Naturforsch. B* **1976**, *31B*, 892–893. (b) McIlwrick, C. R.; Phillips, C. S. G. *J. Chem. Phys. E* **1973**, *6*, 1208–1210. (c) He, M.-Y.; Xiong, G.; Toscano, P. J.; Burwell, R. L., Jr.; Marks, T. J. *J. Am. Chem. Soc.* **1985**, *107*, 641–652.
(22) Meyer, G. *Inorg. Synth.* **1989**, *25*, 146–150.
(23) (a) Fendrick, C. M.; Mintz, E. A.; Schertz, L. D.; Marks, T. J.; Day, V. W. *Organometallics* **1984**, *3*, 819–821. (b) Fendrick, C. M.; Schertz, L. D.; Day, V. W.; Marks, T. J. *Organometallics* **1988**, *7*, 1828–1830.
(24) Faller, J. W.; Kuo-Hua, C. *Organometallics* **1984**, *3*, 927–932.
(25) Halterman, R. L. Ph.D. Thesis, University of California at Berkeley, CA, 1987.
(26) Tessier-Youngs, C.; Beachley, O. T., Jr. *Inorg. Synth.* **1986**, *24*, 95–97.
(27) Cowley, A. H.; Kemp, R. A. *Synth. React. Inorg. Met.-Org. Chem.* **1981**, *11*, 591–595.
(28) Manzer, L. E. *J. Am. Chem. Soc.* **1978**, *100*, 8068–8073.
(29) Schmidbauer, H.; Tronich, W. *Chem. Ber.* **1968**, *101*, 3556–3561.
(30) Brown, C. A. *J. Org. Chem.* **1974**, *39*, 3913–3918.
(31) Al-Hashimi, S.; Smith, J. D. *J. Organomet. Chem.* **1978**, *153*, 253–263.
(32) Hart, A. J.; O'Brien, D. H.; Russell, C. R. *J. Organomet. Chem.* **1974**, *72*, C19–C22.

mL), and dried *in vacuo*. Yield: 35.7 g (92%) of Na[(+)neomenthylCp] as colorless, highly air- and moisture-sensitive needles. The product was recrystallized from THF/pentane for the subsequent ligand synthesis.

^{1}H NMR (THF-d_8): δ 5.64 (t, 2H), 5.58 (t, 2H), 3.13 (br s, 1H), 2.13 (m, 1H), 1.83–1.46 (m, 4H), 1.27 (m, 2H), 0.95 (m, 2H), 0.84 (d, 3H), 0.80 (d, 3H), 0.57 (d, 3H). ^{13}C NMR: δ 121.9, 105.7, 101.8, 50.9, 46.6, 40.5, 37.6, 30.8, 28.5, 26.0, 24.1, 22.7, 21.0.

Na[(–)-menthylCp] (2b). This compound was prepared from NaH (4.45 g, 0.185 mol) and [(–)-menthylCp]H (35.0 g, 0.171 mol) in THF (600 mL) using the method used for Na[(+)-neomenthylCp] (**2a**) above. Crystallization from a pentane/THF mixture afforded 32 g (83%) of Na[(–)-menthylCp] as colorless, highly air- and moisture-sensitive needles.

^{1}H NMR (THF-d_8): δ 5.57 (t, 2H), 5.52 (t, 2H), 2.29 (m, 1H), 1.62 (m, 1H), 1.39 (br m, 1H), 1.26 (m, 1H), 1.12–1.03 (m, 6H), 0.89 (d, 3H), 0.70 (d, 3H), 0.66 (d, 3H). ^{13}C NMR (THF-d_8): δ 124.6, 101.7, 101.6, 51.6, 48.5, 44.2, 37.0, 35.0, 27.7, 26.2, 23.6, 22.4, 16.3.

Li_2Me_2SiCp''[(+)-neomenthylCp] (3a). A 250 mL flask with a Teflon inlet valve was charged with Na[(+)-neomenthylCp] (11.27 g, 0.0498 mol) in the glovebox. THF (150 mL) was added via syringe to the reaction flask. The mixture was stirred, completely dissolving the solids and affording a clear, pale yellow solution. Under an argon flush, a solution of $Me_2Si(Cp''H)Cl$ (10.71 g, 0.0499 mol) in THF (40 mL) was syringed into the stirred solution of the sodium salt. Immediate precipitation of a flocculent, colorless solid (NaCl) occurred. The suspension was stirred at ambient temperature for 10 h. The solvent was then removed *in vacuo*, and pentane (150 mL) was added to the reaction flask. The resulting mixture was filtered, and the colorless precipitate was washed once with pentane (30 mL). A solution of $LiCH_2SiMe_3$ (9.09 g, 0.0965 mol) in pentane (50 mL) was added slowly to the combined extracts of $Me_2Si(Cp''H)$[(+)-neomenthylCp]H from a 100 mL side-arm flask. The rate of addition was controlled by monitoring the evolution of gaseous $SiMe_4$ from the exothermic reaction. After addition was complete, the colorless mixture slowly gelled. The gel was dissolved by addition of a small amount of THF (5 mL). A pale yellow oil gradually separated from the supernatant and was removed by decantation. Prolonged evacuation of this oil yielded 19.1 g (97%) of Li_2Me_2SiCp''[(+)-neomenthylCp] as a solvent-free, colorless solid foam.

^{1}H NMR (THF-d_8): δ 5.84 (t, 1H), 5.77 (t, 1H), 5.75 (t, 1H), 3.17 (br s, 1H), 2.06 (s, 6H), 2.02 (m, 1H), 1.91 (s, 6H), 1.82–1.58 (m, 4H), 1.24 (m, 2H), 0.99–0.80 (m, 2H), 0.88 (d, 3H), 0.79 (d, 3H), 0.71 (d, 3H), 0.39 (s, 3H), 0.38 (s, 3H). ^{13}C NMR (THF-d_8): δ 124.2, 116.6, 113.8, 113.4, 111.3, 110.6, 108.0, 104.3, 50.5, 46.5, 39.5, 37.3, 30.7, 28.2, 26.6, 23.8, 22.4, 21.5, 14.8, 11.6, 5.02, 4.50.

Li_2Me_2SiCp''[(–)-menthylCp] (3b). This compound was prepared from Na[(–)-menthylCp] (11.27 g, 49.8 mmol) and $Me_2Si(Cp''H)Cl$ (10.71 g, 49.9 mmol) by using the same procedure as used for the synthesis of Li_2Me_2SiCp''[(+)-neomenthylCp]. Total yield: 19.1 g (97%) of Li_2Me_2SiCp''[(–)-menthylCp] as a solvent-free, colorless solid foam.

^{1}H NMR (THF-d_8): δ 5.78 (d, 2H), 5.60 (t, 1H), 2.30 (t, 1H), 2.05 (s, 6H), 1.89 (s, 6H), 1.82–1.60 (m, 4H), 1.35 (m, 2H), 1.08–0.88 (m, 2H), 0.85 (d, 3H), 0.74 (d, 3H), 0.68 (d, 3H), 0.40 (s, 6H). ^{13}C NMR (THF-d_8): δ 128.1, 121.9, 116.1, 112.0, 109.5, 104.7, 101.5, 50.4, 48.7, 43.2, 34.7, 27.9, 26.0, 24.7, 23.3, 22.3, 16.1, 14.5, 11.5, 5.4, 4.2.

Li_2Me_2SiCp''[(–)-phenylmenthylCp] (3c). A 100 mL flask with a Teflon inlet valve was charged with $LiCH_2SiMe_3$ (2.04 g, 21.7 mmol). Pentane (40 mL) was condensed *in vacuo* into the flask at –78 °C. After the flask was back-filled with argon, a solution of [(–)-phenylmenthylCp]H (5.96 g, 21.3 mmol) in pentane (30 mL) was added to the reaction flask via syringe under an Ar flush. Evolution of $SiMe_4$ was immediately evident from the exothermic reaction. A pale yellow oil separated from the supernatant after 1 h. Solvent was next removed *in vacuo*, and the resulting colorless, solid foam was dried under dynamic vacuum for 12 h. THF (50 mL) was then condensed *in vacuo* into the reaction flask at –78 °C. Upon the solution warming to ambient temperature, the Li[(–)-phenylmenthylCp] completely dissolved, affording a clear, pale yellow solution. Under an argon flush, a solution of $Me_2Si(Cp''H)Cl$ (4.64 g, 21.6 mmol) in THF (40 mL) was added via syringe to the stirred solution. The reaction mixture immediately became colorless and was subsequently stirred at ambient temperature for 2 h. The solvent was then removed *in vacuo*, and the resulting pale yellow oil was dried under dynamic vacuum for 1 h. Pentane (50 mL) was condensed *in vacuo* into the flask at –78 °C. The mixture was warmed to ambient temperature and filtered. The colorless precipitate (LiCl) was extracted once with pentane (5 mL). The combined colorless filtrate was treated carefully with a solution of $LiCH_2SiMe_3$ (3.81 g, 40.5 mmol) in pentane (20 mL). The rate of addition was controlled by carefully monitoring the evolution of $SiMe_4$. After evolution ceased, a pale yellow oil gradually separated from the mother liquod and was subsequently decanted away. Prolonged evacuation of the oil afforded 8.69 g (93% yield) of Li_2Me_2SiCp''[(–)-phenylmenthylCp] as a pale yellow solid foam.

^{1}H NMR (THF-d_8): δ 7.21 (d, 2H), 7.15 (d, 2H), 6.99 (t, 1H), 5.83 (br s, 1H), 5.77 (br s, 1H), 5.69 (br s, 1H), 2.47 (br t, 1H), 2.11 (s, 6H), 2.03 (br m, 1H), 1.92 (s, 6H), 1.64 (br s, 1H), 1.49–1.01 (m, 4H), 0.92 (m, 3H), 0.90–0.76 (m, 2H), 0.80 (s, 3H), 0.633 (s, 3H), 0.400 (s, 6H). ^{13}C NMR (THF-d_8): δ 159.2, 129.6, 128.1, 126.5, 124.9, 116.5, 113.4, 112.2, 111.5, 110.6, 110.1, 104.7, 54.5, 51.0, 43.4, 42.8, 36.9, 34.7, 31.6, 30.9, 23.1, 20.6, 14.8, 11.6, 5.2, 5.1.

(*R*)-Me_2SiCp''[(+)-neomenthylCp]$La(\mu\text{-}Cl)_2Li(ether)_2$ [(*R*)-4a]. A 250 mL flask with a Teflon inlet valve was charged with $LaCl_3$ (3.72 g, 15.2 mmol) and Li_2Me_2SiCp''[(+)-neomenthylCp] (6.02 g, 15.3 mmol). THF (150 mL) was condensed into the reaction flask *in vacuo* at –78 °C. The reaction mixture was stirred for 12 h at ambient temperature under argon. The milky white suspension was then refluxed for 24 h. The colorless solid $LaCl_3$ gradually dissolved, upon warming, to form a clear, homogeneous, amber solution. The mixture was next cooled to room temperature, and the solvent was removed *in vacuo*. The resulting colorless, gummy solid was dried under high vacuum for 2 h. Diethyl ether (100 mL) was condensed into the reaction flask *in vacuo* at –78 °C. The solid was triturated with diethyl ether at –10 °C, and the resulting mixture was filtered. The colorless precipitate (LiCl) was extracted once with diethyl ether (25 mL). The clear, amber filtrate was evaporated to yield a gummy, brown solid, which was exchanged repetitively with diethyl ether (100 mL) until a colorless solid precipitated upon solvent removal. Usually 5–6 repetitions were necessary. The mixture was next warmed to 0 °C and the solid redissolved. This solution was then slowly cooled to –78 °C, and the resulting solid was isolated via cold (–78 °C) filtration. Vacuum-drying afforded 4.01 g (35% yield) of (*R*)-Me_2SiCp''[(+)-neomenthylCp]$La(\mu\text{-}Cl)_2Li(ether)_2$ as colorless microcrystals. A second crop of 1.33 g (12% yield) of product could be recovered in a similar fashion from the mother liquor (total yield: 47%). The product was recrystallized additionally from cold (–78 °C) diethyl ether. The colorless microcrystals slowly lose diethyl ether as a solid *in vacuo*, while prolonged evacuation causes complete loss of diethyl ether. Satisfactory analyses could be obtained only from the diethyl ether-free LiCl adduct.

^{1}H NMR (THF-d_8): δ 6.19 (t, 1H), 5.78 (t, 1H), 5.74 (t, 1H), 3.39 (q, 8H), 3.43 (br s, 1H), 2.16 (d, 1H), 2.13 (s, 3H), 2.11 (s, 3H), 2.04 (m, 1H), 1.89 (s, 3H), 1.88 (s, 3H), 1.49–0.87 (m, 7H), 1.12 (t, 12H), 0.96 (d, 3H), 0.83 (d, 3H), 0.62 (s, 3H), 0.60 (s, 3H), 0.59 (d, 3H). ^{13}C NMR (THF-d_8): δ 134.9, 125.6, 123.9, 123.8, 123.7, 119.2, 118.3, 116.1, 113.0, 105.4, 66.3, 50.7, 44.1, 38.0, 37.4, 30.2, 29.0, 25.0, 24.2, 22.8, 21.0, 15.7, 15.6, 15.3, 11.7, 1.6, 1.2. Anal. Calcd for the ether-free product $C_{26}H_{40}Cl_2LaLiSi$: C, 52.27; H, 6.75; Cl, 11.87. Found: C, 52.15; H, 7.00; Cl, 11.57.

(*R*)-Me_2SiCp''[(+)-neomenthylCp]$Nd(\mu\text{-}Cl)_2Li(ether)_2$[(*R*)-4b]. This compound was prepared from $NdCl_3$ (1.99 g, 7.98 mmol) and Li_2Me_2SiCp''[(+)-neomenthylCp] (3.008 g, 7.62 mmol) in THF (100 mL) using the procedure used above for (*R*)-Me_2SiCp''[(+)-neomenthylCp]$La(\mu\text{-}Cl)_2Li(ether)_2$. The diethyl ether exchange was performed at ambient temperature. Crystallization from cold (–78 °C) diethyl ether afforded 2.235 g (39% yield) of (*R*)-Me_2SiCp''[(+)-neomenthylCp]$Nd(\mu\text{-}Cl)_2Li(ether)_2$ as pale blue prisms. An additional 1.460 g (26% yield) of product was crystallized from the mother liquor (total yield: 65%). The product was further recrystallized from cold (–78 °C) diethyl ether.

^{1}H NMR (diethyl ether-d_{10}): δ 34.24 (br s, 1H), 24.37 (br s, 1H), 20.38 (br s, 1H), 20.08 (br s, 3H), 19.68 (s, 3H), 17.65 (br s, 1H), 12.90 (br s, 1H), 11.37 (s, 1H), 9.25 (br s, 1H), 7.27 (s, 1H), 5.90 (br s, 3H), 5.56 (br s, 1H), 4.24 (br s, 1H), 3.47 (br s, 1H), 3.37 (q, 8H), 1.95 (br s, 3H), 1.10 (t, 12H), 1.12 (br s, 3H), –1.74 (br s, 3H), –2.01 (m, 1H), –8.58 (br s, 3H), –10.76 (br s, 3H), –12.60 (br s, 3H), –25.75 (br s, 1H). Anal. Calcd for $C_{34}H_{60}Cl_2LiNdO_2Si$: C, 54.37; H, 8.05. Found: C, 53.95; H, 7.98.

(*R*)-Me_2SiCp''[(+)-neomenthylCp]$Sm(\mu\text{-}Cl)_2Li(ether)_2$ [(*R*)-4c]. A 250 mL flask with a teflon inlet valve was charged with $SmCl_3$ (2.67 g, 10.4 mmol) and Li_2Me_2SiCp''[(+)-neomenthylCp] (4.10 g, 10.4 mmol). THF (150 mL) was then condensed into the reaction flask *in vacuo* at –78 °C. The reaction mixture was stirred for 16 h at 25 °C under argon and then refluxed for 12 h. The orange-yellow solution was next cooled to 25 °C, and the solvent was removed *in vacuo*. The resulting orange, gummy solid was dried under high vacuum for 6 h. Diethyl ether (100 mL) was then condensed into the reaction flask *in vacuo* at –78 °C. The solid was triturated with diethyl ether at –40 °C, and the resulting mixture was filtered. The colorless precipitate (LiCl) was extracted once with

cold diethyl ether (25 mL). The clear, orange filtrate was evaporated to a gummy, orange solid, which was then exchanged repetitively with diethyl ether (50 mL) at −40 °C, until a crystalline solid appeared upon solvent removal. Usually 5–6 repetitions were necessary. Crystallization from cold (−78 °C) diethyl ether afforded (*R*)-Me_2SiCp''[(+)-neomenthylCp]Sm(μ-Cl)$_2$Li(ether)$_2$ as deep orange plates (2.05 g, 26% yield). A further 1.65 g (21% yield) of product was recovered from the mother liquor (total yield: 47%) by concentration and cooling to −78 °C.

^{1}H NMR (THF-d_8): δ 11.98 (br s, 1H), 6.14 (br s, 1H), 5.61 (d, 1H), 4.80 (s, 3H), 4.25 (br s, 1H), 3.38 (qu, 8H), 3.20 (s, 1H), 2.24 (s, 3H), 1.50 (d, 3H), 1.42 (s, 3H), 1.11 (t, 12H), 0.89 (d, 3H), 0.72 (s, 3H), 0.21 (d, 3H), 0.19 (s, 3H), −0.25 (s, 3H), −0.43 (s, 3H). CD (THF), λ_{max} ([θ]): 309 (−7467), 275 (−22 587) nm. Anal. Calcd for $C_{34}H_{60}Cl_2LiO_2SiSm$: C, 53.93; H, 7.99. Found: C, 53.88; H, 8.58.

(*S*)-Me_2SiCp''[(+)-neomenthylCp]Sm(μ-Cl)$_2$Li(ether)$_2$ [(*S*)-4c]. This compound was prepared from $SmCl_3$ (4.28 g, 16.7 mmol) and Li_2Me_2SiCp''[(+)-neomenthylCp] (6.01 g, 15.2 mmol) in THF (100 mL) using the above method used for (*R*)-Me_2SiCp''[(+)-neomenthylCp]La(μ-Cl)$_2$Li(ether)$_2$. The diethyl ether exchanges were performed at room temperature. Crystallization from cold (−78 °C) diethyl ether afforded 3.61 g (31% yield) of (*S*)-Me_2SiCp''[(+)-neomenthylCp]Sm(μ-Cl)$_2$Li(ether)$_2$ as deep orange plates. A further 3.07 g (27% yield) of product was retrieved from the mother liquor (total yield: 58%) by concentration and cooling to −78 °C. The product was additionally recrystallized from cold diethyl ether.

^{1}H NMR (diethyl ether-d_{10}): δ 15.47 (br s, 1H), 6.83 (br s, 1H), 5.73 (br s, 1H), 4.59 (br s, 1H), 3.38 (q, 8H), 3.22 (m, 1H), 2.32 (d, 3H), 2.20 (s, 3H), 2.01 (s, 3H), 1.86 (s, 3H), 1.68 (m, 2H), 1.54 (m, 1H), 1.11 (t, 12H), 0.86 (s, 3H), 6.81 (m, 1H), 0.09 (m, 1H), −0.66 (br t, 1H), −1.34 (s, 3H), −1.80 (d, 3H), −3.74 (s, 1H), −4.58 (s, 3H), −4.65 (m, 1H). CD (diethyl ether), λ_{max} ([θ]): 322 (−1040), 270 (+21 400) nm. Anal. Calcd for $C_{34}H_{60}Cl_2LiO_2SiSm$: C, 53.93; H, 7.99. Found: C, 54.18; H, 8.14.

(*R*)-Me_2SiCp''[(+)-neomenthylCp]Y(μ-Cl)$_2$Li(ether)$_2$ [(*R*)-4d]. This compound was prepared from YCl_3 (2.71 g, 13.8 mmol) and Li_2Me_2SiCp''[(+)-neomenthylCp] (5.02 g, 12.7 mmol) in THF (100 mL) using the general procedure used for (*R*)-Me_2SiCp''[(+)-neomenthylCp]La(μ-Cl)$_2$Li(ether)$_2$ above. The reactants completely dissolved at ambient temperature; no reflux period was required. The diethyl ether exchanges were performed at room temperature. Crystallization from cold (−78 °C) diethyl ether afforded 3.62 g (41% yield) of (*R*)-Me_2SiCp''[(+)-neomenthylCp]Y(μ-Cl)$_2$Li(ether)$_2$ as large, colorless prisms. A second crop of 1.93 g (22% yield) was recovered from the mother liquor (total yield: 63%) by concentration and cooling to −78 °C. The product was further recrystallized from cold (−78 °C) diethyl ether.

^{1}H NMR (diethyl ether-d_{10}): δ 6.28 (t, 1H), 5.66 (m, 2H), 3.49 (br s, 1H), 3.39 (q, 8H), 2.28 (br d, 1H), 1.96 (s, 3H), 1.93 (s, 3H), 1.90 (m, 1H), 1.88 (s, 3H), 1.86 (s, 3H), 1.80–0.87 (m, 7H), 1.12 (t, 12H), 1.03 (d, 3H), 0.86 (d, 3H), 0.85 (d, 3H), 0.72 (s, 3H), 0.71 (s, 3H). ^{13}C NMR (diethyl ether-d_{10}): δ 136.4, 126.1, 125.0, 122.3, 121.1, 118.9, 113.1, 113.0, 112.9, 104.6, 66.3, 52.9, 42.4, 37.5, 36.5, 30.4, 26.2, 25.6, 23.4, 22.9, 22.2, 15.6, 14.2, 14.0, 12.0, 11.9, 1.1, 0.65. CD (diethyl ether), λ_{max} ([θ]): 314 (−6390), 269 (−18 100) nm. Anal. Calcd for $C_{34}H_{60}Cl_2LiO_2SiY$: C, 58.70; H, 8.69. Found: C, 59.17; H, 8.12.

(*R*)-Me_2SiCp''[(+)-neomenthylCp]Lu(μ-Cl)$_2$Li(ether)$_2$ [(*R*)-4e]. The title compound was prepared from $LuCl_3$ (3.13 g, 11.1 mmol) and Li_2Me_2SiCp''[(+)-neomenthylCp] (4.18 g, 10.6 mmol) in THF (100 mL) according to the procedure used for (*R*)-Me_2SiCp''[(+)-neomenthylCp]La(μ-Cl)$_2$Li(ether)$_2$ above. The reactants completely dissolved in THF at ambient temperature; reflux was unnecessary. The diethyl ether exchanges were also performed at ambient temperature. Crystallization from cold (−78 °C) diethyl ether afforded 3.92 g (47% yield) of (*R*)-Me_2SiCp''[(+)-neomenthylCp]Lu(μ-Cl)$_2$Li(ether)$_2$ as large, colorless prisms. An additional 0.86 g (10%) was retrieved from the filtrate extracts in a similar manner (total yield: 57%). The product was subsequently recrystallized from cold (−78 °C) diethyl ether.

^{1}H NMR (diethyl ether-d_{10}): δ 6.21 (t, 1H), 5.59 (d, 2H), 3.51 (br s, 1H), 3.38 (q, 8H), 2.26 (br d, 1H), 1.95 (s, 3H), 1.93 (m, 1H), 1.92 (s, 3H), 1.87 (s, 3H), 1.86 (s, 3H), 1.79–1.51 (m, 4H), 1.24–0.91 (m, 3H), 1.18 (t, 12H), 1.00 (d, 3H), 0.87 (d, 3H), 0.85 (d, 3H), 0.72 (s, 3H), 0.70 (s, 3H). ^{13}C NMR (diethyl ether-d_{10}): δ 135.9, 125.9, 124.2, 120.7, 119.1, 118.9, 112.9, 111.4, 111.0, 104.3, 66.3, 53.0, 42.3, 37.5, 36.5, 30.5, 26.3, 25.8, 23.4, 22.9, 22.3, 15.6, 14.3, 14.1, 12.1, 12.0, 1.1, 0.53. CD (diethyl ether), λ_{max} ([θ]): 308 (−4550), 260 (−19 800) nm. Anal. Calcd for $C_{34}H_{60}Cl_2LiLuO_2Si$: C, 52.24; H, 7.74. Found: C, 52.23; H, 7.51.

(*R*)-Me_2SiCp''[(−)-menthylCp]Sm(μ-Cl)$_2$Li(ether)$_2$ [(*R*)-4f]. A 100 mL flask with a Teflon inlet valve was charged with $SmCl_3$ (2.86 g, 11.1 mmol) and Li_2Me_2SiCp''[(−)-menthylCp] (4.0 g, 10.1 mmol). THF (100 mL) was condensed into the reaction flask *in vacuo* at −78 °C. The reaction mixture was stirred for 12 h at 25 °C under argon, with both reactants dissolving at this temperature. The solvent was next removed *in vacuo*, and the resulting yellow-orange, gummy solid was dried under high vacuum for 2 h. Diethyl ether (50 mL) was then condensed into the reaction flask *in vacuo* at −78 °C. The solid was next triturated with the ether at 25 °C, and the resulting mixture was filtered. The colorless precipitate (LiCl) was extracted once with diethyl ether (25 mL). The clear orange filtrate was evaporated to a gummy, orange solid, which was exchanged (dissolved, evaporated) repetitively with 25 mL of ether at 25 °C until an orange solid precipitated upon solvent removal. Usually 5–6 repetitions were necessary. Crystallization from cold (−78 °C) diethyl ether, cold filtration, and vacuum-drying afforded 3.0 g (40%) of (*R*)-Me_2SiCp''[(−)-menthylCp]Sm(μ-Cl)$_2$Li(ether)$_2$ as deep orange prisms. A further 1.5 g (20% yield) of product was recovered from the mother liquor (total yield: 60%) by concentration and cooling to −78 °C. The product was additionally recrystallized from cold diethyl ether.

^{1}H NMR (THF-d_8): δ 13.31 (s, 1H), 6.43 (s, 1H), 4.68 (s, 1H), 3.91 (t, 1H), 3.64 (m, 8H), 3.38 (q, 8H), 2.32 (d, 3H), 2.37 (s, 3H), 1.82 (d, 3H), 1.50 (m, 3H), 1.40 (s, 3H), 1.18 (d, 3H), 1.05 (t, 12H), 1.03 (s, 3H), 0.95 (m, 1H), 0.90 (s, 3H), 0.50 (m, 1H), −0.12 (d, 3H), −0.58 (s, 3H), −1.30 (q, 1H), −1.78 (s, 3H), −2.23 (d, 1H). CD (diethyl ether), λ_{max} ([θ]): 312 (+2669), 270 (−21 197) nm. Anal. Calcd for $C_{34}H_{60}Cl_2LiO_2SiSm$: C, 53.93; H, 7.99. Found: C, 53.42; H, 7.82.

4/1 (*S*)/(*R*)-Me_2SiCp''[(−)-menthylCp]Sm(μ-Cl)$_2$Li(ether)$_2$ [(*S*,*R*)-4f]. A 50 mL flask with a Teflon inlet valve was loaded with (*R*)-Me_2SiCp''[(−)-menthylCp]Sm(μ-Cl)$_2$Li(ether)$_2$ (2.0 g, 2.64 mmol). THF (30 mL) was condensed into the reaction flask *in vacuo* at −78 °C. The mixture was warmed to 25 °C and stirred for 10 days under argon. The solvent was then removed *in vacuo*, and the resulting yellow oil was dried under high vacuum for 12 h. Diethyl ether (15 mL) was condensed into the reaction flask *in vacuo* at −78 °C. The clear yellow solution was evaporated to a gummy, yellow solid, which was exchanged repetitively with diethyl ether (15 mL) at −78 °C until an orange-yellow microcrystalline solid was obtained upon solvent removal. Vacuum-drying afforded 1.94 g (97% yield) of a 4/1 mixture of (*S*)/(*R*)-Me_2SiCp''[(−)-menthylCp]Sm(μ-Cl)$_2$Li(ether)$_2$ as a microcrystalline powder.

^{1}H NMR (THF-d_8): δ 13.31 (s, 1H), 11.75 (s, 1H), 6.70 (s, 1H), 6.43 (s, 1H), 6.10 (d, 1H), 4.68 (s, 1H), 4.40 (s, 1H), 3.91 (t, 1H), 3.64 (m, 8H), 3.38 (q, 8H), 2.78 (t, 1H), 2.56 (m, 1H), 2.50 (s, 3H), 2.32 (d, 3H), 2.37 (s, 3H), 2.30 (t, 1H), 2.10 (d, 1H), 1.94 (d, 1H), 1.90 (m, 1H), 1.82 (d, 3H), 1.61 (s, 3H), 1.50 (m, 3H), 1.41 (d, 3H), 1.40 (s, 3H), 1.18 (d, 3H), 1.05 (t, 12H), 1.03 (s, 3H), 1.0 (d, 3H), 0.95 (m, 1H), 0.90 (s, 3H), 0.70 (s, 3H), 0.6 (d, 3H), 0.50 (m, 1H), 0.09 (s, 3H), 0.00 (s, 3H), −0.12 (d, 3H), −0.58 (s, 3H), −0.57 (s, 3H), −1.30 (q, 1H), −1.78 (s, 3H), −2.23 (d, 1H). Anal. Calcd for $C_{34}H_{58}Cl_2LiO_2SiSm$: C, 53.93; H, 7.99. Found: C, 54.08; H, 7.88.

(*R*)-Me_2SiCp''[(−)-menthylCp]Y(μ-Cl)$_2$Li(ether)$_2$ [(*R*)-4g]. This compound was prepared from YCl_3 (2.71 g, 11.1 mmol) and Li_2Me_2SiCp''[(−)-menthylCp] (4.0 g, 10.1 mmol) in THF (100 mL) using the procedure described for (*R*)-Me_2SiCp''[(−)-menthylCp]Sm(μ-Cl)$_2$Li(ether)$_2$. The ether exchange was performed at 25 °C, and crystallization from cold (−78 °C) diethyl ether afforded 3.0 g (43% yield) of (*R*)-Me_2SiCp''[(−)-menthylCp]Y(μ-Cl)$_2$Li(ether)$_2$ as large, colorless prisms. A second crop of 1.5 g (21% yield) was recovered from the mother liquor (total yield: 64%) by concentration and cooling to −78 °C. The product was further recrystallized from cold (−78 °C) diethyl ether.

^{1}H NMR (THF-d_8): δ 6.00 (t, 1H), 5.57 (d, 2H), 3.39 (q, 8H), 2.63 (m, 1H), 2.44 (t, 1H), 1.97 (s, 3H), 1.94 (s, 3H), 1.90 (m, 2H), 1.85 (s, 3H), 1.81 (s, 3H), 1.70 (m, 1H), 1.65 (d, 1H), 1.36 (m, 1H), 1.11 (t, 12H), 1.06 (m, 2H), 0.88 (d, 3H), 0.83 (m, 1H), 0.78 (d, 3H), 0.71 (d, 3H), 0.67 (s, 3H), 0.62 (s, 3H). ^{13}C NMR (THF-d_8): δ 136.4, 126.1, 125.0, 122.3, 121.1, 118.9, 113.1, 113.0, 112.9, 104.6, 66.3, 52.9, 42.4, 37.5, 36.5, 30.4, 26.2, 25.6, 23.4, 22.9, 22.2, 15.6, 14.2, 14.0, 12.0, 11.9, 1.1, 0.7. CD (diethyl ether), λ_{max} ([θ]): 294 (+4373), 264 (−32 046) nm. Anal. Calcd for $C_{34}H_{60}Cl_2LiO_2SiY$: C, 58.70; H, 8.69. Found: C, 58.64; H, 8.72.

(*R*)-Me_2SiCp''[(−)-menthylCp]Lu(μ-Cl)$_2$Li(ether)$_2$ [(*R*)-4h]. This compound was prepared from $LuCl_3$ (3.13 g, 11.1 mmol) and Li_2Me_2SiCp''[(−)-menthylCp] (4.0 g, 10.1 mmol) in THF (100 mL) using the procedure described for (*R*)-Me_2SiCp''[(−)-menthylCp]Sm(μ-Cl)$_2$Li(ether)$_2$. The diethyl ether exchange was performed at 25 °C, and crystallization from cold (−78 °C) diethyl ether afforded 4.10 g (52%

yield) of (*R*)-Me_2SiCp''[(−)-menthylCp]Lu(μ-Cl)$_2$Li(ether)$_2$ as large, colorless prisms. An additional 1.40 g (18% yield) was recovered from the mother liquor (total yield: 70%) by concentration and cooling to −78 °C. The product was further recrystallized from cold (−78 °C) diethyl ether.

^{1}H NMR (THF-d_8): δ 6.00 (t, 1H), 5.58 (d, 2H), 3.38 (q, 8H), 2.68 (d, 1H), 2.42 (t, 1H), 1.97 (s, 3H), 1.94 (s, 3H), 1.86 (s, 3H), 1.82 (s, 3H), 1.78–1.58 (m, 4H), 1.36 (m, 1H), 1.11 (t, 12H), 1.06 (m, 2H), 0.88 (d, 3H), 0.84 (m, 1H), 0.76 (d, 3H), 0.71 (d, 3H), 0.67 (s, 3H), 0.64 (s, 3H). ^{13}C NMR (THF-d_8): δ 137.9, 125.2, 122.6, 120.1, 117.5, 116.6, 111.6, 111.0, 107.9, 103.4, 66.3, 51.2, 42.3, 41.6, 36.6, 31.3, 27.4, 25.8, 23.3, 22.2, 18.5, 15.7, 14.8, 12.3, 11.9, 1.3, 0.7. CD (diethyl ether), λ_{max} ([θ]): 285 (+3018), 256 (−34 260) nm. Anal. Calcd for $C_{34}H_{60}Cl_2LiLuO_2Si$: C, 52.24; H, 7.74. Found: C, 51.84; H, 7.71.

(*S*)-Me_2SiCp''[(−)-phenylmenthylCp]Y(μ-Cl)$_2$Li(ether)$_2$ [(*S*)-4i]. The procedure for (*R*)-Me_2SiCp''[(+)-neomenthylCp]Y(μ-Cl)$_2$Li(ether)$_2$ was employed with YCl_3 (1.37 g, 7.02 mmol) and Li_2Me_2SiCp''[(−)-phenylmenthylCp] (3.10 g, 7.04 mmol) in THF (60 mL). Crystallization from cold (−78 °C) diethyl ether afforded 2.16 g (48% yield) of (*S*)-Me_2SiCp''[(−)-phenylmenthylCp]Y(μ-Cl)$_2$Li(ether)$_2$ as a colorless, microcrystalline solid. The product was additionally recrystallized from cold (−78 °C) diethyl ether.

^{1}H NMR (diethyl ether-d_{10}): δ 7.09 (d, 5H), 6.96 (m, 1H), 6.20 (t, 1H), 5.64 (t, 1H), 5.60 (t, 1H), 3.38 (q, 8H), 2.83 (br d, 1H), 2.51 (br t, 1H), 2.02 (s, 3H), 1.92 (s, 3H), 1.88 (s, 3H), 1.86 (s, 3H), 1.61–0.78 (m, 7H), 1.16 (s, 3H), 1.11 (t, 12H), 0.85 (d, 3H), 0.74 (s, 3H), 0.68 (s, 3H), 0.52 (s, 3H). ^{13}C NMR (THF-d_8): δ 154.7, 138.0, 128.3, 126.2, 125.0, 124.8, 123.4, 121.7, 118.3, 118.1, 113.5, 111.5, 109.2, 66.3, 56.8, 46.4, 42.6, 42.4, 37.3, 34.4, 31.4, 30.9, 23.0, 20.5, 15.7, 14.9, 14.5, 12.3, 12.1, 1.7, 0.9. CD (diethyl ether), λ_{max} ([θ]): 322 (−904), 295 (−1010), 269 (+12 500) nm. Anal. Calcd for $C_{40}H_{64}Cl_2LiO_2SiY$: C, 62.25; H, 8.36. Found: C, 62.04; H, 8.01.

(*S*)-Me_2SiCp''[(−)-menthylCp]Sm(μ-Cl)$_2$Li(DME) [(*S*)-5a]. A 100 mL flask with a Teflon inlet valve was charged with $SmCl_3$ (2.86 g, 11.1 mmol) and Li_2Me_2SiCp''[(−)-menthyl]Cp (4.0 g, 10.1 mmol). THF (100 mL) was condensed into the reaction flask *in vacuo* at −78 °C. The reaction mixture was stirred for 12 h at 25 °C under argon. The solvent was then removed *in vacuo*, and the resulting yellow-orange, gummy solid was dried under high vacuum for 12 h. 1,2-Dimethoxyethane (DME; 50 mL) was added to the solid, and the yellow solution was stirred at 25 °C for 1 h. The solvent was then removed *in vacuo*, and the resulting yellow, crystalline solid was dried under high vacuum for 2 h. Diethyl ether (50 mL) was next condensed into the reaction flask *in vacuo* at −78 °C. The solids were stirred at 0 °C for 20 min, and the resulting suspension was filtered. The colorless precipitate (LiCl) was extracted once with diethyl ether (25 mL). The clear yellow filtrate was evaporated until a yellow solid appeared. The mixture was then warmed to 25 °C and the solid redissolved. This solution was slowly cooled to −30 °C, and the resulting solid was isolated via cold filtration. Vacuum-drying afforded 4.0 g (60% yield) of (*S*)-Me_2SiCp''[(−)-menthylCp]Sm(μ-Cl)$_2$Li(DME) as yellow prisms. A further 1.9 g (28% yield) of product was recovered from the mother liquor (total yield: 88%) by concentration and cooling to −78 °C. The product was additionally recrystallized from cold (−30 °C) diethyl ether.

^{1}H NMR (THF-d_8): δ 11.75 (s, 1H), 6.70 (s, 1H), 6.10 (d, 1H), 4.40 (s, 1H), 3.40 (s, 4H), 3.25 (s, 6H), 2.78 (t, 1H), 2.56 (m, 1H), 2.50 (s, 3H), 2.30 (t, 1H), 2.10 (d, 1H), 1.94 (d, 1H), 1.90 (m, 1H), 1.60 (s, 3H), 1.4 (d, 3H), 1.0 (d, 3H), 0.70 (s, 3H), 0.6 (d, 3H), 0.09 (s, 3H), 0.00 (s, 3H), −0.58 (s, 3H). CD (THF), λ_{max} ([θ]): 298 (+31 740), 262 (+12 600) nm. Anal. Calcd for $C_{30}H_{50}Cl_2LiO_2SiSm$: C, 51.54; H, 7.21. Found: C, 51.53; H, 7.60.

(*S*)-Me_2SiCp''[(−)-menthylCp]Lu(μ-Cl)$_2$Li(DME) [(*S*)-5b]. This compound was prepared from $LuCl_3$ (3.13 g, 11.1 mmol) and Li_2Me_2SiCp''-[(−)-menthylCp] (4.0 g, 10.1 mmol) in THF (100 mL) using the procedure described for (*R*)-Me_2SiCp''[(−)-menthylCp]Sm(μ-Cl)$_2$Li(DME) above. Crystallization from cold (−78 °C) diethyl ether afforded 3.80 g (52% yield) of (*R*)-Me_2SiCp''[(−)-menthylCp]Lu(μ-Cl)$_2$Li(DME) as large, colorless prisms. An additional 2.70 g (37% yield) was recovered from the mother liquor (total yield: 89%) by concentration and cooling to −78 °C. The product was further recrystallized from cold (−78 °C) DME.

^{1}H NMR (THF-d_8): δ 6.09 (t, 1H), 5.55 (t, 1H), 5.42 (t, 1H), 3.40 (s, 4H), 3.25 (s, 6H), 2.53 (dt, 2H), 1.97 (s, 3H), 1.85 (s, 3H), 1.69 (m, 3H), 1.60 (dq, 2H), 1.41 (m, 2H), 1.21 (m, 4H), 0.91 (m, 3H), 0.85 (d, 3H), 0.77 (d, 3H), 0.68 (d, 3H), 0.63 (s, 3H), 0.60 (s, 3H); ^{13}C NMR (THF-d_8): δ 135.1, 123.9, 122.9, 119.3, 116.9, 116.6, 111.2, 109.8, 109.2, 102.3, 72.7, 58.9, 52.3, 42.8, 41.9, 37.1, 31.3, 27.6, 25.9, 24.8, 23.5, 22.3, 16.2, 15.8, 14.8, 14.6, 12.4, 12.2, 1.2, 0.91. CD (THF), λ_{max} ([θ]): δ 294 (+31 200), 256 (+12 600) nm. Anal. Calcd for $C_{30}H_{50}Cl_2LiLuO_2Si$: C, 49.75; H, 6.91. Found: C, 49.37; H, 6.58.

(*R*)-Me_2SiCp''[(+)-neomenthylCp]Sm(μ-Cl)$_2$Li(DME) [(*R*)-5c]. A 100 mL flask with a Teflon inlet valve was charged with $SmCl_3$ (2.33 g, 9.08 mmol) and Li_2Me_2SiCp''[(+)-neomenthyl]Cp (3.5 g, 8.87 mmol). THF (70 mL) was condensed into the reaction flask *in vacuo* at −78 °C. The reaction mixture was stirred for 24 h at 25 °C under argon, the solvent was then removed *in vacuo*, and the resulting yellow-orange, gummy solid was dried under high vacuum for 12 h. 1,2-Dimethoxyethane (DME; 50 mL) was added to the solid, and the resulting yellow solution was stirred at 0 °C for 1 h. The solvent was then removed *in vacuo*, and the resulting yellow crystalline solid was dried under high vacuum for 6 h. This procedure was repeated with drying under high vacuum for 12 h. Diethyl ether (50 mL) was then condensed into the reaction flask *in vacuo* at −78 °C. The suspension was stirred for 20 min at −30 °C, and the resulting suspension was cold filtered. The colorless precipitate (LiCl) was extracted once with diethyl ether (25 mL). The clear yellow filtrate was concentrated and slowly cooled to −50 °C; the resulting solid was then isolated via cold filtration. Vacuum-drying afforded 1.95 g (31% yield) of (*R*)-Me_2SiCp''[(+)-neomenthylCp]Sm(μ-Cl)$_2$Li(DME) as yellow prisms. A further 1.44 g (23% yield) of product was recovered from the mother liquor (total yield: 54%) by concentration and cooling to −78 °C. The product was additionally recrystallized from cold (−50 °C) diethyl ether.

^{1}H NMR (THF-d_8): δ 11.92 (s, 1H), 6.22 (s, 1H), 5.61 (d, 1H), 4.77 (s, 1H), 3.46 (s, 4H), 3.30 (s, 6H), 2.52 (s, 3H), 2.10 (m, 1H), 1.52 (s, 3H), 1.54 (d, 3H), 0.91 (d, 3H), 0.72 (s, 3H), 0.47 (d, 3H), 0.37 (s, 3H), −0.10 (s, 3H), −0.36 (s, 3H). Anal. Calcd for $C_{30}H_{50}Cl_2LiO_2SiSm$: C, 51.54; H, 7.21. Found: C, 51.76; H, 7.52.

Equilibration of (*R*)- and (*S*)-Me_2SiCp''[(+)-neomenthylCp]Lu(μ-Cl)$_2$Li(ether)$_2$. A 5 mm J. Young NMR tube was charged with approximately 20 mg (0.026 mmol) of [(+)-neomenthylCp]Lu(μ-Cl)$_2$Li(ether)$_2$ and 0.6 mL of THF-d_8. The sample was sealed under nitrogen and placed in an oil bath which was maintained at a constant temperature (±0.2 °C) with a thermostated Haake heater/stirrer. At measured time intervals, the ^{1}H NMR spectrum of the sample was recorded at −25 °C after the equilibration reaction was quenched at −78 °C. Spectra were recorded in this manner after several time intervals to ensure complete equilibration within experimental error. The equilibrium constant for a given temperature was determined from the integrals of the cyclopentadienyl ^{1}H resonances at δ 6.32 (*R*) and 6.15 ppm (*S*) using a long (10 s) pulse delay to avoid saturation. These data were fit to the van't Hoff equation via linear least-squares methods, and ΔH and ΔS for the epimerization process were extracted from the slope and *y*-intercept, respectively, of the resulting plot. Thermal decomposition of the complex was <5% based on the limits of NMR detectability.

Equilibration of (*R*)- and (*S*)-Me_2SiCp''[(−)-menthylCp]Ln(μ-Cl)$_2$Li(ether)$_2$. The procedure for the above (+)-neomenthyl equilibration study was followed, monitoring the (*R*)- and (*S*)-cyclopentadienyl resonances at δ 13.31 and 11.75 ppm for Ln = Sm, δ 6.07 and 6.12 ppm for Ln = Y, and δ 6.00 and 6.09 ppm for Ln = Lu.

Isomerization of (*S*)-Me_2SiCp''[(−)-phenylmenthylCp]Y(μ-Cl)$_2$Li(ether)$_2$. A 5 mm NMR tube with a Teflon valve was charged with 0.0323 g (0.042 mmol) of (*S*)-Me_2SiCp''[(−)-phenylmenthylCp]Y(μ-Cl)$_2$Li(ether)$_2$. Diethyl ether-d_{10} (ca. 0.6 mL) was vacuum-transferred into the tube at −78 °C. The tube was then back-filled with argon and warmed to ambient temperature (22 °C ± 1 °C). An initial (t = 0) ^{1}H NMR spectrum was immediately recorded on the Varian XL-400. The rate of disappearance of starting material was then monitored with time. The mole fraction of the initial (*S*)-epimer (S_0) was determined by the relative areas of the integrals of the well-separated cyclopentadienyl proton resonances at δ 6.20 (*S*) and 6.14 ppm (*R*). The data for this reaction could be fit by a least-squares analysis to eq 1, where S_0 is the initial mole fraction of the (*S*)-isomer and S is the mole fraction at time t. The

$$\ln(S_0/S) = k't \quad (1)$$

first-order rate constant, k', was extracted from the slope of the least-squares-determined curve. After 14 days, the reaction had proceeded to equilibrium (S_{eq} = 0.17). The product was characterized *in situ* spectroscopically.

(*R*)-Me_2SiCp''[(−)-phenylmenthylCp]Y(μ-Cl)$_2$Li(ether)$_2$. ^{1}H NMR (diethyl ether-d_{10}): δ 7.09 (m, 5H), 6.97 (m, 1H), 6.14 (t, 1H), 5.76 (t, 1H), 5.56 (t, 1H), 3.38 (q, 8H), 2.59 (br d, 1H), 2.44 (br t, 1H), 2.08 (s, 3H), 1.91 (s, 3H), 1.86 (s, 3H), 1.85 (s, 3H), 1.64–0.89 (m, 7H), 1.17

(s, 3H), 1.12 (t, 12H), 0.83 (d, 3H), 0.78 (s, 3H), 0.68 (s, 3H), 0.59 (s, 3H). ^{13}C NMR (diethyl ether-d_{10}): δ 153.4, 143.2, 128.4, 127.8, 126.3, 125.3, 124.9, 124.3, 120.7, 117.4, 114.9, 114.2, 111.3, 105.3, 66.3, 56.7, 46.2, 42.7, 42.0, 37.0, 34.7, 31.4, 29.7, 22.5, 22.4, 15.6, 14.7, 14.2, 11.9, 11.7, 1.5, 0.31.

(*R,S*)-Me$_2$SiCp′[(+)-neomenthylCp]NdCH(SiMe$_3$)$_2$[(*R,S*)-6b]. A 50 mL flask was charged with (*R*)-Me$_2$SiCp″[(+)-neomenthylCp]Nd(μ-Cl)$_2$Li(ether)$_2$ (1.56 g, 2.08 mmol) and LiCH(SiMe$_3$)$_2$ (0.403 g, 2.42 mmol). Toluene (40 mL) was condensed into the reaction flask *in vacuo* at −78 °C. After the flask was back-filled with argon, the mixture was placed in a cold bath thermostated at −5 °C. The reaction was allowed to proceed with stirring for 12 h under these conditions and subsequently for 2 h at ambient temperature. The solvent was then removed *in vacuo*, and the resulting green oil was dried under high vacuum for 2 h to remove entrained toluene. Pentane (40 mL) was next condensed into the flask *in vacuo* at −78 °C. Upon warming, the mixture was filtered. A colorless solid was isolated and extracted once with pentane (10 mL). The combined clear, green filtrate was concentrated *in vacuo* to ca. 10 mL and slowly cooled to −78 °C. Cold filtration afforded 0.808 g (57% yield) of (*R,S*)-Me$_2$SiCp″[(+)-neomenthylCp]NdCH(SiMe$_3$)$_2$ as dichroic green plates. An additional 0.203 g (14% yield) of product was isolated from the mother liquor by concentration and cooling to −78 °C (total yield: 71%). The product was subsequently recrystallized from cold (−78 °C) pentane.

^{1}H NMR (toluene-d_8): δ 83.16 (br, 1H), 64.83 (br, 1H), 23.71 (br s, 1H), 21.58 (br s, 1H), 18.50 (br s, 1H), 15.76 (s, 3H), 15.42 (s, 3H), 14.53 (br s, 1H), 13.83 (s, 3H), 13.7–15.9 (br m, 22H), 12.69 (s, 3H), 12.28 (s, 3H), 11.31 (br s, 3H), 7.98 (s, 3H), 4.92 (s, 3H), −2.36 (s, 3H), −4.30 (br s, 9H), −4.46 (br s, 9H), −5.59 (br s, 3H), −10.88 (s, 3H), −11.12 (br s, 9H), −14.43 (br s, 9H), −28.09 (s, 3H), −28.86 (s, 3H). Anal. Calcd for $C_{33}H_{59}NdSi_3$: C, 57.92; H, 8.67. Found: C, 58.00; H, 8.70.

(*R,S*)-Me$_2$SiCp″[(+)-neomenthylCp]SmCH(SiMe$_3$)$_2$[(*R,S*)-6c]. The procedure used for (*R,S*)-Me$_2$SiCp″[(+)-neomenthylCp]NdCH(SiMe$_3$)$_2$ above was followed with (*S*)-Me$_2$SiCp″[(+)-neomenthylCp]Sm(μ-Cl)$_2$Li(ether)$_2$ (1.75 g, 2.31 mol) and LiCH(SiMe$_3$)$_2$ (0.470 g, 2.83 mmol) in toluene (80 mL). Crystallization from cold (−78 °C) pentane afforded 0.46 g (38% yield) of (*R,S*)-Me$_2$SiCp″[(+)-neomenthylCp]SmCH(SiMe$_3$)$_2$ as deep red-orange plates. An additional 0.43 g (36% yield) of product was recovered from the mother liquor by concentration and cooling to −78 °C (total yield: 74%). The product was additionally recrystallized from cold pentane.

^{1}H NMR (toluene-d_8): δ 17.36 (s, 1H), 16.66 (s, 1H), 15.78 (br s, 1H), 15.48 (br s, 1H), 12.97 (s, 1H), 12.27 (s, 1H), 6.29 (d, 1H), 5.39 (s, 1H), 4.83 (br s, 1H), 3.63 (m, 1H), 3.49 (s, 3H), 3.37 (s, 3H), 3.33 (m, 1H), 3.17 (m, 1H), 3.02 (br s, 6H), 2.73 (m, 1H), 2.52 (d, 3H), 2.29 (m, 1H), 2.17 (br s, 1H), 2.00 (d, 3H), 1.91 (m, 1H), 1.73 (s, 3H), 1.62 (d, 3H), 1.61 (d, 3H), 1.56 (m, 1H), 1.31 (m, 1H), 1.26 (m, 1H), 1.14 (m, 1H), 0.95 (d, 3H), 0.88 (t, 1H), 0.73 (s, 3H), 0.36 (s, 3H), 0.30 (m, 1H), −0.67 (s, 3H), −0.85 (br s, 1H), −1.22 (br s, 1H), −1.41 (br s, 1H), −1.64 (m, 1H), −1.63 (s, 9H), −1.86 (br s, 1H), −1.88 (s, 9H), −1.94 (d, 3H), −3.09 (s, 1H), −4.11 (s, 3H), −5.32 (s, 3H), −6.02 (br s, 9H), −7.09 (br s, 9H), −7.62 (s, 3H), −7.63 (s, 3H). Anal. Calcd for $C_{33}H_{59}Si_3Sm$: C, 57.40; H, 8.61. Found: C, 57.75; H, 8.61.

(*R*)-Me$_2$SiCp″[(+)-neomenthylCp]SmCH(SiMe$_3$)$_2$[(*R*)-6c]. A 50 mL flask was charged with (*R*)-Me$_2$SiCp″[(+)-neomenthylCp]Sm(μ-Cl)$_2$Li(ether)$_2$ (0.801 g, 1.06 mmol), and an attached side-arm addition flask was charged with LiCH(SiMe$_3$)$_2$ (0.175 g, 1.06 mmol). Toluene (40 mL) was condensed into the side-arm flask *in vacuo* at −78 °C. After the flask was back-filled with argon, the toluene solution of LiCH(SiMe$_3$)$_2$ was warmed to 25 °C and decanted onto the samarium chloride. The reaction was then allowed to proceed with stirring for 12 h at 25 °C. The solvent was next removed *in vacuo*, and the resulting orange-red oil was dried under high vacuum for 6 h to remove the entrained toluene. The gummy solid was then triturated with pentane (4 × 40 mL), and the mixture was filtered. A colorless solid was isolated which was extracted once with pentane (30 mL). Crystallization from cold (−78 °C) pentane afforded 0.19 g (26% yield) of (*R,S*)-Me$_2$SiCp″[(+)-neomenthylCp]-SmCH(SiMe$_3$)$_2$ as deep red-orange prisms. Concentration and cooling of the filtrate afforded 0.36 g (49% yield) of (*R*)-Me$_2$SiCp″[(+)-neomenthylCp]SmCH(SiMe$_3$)$_2$ as a deep red-orange microcrystalline solid.

^{1}H NMR (benzene-d_6): δ 21.41 (br s, 1H), 16.77 (s, 1H), 15.78 (br s, 1H), 15.48 (br s, 1H), 12.36 (s, 1H), 6.29 (d, 1H), 4.83 (br s, 1H), 3.51 (s, 3H), 3.02 (s, 3H), 2.09 (d, 3H), 1.73 (s, 3H), 0.99 (d, 3H), 0.31 (s, 3H), −1.59 (s, 9H), −1.72 (d, 3H), −4.05 (s, 3H), −7.02 (br s, 9H), −7.76 (s, 3H). CD (heptane), λ_{max} ([θ]): 329 (−5937), 287 (−9258) nm. Anal. Calcd for $C_{33}H_{59}Si_3Sm$: C, 57.40; H, 8.61. Found: C, 57.75; H, 8.93.

(*S*)-Me$_2$SiCp″[(+)-neomenthylCp]SmCH(SiMe$_3$)$_2$[(*S*)-6c]. A 25 mL flask with a Teflon inlet valve was charged with (*S*)-Me$_2$SiCp″[(+)-neomenthylCp]Sm(μ-Cl)$_2$Li(ether)$_2$ (0.464 g, 0.613 mmol) and KCH(SiMe$_3$)$_2$ (0.122 g, 0.613 mmol) in the glovebox. On the vacuum line, toluene (20 mL) was syringed into the flask under an Ar flush, and stirring was initiated. Precipitation of a colorless solid occurred immediately, with a concomitant color change of the solution from yellow-orange to red-orange. The mixture was stirred at ambient temperature for 4 h, and then the solvent was removed *in vacuo*. Pentane (20 mL) was vacuum-transferred into the reaction flask at −78 °C. The flask was back-filled with Ar and then warmed to ambient temperature. The mixture was filtered, and the colorless precipitate was extracted with pentane (5 mL). The orange filtrate was concentrated *in vacuo* to ca. 5 mL. Slow cooling to −78 °C followed by cold (−78 °C) filtration afforded 0.111 g (26% yield) of an approximately 3:1 (*S*):(*R*) mixture of Me$_2$SiCp″[(+)-neomenthylCp]SmCH(SiMe$_3$)$_2$ as red-orange crystals. The filtrate was concentrated *in vacuo* at −78 °C until an orange microcrystalline solid precipitated. Filtration of the solid afforded 0.296 g (70% yield) of (*S*)-Me$_2$SiCp″[(+)-neomenthylCp]SmCH(SiMe$_3$)$_2$.

^{1}H NMR (toluene-d_8): δ 17.38 (s, 1H), 15.50 (br s, 1H), 12.97 (s, 1H), 5.41 (s, 1H), 3.65 (m, 1H), 3.37 (s, 3H), 3.33 (m, 1H), 3.00 (s, 3H), 2.72 (m, 1H), 2.52 (d, 3H), 2.17 (m, 1H), 1.91 (m, 1H), 1.71 (s, 3H), 1.63 (d, 3H), 1.31 (m, 1H), 0.83 (t, 1H), 0.73 (s, 3H), 0.30 (m, 1H), −0.67 (s, 3H), −1.39 (br s, 1H), −1.64 (m, 1H), −1.85 (s, 9H), −1.94 (d, 3H), −6.02 (br s, 9H), −7.61 (s, 3H). CD (heptane), λ_{max} ([θ]): 317 (+4920), 281 (+14 900) nm. Anal. Calcd for $C_{33}H_{59}Si_3Sm$: C, 57.40; H, 8.61. Found: C, 57.62; H, 8.81.

(*R,S*)-Me$_2$SiCp″[(+)-neomenthylCp]YCH(SiMe$_3$)$_2$ [(*R,S*)-6d]. The procedure used for (*R,S*)-Me$_2$SiCp″[(+)-neomenthylCp]NdCH(SiMe$_3$)$_2$ above was employed with (*R*)-Me$_2$SiCp″[(+)-neomenthylCp]Y(μ-Cl)$_2$Li(ether)$_2$ (2.23 g, 3.20 mmol) and LiCH(SiMe$_3$)$_2$ (0.601 g, 3.61 mmol) in toluene (80 mL). Crystallization from cold (−78 °C) pentane yielded 1.21 g (60%) of (*R,S*)-Me$_2$SiCp″[(+)-neomenthylCp]YCH(SiMe$_3$)$_2$ as large colorless prisms. A second crop of 0.51 g (25% yield) was isolated from the filtrate extracts by concentration and cooling to −78 °C (total yield: 85%). The product was further recrystallized from cold pentane.

^{1}H NMR (benzene-d_6): δ 7.11 (t, 1H), 7.03 (t, 1H), 6.07 (t, 1H), 5.87 (t, 1H), 5.71 (t, 1H), 5.70 (t, 1H), 3.32 (m, 1H), 3.08 (br s, 1H), 2.44 (br d, 1H), 2.12–0.73 (m, 17H), 1.97 (s, 3H), 1.94 (s, 6H), 1.92 (s, 6H), 1.90 (s, 3H), 1.89 (s, 3H), 1.74 (s, 3H), 1.72 (s, 3H), 0.99 (d, 3H), 0.97 (d, 6H), 0.92 (d, 3H), 0.82 (d, 3H), 0.81 (s, 3H), 0.80 (s, 3H), 0.70 (s, 3H), 0.69 (s, 3H), 0.68 (d, 3H), 0.27 (s, 18H), 0.05 (s, 9H), 0.03 (s, 9H), −0.55 (d, J_{Y-H} = 2.8 Hz, 1H), −0.56 (d, J_{Y-H} = 2.4 Hz, 1H). Anal. Calcd for $C_{33}H_{59}Si_3Y$: C, 63.01; H, 9.45. Found: C, 62.86; H, 9.51.

(*R,S*)-Me$_2$SiCp″[(+)-neomenthylCp]LuCH(SiMe$_3$)$_2$[(*R,S*)-6e]. The procedure used for (*R,S*)-Me$_2$SiCp″[(+)-neomenthylCp]NdCH(SiMe$_3$)$_2$ above was followed using (*R*)-Me$_2$SiCp″[(+)-neomenthylCp]Lu(μ-Cl)$_2$Li(ether)$_2$ (1.87 g, 2.39 mmol) and LiCH(SiMe$_3$)$_2$ (0.512 g, 3.07 mmol) in toluene (40 mL). Crystallization from cold (−78 °C) pentane afforded 1.004 g (59% yield) of (*R,S*)-Me$_2$SiCp″[(+)-neomenthylCp]-LuCH(SiMe$_3$)$_2$ as large, colorless prisms. An additional 0.341 g (20% yield) of colorless microcrystals was recovered from the mother liquor by concentration and cooling to −78 °C (total yield: 79%). The product was subsequently recrystallized from cold (−78 °C) pentane.

^{1}H NMR (C_6D_6): δ 7.12 (t, 1H), 7.03 (t, 1H), 6.14 (t, 1H), 5.93 (t, 1H), 5.68 (t, 1H), 5.65 (t, 1H), 3.24 (m, 1H), 3.07 (br s, 1H), 2.45 (br d, 1H), 2.09–0.82 (m, 17H), 2.04 (s, 3H), 1.98 (s, 3H), 1.93 (s, 3H), 1.92 (s, 3H), 1.91 (s, 6H), 1.73 (s, 3H), 1.71 (s, 3H), 0.97 (d, 3H), 0.95 (d, 3H), 0.94 (d, 3H), 0.93 (d, 3H), 0.86 (d, 3H), 0.83 (s, 3H), 0.82 (s, 3H), 0.70 (s, 3H), 0.69 (d, 3H), 0.67 (s, 3H), 0.30 (s, 9H), 0.29 (s, 9H), 0.08 (s, 9H), 0.06 (s, 1H), −0.48 (s, 1H). Anal. Calcd for $C_{33}H_{59}LuSi_3$: C, 55.43; H, 8.32. Found: C, 55.85; H, 8.68.

(*R*)-Me$_2$SiCp″[(−)-menthylCp]SmCH(SiMe$_3$)$_2$[(*R*)-6f]. A 50 mL flask was charged with (*R*)-Me$_2$SiCp″[(−)-menthylCp]Sm(μ-Cl)$_2$Li(ether)$_2$ (1.56 g, 2.08 mmol) and LiCH(SiMe$_3$)$_2$ (0.403 g, 2.42 mmol). Toluene (40 mL) was condensed into the reaction flask *in vacuo* at −78 °C. After the flask was back-filled with argon, the mixture was placed in a cold bath thermostated at 0 °C. The reaction was allowed to proceed with stirring for 12 h under these conditions and subsequently for 2 h at 25 °C. The solvent was then removed *in vacuo*, and the resulting orange-red oily solid was dried under high vacuum for 2 h to remove entrained toluene. Pentane (40 mL) was next condensed into the flask *in vacuo* at −78 °C. Upon warming, the mixture was stirred for 20 min. Pentane

was next removed *in vacuo*, and the procedure was repeated. The mixture was then filtered, and a light-yellow solid was isolated (LiCl). This solid was extracted once with pentane (10 mL). The combined clear, orange-red filtrate was concentrated *in vacuo* to ca. 10 mL and slowly cooled to −78 °C. Cold filtration afforded 0.808 g (57% yield) of (*R*)-Me_2SiCp″[(−)-menthylCp]SmCH($SiMe_3$)$_2$ as red needles. An additional 0.203 g (14% yield) of product was isolated from the mother liquor by concentration and cooling to −78 °C (total yield: 71%). The product was subsequently recrystallized from cold (−78 °C) pentane.

^{1}H NMR (toluene-d_8): δ 16.91 (br s, 1H), 16.62 (br s, 1H), 11.12 (br s, 1H), 5.48 (t, 1H), 4.63 (t, 1H), 3.21 (s, 6H), 2.63 (s, 3H), 2.58 (d, 3H), 2.21 (m, 1H), 1.98 (s, 3H), 1.88 (m, 2H), 1.62 (d, 3H), 1.23 (m, 1H), 0.18 (s, 3H), −2.75 (s, 3H), −2.43 (s, 3H), −2.92 (s, 9H), −3.43 (m, 1H), −4.78 (br s, 9H), −7.02 (br s, 3H), −8.73 (d, 1H). CD (heptane), λ_{max} ([θ]): 322 (−9044), 288 (−14 116) nm. Anal. Calcd for $C_{33}H_{59}Si_3Sm$: C, 57.40; H, 8.61. Found: C, 56.87; H, 8.20.

70/30 (*S*)/(*R*)-Me_2SiCp′[(−)-menthylCp]SmCH($SiMe_3$)$_2$[(*S*/*R*)-6f]. The procedure for (*R*)-Me_2SiCp″[(−)-menthylCp]SmCH($SiMe_3$)$_2$ above was followed with a 4/1 mixture of (*S*)/(*R*)-Me_2SiCp″[(−)-menthylCp]Sm(μ-Cl)$_2$Li(ether)$_2$ (1.56 g, 2.08 mmol) and LiCH($SiMe_3$)$_2$ (0.403 g, 2.42 mmol) in toluene (40 mL). The combined clear, orange-red filtrate was concentrated *in vacuo* to dryness, and a 70/30 mixture of (*S*)/(*R*)-Me_2SiCp″[(−)-menthylCp]SmCH($SiMe_3$)$_2$ was obtained as a microcrystalline powder. The product was dried under vacuum for 12 h and used without further purification.

^{1}H NMR (toluene-d_8) ((*S*)-isomer resonances): δ 16.22 (br s, 1H), 14.73 (br s, 1H), 12.27 (br s, 1H), 4.63 (t, 1H), 3.41 (s, 3H), 3.22 (m, 2H), 3.03 (s, 3H), 2.02 (m, 2H), 1.77 (s, 3H), 1.43 (d, 3H), 1.39 (d, 3H), 0.97 (m, 2H), 0.63 (d, 3H), 0.58 (s, 3H), −0.38 (s, 3H), −1.39 (s, 9H), −2.31 (s, 1H), −3.73 (s, 2H), −4.41 (s, 2H), −6.53 (br s, 9H), −7.42 (br s, 3H). CD (heptane), λ_{max} ([θ]): 325 (+9317), 288 (+6739) nm. Anal. Calcd for $C_{33}H_{59}Si_3Sm$: C, 57.40; H, 8.61. Found: C, 56.99; H, 8.06.

(*R*)-Me_2SiCp′[(−)-menthylCp]YCH($SiMe_3$)$_2$[(*R*)-6g]. The procedure described above for (*R*)-Me_2SiCp″[(−)-menthylCp]SmCH($SiMe_3$)$_2$ was followed using (*R*)-Me_2SiCp′[(−)-menthylCp]Y(μ-Cl)$_2$Li(ether)$_2$ (1.10 g, 1.6 mmol) and LiCH($SiMe_3$)$_2$ (0.27 g, 1.6 mmol) in toluene (40 mL). Crystallization from cold (−78 °C) pentane yielded 0.60 g (60%) of (*R*)-Me_2SiCp″[(−)-menthylCp]YCH($SiMe_3$)$_2$ as large colorless needles. A second crop of 0.11 g (11% yield) was recovered from the filtrate by concentration and cooling to −78 °C (total yield: 71%). The product was further recrystallized from cold (−78 °C) pentane.

^{1}H NMR (benzene-d_6): δ 6.95 (t, 1H), 5.88 (t, 1H), 5.65 (t, 1H), 2.61 (dt, 1H), 1.93 (s, 3H), 1.89 (s, 3H), 1.88 (s, 3H), 1.75 (s, 3H), 1.70 (m, 1H), 1.65 (dq, 1H), 1.46 (m, 1H), 1.31 (q, 1H), 1.06 (m, 2H), 0.98 (d, 3H), 0.93 (d, 3H), 0.78 (s, 3H), 0.71 (d, 3H), 0.70 (s, 3H), 0.25 (s, 9H), 0.08 (s, 9H), −0.51 (d, J_{Y-H} = 2.6 Hz, 1H). ^{13}C NMR (benzene-d_6): δ 140.6, 126.3, 126.2, 124.1, 121.9, 118.0, 114.7, 111.8, 115.7, 106.8, 51.8, 42.8, 41.4, 35.6, 33.3, 28.6 (d), 27.3, 25.1, 22.8, 21.8, 15.8, 14.4, 13.7, 12.0, 11.9, 4.8, 3.7, 0.6, 0.3. CD (heptane), λ_{max} ([θ]): 314 (−4935), 279 (−12 582) nm. Anal. Calcd for $C_{33}H_{59}Si_3Y$: C, 63.01; H, 9.45. Found: C, 62.65; H, 9.89.

(*R*)-Me_2SiCp′[(−)-menthylCp]LuCH($SiMe_3$)$_2$ [(*R*)-6h]. The procedure described above for (*R*)-Me_2SiCp″[(−)-menthylCp]SmCH($SiMe_3$)$_2$ was followed using (*R*)-Me_2SiCp″[(−)-menthylCp]Lu(μ-Cl)$_2$Li(ether)$_2$ (2.00 g, 2.55 mmol) and LiCH($SiMe_3$)$_2$ (0.432 g, 2.6 mmol) in toluene (40 mL). Crystallization from cold (−78 °C) pentane yielded 1.10 g (60%) of (*R*)-Me_2SiCp″[(−)-menthylCp]LuCH($SiMe_3$)$_2$ as large colorless prisms. An additional 0.365 g (20% yield) was recovered from the filtrate by concentration and cooling to −78 °C (total yield: 80%). The product was further recrystallized from cold (−78 °C) pentane.

^{1}H NMR (benzene-d_6): δ 6.95 (t, 1H), 5.92 (t, 1H), 5.63 (t, 1H), 2.54 (dt, 1H), 1.98 (s, 3H), 1.91 (s, 3H), 1.88 (s, 3H), 1.71 (s, 3H), 1.65 (m, 4H), 1.4 (m, 1H), 1.31 (q, 1H), 1.06 (m, 2H), 0.98 (d, 3H), 0.93 (d, 3H), 0.81 (s, 3H), 0.72 (d, 3H), 0.70 (s, 3H), 0.31 (s, 9H), 0.11 (s, 9H), −0.45 (s, 1H). ^{13}C NMR (benzene-d_6): δ 139.1, 125.6, 125.5, 123.2, 120.5, 117.4, 115.0, 113.6, 111.0, 106.2, 51.8, 42.1, 41.3, 35.5, 33.3, 27.9, 27.3, 25.1, 22.9, 21.8, 15.8, 14.5, 14.2, 12.2, 11.9, 5.4, 3.2, 0.8, 0.03. CD (heptane), λ_{max} ([θ]): 317 (−6912), 283 (−12 615) nm. Anal. Calcd for $C_{33}H_{59}LuSi_3$: C, 55.43; H, 8.32. Found: C, 54.47; H, 8.00.

(*R*)-Me_2SiCp′[(−)-phenylmenthylCp]YCH($SiMe_3$)$_2$[(*R*)-6i]. A 25 mL flask was equipped with a magnetic stirring bar and a bent addition tube. In the glovebox, the reaction flask was charged with LiCH($SiMe_3$)$_2$ (0.140 g, 0.84 mmol) and the addition tube with (*S*)-Me_2SiCp″[(−)-phenylmenthylCp]Y(μ-Cl)$_2$Li(ether)$_2$ (0.539 g, 0.71 mmol). On the vacuum line, toluene (15 mL) was condensed *in vacuo* into the reaction flask at −78 °C. The mixture was warmed to ambient temperature, and (*S*)-Me_2SiCp″[(−)-phenylmenthylCp]Y(μ-Cl)$_2$Li(ether)$_2$ was added all at once to the stirring solution. A colorless solid (LiCl) immediately precipitated. The mixture was stirred for an additional 2 h. Solvent was then removed *in vacuo*, and the colorless, oily solid was dried under high vacuum for 2 h. Pentane (15 mL) was next vacuum-transferred into the reaction flask at −78 °C. The mixture was filtered upon warming, and the colorless precipitate was extracted once with pentane (5 mL). The combined colorless filtrate was then concentrated *in vacuo* to 5 mL and slowly cooled to −78 °C. A colorless solid precipitated which was isolated by cold (−78 °C) filtration and dried under high vacuum for 2 h. Yield: 0.339 g (67%) of (*R*)-Me_2SiCp″[(−)-phenylmenthylCp]YCH($SiMe_3$)$_2$ as a colorless microcrystalline solid.

^{1}H NMR (benzene-d_6): δ 7.13 (d, 2H), 7.09 (t, 2H), 7.01 (m, 1H), 6.78 (t, 1H), 5.76 (t, 1H), 5.48 (t, 1H), 2.72 (br t, 1H), 1.97 (s, 3H), 1.89 (s, 3H), 1.87 (s, 3H), 1.75 (s, 3H), 1.70–0.76 (m, 8H), 1.22 (s, 3H), 0.87 (s, 3H), 0.85 (d, 3H), 0.84 (s, 3H), 0.67 (s, 3H), 0.24 (s, 9H), 0.12 (s, 9H), −0.47 (d, $^2J_{Y-H}$ = 2.4 Hz, 1H). ^{13}C NMR (benzene-d_6): δ 152.4, 143.2, 129.3, 128.1, 127.1, 125.9, 125.0, 122.2, 117.7, 116.5, 115.2, 114.7, 113.1, 107.2, 55.3, 47.0, 41.5, 41.4, 35.9, 33.1, 30.0, 29.2 (d, $^2J_{Y-H}$ = 45 Hz), 28.2, 23.9, 22.3, 14.6, 14.0, 12.1, 12.0, 4.9, 4.7, 0.9, 0.2. CD (heptane), λ_{max} ([θ]): 358 (+1050), 314 (−1680), 279 (−5490) nm. Anal. Calcd for $C_{39}H_{63}Si_3Y$: C, 66.44; H, 9.01. Found: C, 66.03; H, 8.87.

(*R*)-Me_2SiCp″[(+)-neomenthylCp]LaN($SiMe_3$)$_2$[(*R*)-7a]. A 100 mL reaction flask equipped with a 50 mL side-arm addition flask was charged with (*R*)-Me_2SiCp″[(+)-neomenthylCp]La(μ-Cl)$_2$Li(ether)$_2$ (1.502 g, 2.014 mmol). The side-arm flask was charged with KN($SiMe_3$)$_2$ (0.803 g, 4.03 mmol). Diethyl ether was condensed *in vacuo* into both the reaction flask (40 mL) and the addition flask (20 mL) at −78 °C. Both solutions were warmed to ambient temperature. The solution of amide was slowly added to the stirred suspension of (*R*)-Me_2SiCp″[(+)-neomenthylCp]La(μ-Cl)$_2$Li(ether)$_2$. After addition was complete, the mixture was further stirred at ambient temperature for 12 h. The solvent was then removed *in vacuo*, and the resulting colorless, waxy solid was dried under high vacuum for 1 h. Pentane (50 mL) was condensed into the reaction flask *in vacuo* at −78 °C. Upon warming to ambient temperature, the mixture was filtered. A colorless precipitate was isolated and extracted once with pentane (10 mL). The combined, colorless filtrate was concentrated *in vacuo* until a colorless solid precipitated. The solid was redissolved by warming, and the colorless solution slowly cooled to −78 °C. Cold filtration afforded 0.252 g (18%) of (*R*,*S*)-Me_2SiCp″[(+)-neomenthylCp]LaN($SiMe_3$)$_2$ as large, colorless prisms. The mother liquor was further concentrated *in vacuo* until additional precipitation occurred. The mixture was slowly cooled to −78 °C, and the product was isolated by cold filtration. This procedure afforded 0.777 g (57% yield) of diastereomerically pure (*R*)-Me_2SiCp″[(+)-neomenthylCp]LaN($SiMe_3$)$_2$ as colorless plates. The product was additionally recrystallized from cold (−78 °C) pentane.

^{1}H NMR (benzene-d_6): δ 6.48 (t, 1H), 5.87 (m, 2H), 3.23 (br s, 1H), 2.33 (br d, 1H), 2.08 (s, 3H), 2.07 (s, 3H), 2.06 (m, 1H), 1.96 (s, 3H), 1.93 (s, 3H), 1.79 (br d, 1H), 1.49–1.07 (m, 5H), 1.04 (d, 3H), 0.87 (m, 1H), 0.79 (s, 3H), 0.77 (s, 3H), 0.58 (d, 3H), 0.12 (s, 9H), 0.11 (s, 9H). ^{13}C NMR (benzene-d_6): δ 139.6, 126.4, 126.0, 125.9, 125.6, 120.2, 119.5, 118.7, 118.6, 112.6, 50.0, 42.5, 38.1, 36.6, 29.6, 28.9, 23.7, 23.6, 22.7, 20.2, 14.2, 13.8, 11.9, 11.5, 2.8, 2.5, 0.56, 0.51. CD (heptane), λ_{max} ([θ]): 291 (−6080), 264 (+3230) nm. Anal. Calcd for $C_{32}H_{58}LaNSi_3$: C, 56.52; H, 8.59; N, 2.06. Found: C, 56.66; H, 8.94; N, 1.88.

(*R*)-Me_2SiCp′[(+)-neomenthylCp]SmN($SiMe_3$)$_2$[(*R*)-7b]. A 50 mL flask with a Teflon inlet valve was charged with (*R*)-Me_2SiCp″[(+)-neomenthylCp]Sm(μ-Cl)$_2$Li(DME) (1.25 g, 1.79 mmol) and KN($SiMe_3$)$_2$ (0.357 g, 1.79 mmol). Toluene (60 mL) was added to the reaction flask via syringe under an argon flush. The mixture was then stirred at 25 °C for 18 h, during which time a colorless solid precipitated from the clear, bright orange solution. The solvent was removed *in vacuo*, and the gummy solid was evacuated for 12 h. Pentane (50 mL) was then condensed into the flask *in vacuo* at −78 °C, the mixture was stirred for 1 h at 25 °C, the solvent was removed *in vacuo*, and the resulting gummy solid was dried under high vacuum for 12 h. This procedure was then repeated. Pentane (30 mL) was next condensed into the flask at −78 °C, the mixture was stirred at 25 °C for 20 min and filtered, and the colorless residue was washed once with pentane (10 mL). The combined filtrate was then concentrated to ca. 15 mL, and the solution was slowly cooled to −78 °C. Crystallization afforded 0.35 g (28% yield) of (*R*,*S*)-Me_2SiCp″[(+)-neomenthylCp]SmN($SiMe_3$)$_2$ as bright orange prisms. An additional 0.12 g (10% yield) of (*R*,*S*)-Me_2SiCp″[(+)-neomenthylCp]SmN($SiMe_3$)$_2$ was crystallized from the mother liquor by concentration and cooling to

–78 °C. The combined filtrates were recrystallized from cold (–78 °C) pentane to yield (*R*)-Me_2SiCp''[(+)-neomenthylCp]$SmN(SiMe_3)_2$ (0.58 g, 47%).

^{1}H NMR (benzene-d_6): δ 16.38 (br s, 1H), 10.23 (br d, 1H), 7.81 (br s, 1H), 5.99 (br S, 1H), 3.03 (S, 3H), 2.77 (s, 3H), 2.73 (d, 3H), 2.08 (s, 3H), 1.78 (s, 3H), 1.34 (d, 3H), –0.89 (d, 3H), –3.78 (s, 3H), –5.39 (s, 3H), –6.71 (s, 9H), –6.97 (br s, 9H). Anal. Calcd for $C_{32}H_{58}NSi_3Sm$: C, 55.58; H, 8.45; N, 2.03. Found: C, 55.21; H, 8.53; N, 2.18.

(*S*)-Me_2SiCp''[(+)-neomenthylCp]$SmN(SiMe_3)_2$ [(*S*)-7b]. A 25 mL flask with a Teflon inlet valve was charged with (*S*)-Me_2SiCp''[(+)-neomenthylCp]$Sm(\mu\text{-}Cl)_2Li(ether)_2$ (0.242 g, 0.320 mmol) and $NaN(SiMe_3)_2$ (0.059 g, 0.322 mmol). Toluene (20 mL) was added via syringe to the reaction flask under an argon flush. The mixture was then stirred at ambient temperature for 2 h, during which time a colorless precipitate separated from the clear, bright orange solution. The solvent was removed *in vacuo*. Pentane (20 mL) was condensed *in vacuo* into the flask at –78 °C. The mixture was warmed to room temperature and filtered. The colorless precipitate was extracted once with pentane (10 mL). The combined filtrate was next concentrated *in vacuo* to ca. 3 mL, and the solution was slowly cooled to –78 °C. Cold (–78 °C) filtration afforded 0.155 g (70% yield) of (*S*)-Me_2SiCp''[(+)-neomenthylCp]$SmN(SiMe_3)_2$ as bright orange prisms. The product was recrystallized from cold (–78 °C) pentane.

^{1}H NMR (toluene-d_8): δ 16.44 (br s, 1H), 5.60 (br s, 1H), 6.12 (br s, 1H), 4.82 (br s, 1H), 4.07 (d, 3H), 3.13 (m, 1H), 2.67 (m, 2H), 3.03 (s, 3H), 2.67 (m, 2H), 2.37 (br s, 3H), 2.13 (s, 3H), 2.09 (s, 3H), 2.00 (d, 3H), 1.73 (d, 1H), 1.25 (m, 1H), 0.88 (m, 1H), 0.10 (br s, 1H), –0.04 (br s, 1H), –0.95 (d, 3H), –3.62 (s, 3H), –3.97 (br s, 1H), –5.67 (s, 3H), –6.12 (s, 9H), –7.25 (br s, 9H). CD (heptane), λ_{max} ([θ]): 331 (+6740), 286 (+16 500) nm. Anal. Calcd for $C_{32}H_{58}NSi_3Sm$: C, 55.58; H, 8.45; N, 2.03. Found: C, 55.74; H, 8.33; N, 2.08.

(*R*)-Me_2SiCp''[(+)-neomenthylCp]$YN(SiMe_3)_2$ [(*R*)-7c]. A 50 mL flask with a Teflon inlet valve was charged with (*R*)-Me_2SiCp''[(+)-neomenthylCp]$Y(\mu\text{-}Cl)_2Li(ether)_2$ (1.033 g, 1.485 mmol) and $NaN(SiMe_3)_2$ (0.388 g, 2.116 mmol). Toluene (40 mL) was added via syringe to the reaction flask under an argon flush. The mixture was then stirred at ambient temperature for 4 h during which time a colorless precipitate formed. The solvent was then removed *in vacuo*, and pentane (40 mL) was vacuum-transferred onto the resulting colorless oil at –78 °C. Upon warming to room temperature, the mixture was filtered, and the colorless precipitate was extracted once with pentane (10 mL). The combined colorless extracts were concentrated *in vacuo* until precipitation of a colorless solid occurred. The concentrate was warmed to redissolve the precipitate and then slowly cooled to –78 °C. Cold (–78 °C) filtration afforded 0.190 g (20% yield) of (*R,S*)-Me_2SiCp''[(+)-neomenthylCp]-$YN(SiMe_3)_2$ as colorless plates. An additional crop of 0.054 g (6% yield) of the (*R,S*) compound was obtained by repetition of this procedure with the mother liquor (total yield: 26%). The filtrate was evaporated to give a pale yellow solid which was dissolved in the minimum amount of pentane. Slow evaporation of this solution gave 0.664 g (71% yield) of (*R*)-Me_2-$SiCp''$[(+)-neomenthylCp]$YN(SiMe_3)_2$ as a pale yellow microcrystalline solid. The product was recrystallized from cold (–78 °C) pentane.

^{1}H NMR (benzene-d_6): δ 6.62 (t, 1H), 5.84 (m, 2H), 3.23 (br s, 1H), 2.53 (br d, 1H), 2.20–2.11 (m, 2H), 2.03 (s, 3H), 2.01 (s, 3H), 1.91 (s, 3H), 1.88 (s, 3H), 1.72 (m, 2H), 1.48–1.26 (m, 2H), 1.06 (d, 3H), 1.03 (d, 3H), 0.89 (m, 2H), 0.80 (s, 3H), 0.78 (s, 3H), 0.72 (d, 3H), 0.13 (s, 9H), 0.11 (s, 9H). ^{13}C NMR (benzene-d_6): δ 137.6, 127.3, 126.8, 126.0, 122.0, 121.7, 120.1, 119.4, 113.8, 113.0, 51.3, 41.0, 37.0, 36.8, 29.4, 28.7, 24.1, 23.3, 22.6, 21.0, 14.7, 14.0, 12.5, 11.9, 3.7, 3.3, 0.37, 0.26. CD (heptane), λ_{max} ([θ]): 349 (–1280), 289 (–2520) nm. Anal. Calcd for $C_{32}H_{58}NSi_3Y$: C, 61.01; H, 9.28; N, 2.22. Found: C, 60.52; H, 8.98; N, 1.78.

(*R*)-Me_2SiCp''[(+)-neomenthylCp]$LuN(SiMe_3)_2$ [(*R*)-7d]. The procedure used for (*R*)-Me_2SiCp''[(+)-neomenthylCp]$YN(SiMe_3)_2$ above was employed with (*R*)-Me_2SiCp''[(+)-neomenthylCp]$Lu(\mu\text{-}Cl)_2Li(ether)_2$ (1.055 g, 1.350 mmol) and $NaN(SiMe_3)_2$ (0.314 g, 1.712 mmol) in toluene (40 mL). A combined 0.418 g (43% yield) of (*R,S*)-Me_2-$SiCp''$[(+)-neomenthylCp]$LuN(SiMe_3)_2$ was obtained as large, colorless plates after two crystallizations. The remaining filtrate was evaporated, yielding a pale yellow powder which was recrystallized from cold (–78 °C) pentane. (*R*)-Me_2SiCp''[(+)-neomenthylCp]$LuN(SiMe_3)_2$, 0.532 g (55% yield), was obtained as a colorless microcrystalline solid.

^{1}H NMR (benzene-d_6): δ 6.69 (t, 1H), 5.82 (t, 1H), 5.80 (t, 1H), 3.21 (br s, 1H), 2.62 (br d, 1H), 2.12 (m, 1H), 2.08 (s, 3H), 1.98 (s, 3H), 1.94 (s, 3H), 1.88 (s, 3H), 1.80–1.68 (m, 2H), 1.50–1.26 (m, 2H), 1.05 (d, 3H), 1.03 (d, 3H), 0.87 (m, 3H), 0.80 (s, 3H), 0.79 (s, 3H), 0.78 (d, 3H), 0.17 (s, 9H), 0.12 (s, 9H). ^{13}C NMR (benzene-d_6): δ 136.1, 127.0, 125.3, 120.4, 120.3, 120.1, 120.0, 113.4, 112.0, 111.7, 51.7, 40.7, 36.7, 36.4, 28.4, 25.1, 24.4, 23.2, 22.5, 21.5, 14.9, 13.9, 12.6, 12.0, 5.9, 4.5, 3.2. CD (heptane), λ_{max} ([θ]): 353 (–964), 289 (–1730) nm. Anal. Calcd for $C_{32}H_{58}LuNSi_3$: C, 53.68; H, 8.16; N, 1.96. Found: C, 53.36; H, 7.99; N, 1.71.

(*S*)-Me_2SiCp''[(–)-menthylCp]$SmN(SiMe_3)_2$ [(*S*)-7e]. A 50 mL flask with a Teflon inlet valve was charged with (*S*)-Me_2SiCp''[(–)-menthylCp]-$Sm(\mu\text{-}Cl)_2Li(DME)$ (0.781 g, 1.0 mmol) and $KN(SiMe_3)_2$ (0.200 g, 1.01 mmol). Toluene (30 mL) was added to the reaction flask via syringe under an argon flush. The mixture was then stirred at 25 °C for 12 h, during which time a colorless solid precipitated from the clear, bright orange solution. The solvent was removed *in vacuo*, and the gummy solid was evacuated for 12 h. Pentane (20 mL) was next condensed into the flask *in vacuo* at –78 °C, and the mixture was stirred at 25 °C for 12 h, during which time a colorless solid precipitated from the clear, orange solution. The solvent was removed *in vacuo*, and the resulting gummy solid was dried for 12 h. Pentane (20 mL) was next condensed into the flask at –78 °C, the mixture was stirred at 25 °C for 20 min, and the solvent was removed *in vacuo*. The dissolution/evaporation procedure was repeated twice, after which the mixture was dissolved in 20 mL pentane and filtered, and the colorless filtration residue was washed once with pentane (10 mL). The combined filtrate was then concentrated *in vacuo* to ca. 5 mL, and the solution was slowly cooled to –78 °C. Crystallization afforded 0.49 g (70% yield) of (*S*)-Me_2SiCp''[(–)-menthylCp]$SmN(SiMe_3)_2$ as bright orange prisms. An additional 0.115 g (17% yield) of smaller orange prisms was crystallized from the mother liquor by further concentration and cooling to –78 °C (total yield: 87%). The product was recrystallized from cold (–78 °C) pentane.

^{1}H NMR (benzene-d_6): δ 14.15 (br s, 1H), 11.03 (br s, 1H), 6.60 (br s, 1H), 4.37 (m, 1H), 3.75 (m, 1H), 2.73 (d, 3H), 2.55 (s, 6H), 2.51 (m, 1H), 2.45–2.15 (m, 4H), 2.25 (s, 3H), 2.10 (s, 3H), 1.53 (d, 3H), 1.28 (q, 1H), 0.95 (m, 1H), 0.13 (d, 3H), –4.45 (s, 3H), –4.65 (s, 3H), –6.82 (s, 9H), –7.05 (s, 9H). CD (heptane), λ_{max} ([θ]): 330 (+6385), 291 (+8010) nm. Anal. Calcd for $C_{32}H_{58}NSi_3Sm$: C, 55.58; H, 8.45; N, 2.03. Found: C, 55.46; H, 8.23; N, 1.70.

(*R*)-Me_2SiCp''[(–)-menthylCp]$SmN(SiMe_3)_2$ [(*R*)-7e]. A 50 mL flask with a Teflon inlet valve was charged with (*R*)-Me_2SiCp''[(–)-menthylCp]-$Sm(\mu\text{-}Cl)_2Li(ether)_2$ (0.755 g, 1.0 mmol) and $KN(SiMe_3)_2$ (0.20 g, 1.01 mmol). Toluene (30 mL) was syringed into the flask under argon flush. The mixture was stirred for 12 h at ambient temperature, at which time a colorless solid precipitated from the clear, bright orange solution. The solvent was next removed *in vacuo*, and the gummy solid was vacuum-dried for 12 h. Pentane (20 mL) was then condensed onto the solids *in vacuo*, and the solution was warmed to ambient temperature and stirred for 20 min. The solvent was removed *in vacuo*, and the procedure was repeated to remove any entrained toluene. The solution was filtered to remove LiCl, and the filtrate was concentrated *in vacuo*. Slow cooling to –78 °C and cold filtration afforded 0.485 g (70% yield) of (*R*)-Me_2-$SiCp''$[(–)-menthylCp]$SmN(SiMe_3)_2$ as bright orange prisms. An additional 0.115 g (17% yield) of product was recovered from the filtrate was concentration and slow cooling to –78 °C. Total yield: 87%. The product was subsequently recrystallized from cold (–78 °C) pentane.

^{1}H NMR (benzene-d_6): δ 15.22 (br s, 1H), 8.59 (br s, 1H), 7.82 (br s, 1H), 5.21 (br s, 1H), 2.82 (s, 3H), 2.80 (d, 3H), 2.78 (m, 2H), 2.68 (m, 1H), 2.55 (s, 3H), 2.45 (s, 3H), 2.29 (m, 2H), 2.09 (s, 3H), 1.91 (d, 3H), 1.72 (d, 3H), 0.51 (dq, 1H), –0.78 (d, 3H), –2.73 (m, 1H), –3.01 (m, 1H), –4.38 (s, 3H), –5.37 (s, 3H), –5.78 (br s, 9H), –6.51 (br s, 9H). CD (heptane), λ_{max} ([θ]): 332 (–6397), 291 (–8008) nm. Anal. Calcd for $C_{32}H_{58}NSi_3Sm$: C, 55.58; H, 8.45; N, 2.03. Found: C, 55.91; H, 8.35; N, 2.11.

(*R*)-Me_2SiCp''[(–)-menthylCp]$YN(SiMe_3)_2$ [(*R*)-7f]. The procedure described above for (*R*)-Me_2SiCp''[(–)-menthylCp]$SmN(SiMe_3)_2$ was employed using (*R*)-Me_2SiCp''[(–)-menthylCp]$Y(\mu\text{-}Cl)_2Li(ether)_2$ (0.696 g, 1.0 mmol) and $KN(SiMe_3)_2$ (0.20 g, 1.01 mmol) in toluene (30 mL). Total yield: 80% of (*R*)-Me_2SiCp''[(–)-menthylCp]$YN(SiMe_3)_2$ as colorless plates. The product was recrystallized from cold (–78 °C) pentane.

^{1}H NMR (toluene-d_8): δ 6.51 (t, 1H), 5.78 (d, 2H), 2.60 (dt, 1H), 2.06 (s, 3H), 1.90 (s, 3H), 1.88 (s, 3H), 1.86 (s, 3H), 1.71 (d, 1H), 1.61 (m, 1H), 1.59 (m, 1H), 1.45 (m, 1H), 1.28 (q, 1H), 1.03 (m, 1H), 0.99 (d, 3H), 0.92 (m, 2H), 0.88 (d, 3H), 0.78 (s, 3H), 0.73 (d, 3H), 0.71 (d, 3H), 0.12 (s, 9H), 0.10 (s, 9H). ^{13}C NMR (toluene-d_8): δ 140.6, 127.3, 126.7, 126.4, 126.3, 118.0, 115.8, 114.7, 111.8, 106.2, 51.8, 42.8, 41.4, 35.6, 33.4, 28.8, 27.3, 25.1, 22.8, 21.8, 15.8, 14.4, 13.7, 12.1, 12.0, 4.9, 3.7, 0.6, 0.3. CD (heptane), λ_{max} ([θ]): 353 (–5960), 292 (–7779) nm.

Anal. Calcd for $C_{32}H_{58}NSi_3Y$: C, 61.01; H, 9.28; N, 2.22. Found: C, 60.92; H, 9.13; N, 2.02.

(*R*)-Me$_2$SiCp″[(–)-menthylCp]LuN(SiMe$_3$)$_2$[(*R*)-7g]. The procedure described above for (*R*)-Me$_2$SiCp″[(–)-menthylCp]SmN(SiMe$_3$)$_2$ was employed using (*R*)-Me$_2$SiCp″[(–)-menthylCp]Lu(μ-Cl)$_2$Li(ether)$_2$ (0.781 g, 1.0 mmol) and KN(SiMe$_3$)$_2$ (0.20 g, 1.01 mmol) in toluene (30 mL). Total yield: 75% of (*R*)-Me$_2$SiCp″[(–)-menthylCp]LuN(SiMe$_3$)$_2$ as colorless plates. The product was recrystallized from cold (–78 °C) pentane.

^{1}H NMR (benzene-d_6): δ 6.51 (t, 1H), 5.80 (t, 1H), 5.72 (t, 1H), 2.55 (dt, 1H), 2.16 (s, 3H), 1.91 (s, 3H), 1.89 (s, 3H), 1.83 (s, 3H), 1.70 (m, 1H), 1.62 (m, 2H), 1.48 (m, 2H), 1.42 (q, 1H), 0.99 (d, 3H), 0.91 (m, 3H), 0.87 (d, 3H), 0.79 (d, 3H), 0.64 (s, 3H), 0.60 (s, 3H), 0.16 (s, 9H), 0.11 (s, 9H). ^{13}C NMR (benzene-d_6): δ 138.6, 127.5, 127.0, 125.5, 116.7, 113.6, 112.6, 112.3, 111.7, 109.1, 51.8, 42.1, 35.6, 33.4, 33.3, 27.3, 27.1, 25.4, 22.9, 22.0, 21.8, 16.0, 14.3, 14.2, 12.9, 12.1, 4.8, 3.8, 0.8. CD (heptane), λ_{max} ([θ]): 353 (–4960), 292 (–7240), 267 (+10 576) nm. Anal. Calcd for $C_{32}H_{58}LuNSi_3$: C, 53.68; H, 8.16; N, 1.96. Found: C, 53.20; H, 8.02; N, 1.62.

(*S*)-Me$_2$SiCp″[(–)-menthylCp]LuN(SiMe$_3$)$_2$[(*S*)-7g]. The procedure described above for (*S*)-Me$_2$SiCp″[(–)-menthylCp]SmN(SiMe$_3$)$_2$ was employed using (*S*)-Me$_2$SiCp″[(–)-menthylCp]Lu(μ-Cl)$_2$Li(DME) (0.781 g, 1.0 mmol) and KN(SiMe$_3$)$_2$ (0.20 g, 1.01 mmol) in toluene (30 mL). Total yield: 75% of (*S*)-Me$_2$SiCp″[(–)-menthylCp]LuN(SiMe$_3$)$_2$ as colorless plates. The product was recrystallized from cold (–78 °C) pentane.

^{1}H NMR (benzene-d_6): δ 6.62 (t, 1H), 5.85 (t, 1H), 5.80 (t, 1H), 2.63 (dt, 1H), 2.13 (s, 3H), 1.91 (s, 3H), 1.89 (s, 3H), 1.78 (s, 3H), 1.73 (m, 1H), 1.62 (m, 1H), 1.48 (m, 1H), 1.31 (q, 1H), 1.00 (d, 3H), 0.95 (m, 1H), 0.90 (d, 3H), 0.81 (s, 3H), 0.75 (d, 3H), 0.71 (d, 3H), 0.16 (s, 9H), 0.11 (s, 9H). ^{13}C NMR (benzene-d_6): δ 140.6, 127.3, 126.7, 126.4, 126.3, 118.0, 115.8, 114.7, 111.8, 106.2, 51.8, 42.8, 41.4, 35.6, 33.4, 28.8, 27.3, 25.1, 22.8, 21.8, 15.8, 14.4, 13.7, 12.1, 12.0, 4.9, 3.7, 0.6, 0.3. CD (heptane), λ_{max} ([θ]): 353 (+5030), 291 (+7250), 267 (–10 400). Anal. Calcd for $C_{32}H_{58}LuNSi_3$: C, 53.68; H, 8.16; N, 1.96. Found: C, 53.38; H, 8.29; N, 1.67.

(*R,S*)-Me$_2$SiCp″[(–)-phenylmenthylCp]YN(SiMe$_3$)$_2$[(*R,S*)-7h]. A 50 mL flask was charged with (*S*)-Me$_2$SiCp″[(–)-phenylmenthylCp]Y(μ-Cl)$_2$Li(ether)$_2$ (1.04 g, 1.35 mmol) and NaN(SiMe$_3$)$_2$ (0.25 g, 1.36 mmol). Diethyl ether (40 mL) was condensed into the reaction flask at –78 °C *in vacuo*. The mixture was warmed to ambient temperature with stirring under argon. Precipitation of a fine, colorless solid (LiCl, NaCl) occurred upon warming. After 2 h at ambient temperature, the solvent was removed from the cloudy, pale yellow mixture *in vacuo*. The remaining colorless solid was dried under high vacuum for 2 h. Pentane (40 mL) was next vacuum-transferred into the flask at –78 °C. After warming to ambient temperature, the mixture was filtered, and the colorless precipitate was extracted once with pentane (5 mL). The clear, pale yellow filtrate was concentrated *in vacuo* until a colorless solid precipitated. The concentrate was warmed to ambient temperature, and the precipitate was redissolved. Slow cooling of the solution to –78 °C followed by cold filtration afforded 0.753 g (79% yield) of an approximately 60(*R*):40(*S*) mixture of Me$_2$SiCp″[(–)-phenylmenthylCp]YN(SiMe$_3$)$_2$ isomers as a pale-yellow powder.

^{1}H NMR (benzene-d_6): δ 7.18–6.96 (m, 10H), 6.43 (t, 1H), 6.32 (t, 1H), 5.62 (t, 1H), 5.57 (t, 1H), 5.54 (t, 1H), 5.36 (t, 1H), 2.68 (td, 1H), 2.47 (td, 1H), 2.39 (d, 1H), 2.07 (s, 3H), 1.98 (s, 3H), 1.93 (s, 3H), 1.88 (s, 3H), 1.88 (s, 3H), 1.87 (s, 3H), 1.86 (s, 3H), 1.18 (s, 3H), 1.14 (s, 3H), 1.11 (d, 3H), 1.10 (d, 3H), 0.93 (s, 3H), 0.92 (s, 3H), 0.79 (s, 3H), 0.76 (s, 3H), 0.72 (s, 3H), 0.15 (s, 9H), 0.11 (s, 9H), 0.09 (s, 9H), 0.08 (s, 9H). Anal. Calcd for $C_{38}H_{62}NSi_3Y$: C, 64.64; H, 8.85; N, 1.98. Found: C, 64.49; H, 8.48; N, 2.12.

(*R*)-Me$_2$SiCp″[(+)-neomenthylCp]Lu(2-C$_6$H$_4$CH$_2$NMe$_2$) [(*R*)-8]. A 25 mL flask with a Teflon inlet valve was charged with (*R*)-Me$_2$SiCp″-[(+)-neomenthylCp]Lu(μ-Cl)$_2$Li(ether)$_2$ (0.512 g, 0.653 mmol) and Li(2-C$_6$H$_4$CH$_2$NMe$_2$) (0.091 g, 0.645 mmol). Toluene (20 mL) was added via syringe under an argon flush to the reaction flask. Stirring of the mixture was initiated, and a colorless solid (LiCl) precipitated immediately. After 4 h, the solvent was removed *in vacuo*, affording a colorless oil. Pentane (20 mL) was vacuum-transferred into the reaction flask at –78 °C *in vacuo*. The mixture was then filtered upon warming to ambient temperature, and the resulting colorless precipitate was extracted once with pentane (5 mL). The colorless filtrate was concentrated *in vacuo* to ca. 5 mL and slowly cooled to –78 °C. Cold filtration yielded 0.378 g (85% yield) of (*R*)-Me$_2$SiCp″[(+)-neomenthylCp]Lu(2-C$_6$H$_4$CH$_2$NMe$_2$) as a colorless, microcrystalline solid. The product was recrystallized as colorless needles from cold (–78 °C) pentane.

^{1}H NMR (benzene-d_6): δ 7.68 (dd, 1H), 7.27 (t, 1H), 7.13 (td, 1H), 6.87 (d, 1H), 6.14 (t, 1H), 5.77 (t, 1H), 5.66 (t, 1H), 3.49 (d, 1H), 3.38 (br s, 1H), 2.88 (d, 1H), 2.09 (s, 3H), 1.97 (s, 3H), 1.93 (s, 3H), 1.78 (m, 2H), 1.70 (s, 3H), 1.67 (s, 3H), 1.56 (s, 3H), 1.55 (m, 2H), 1.34 (br d, 1H), 1.29–1.11 (m, 3H), 1.07 (d, 3H), 0.88 (s, 3H), 0.87 (s, 3H), 0.86 (m, 1H), 0.64 (d, 3H), 0.62 (d, 3H). ^{13}C NMR (benzene-d_6): δ 191.9, 151.3, 143.1, 140.0, 138.0, 122.5, 120.5, 119.3, 117.1, 115.2, 110.4, 109.7, 103.0, 66.9, 50.3, 50.0, 45.9, 40.4, 38.3, 36.1, 29.6, 28.7, 24.2, 23.1, 22.8, 20.4, 14.0, 13.7, 13.1, 11.6, 0.97, 0.33. CD (heptane), λ_{max} ([θ]): 316 (–7110), 276 (–24 700) nm. Anal. Calcd for $C_{35}H_{52}LuNSi$: C, 60.94; H, 7.60; N, 2.03. Found: C, 60.72; H, 7.43; N, 1.98.

(*R*)-Me$_2$SiCp″[(+)-neomenthylCp]Lu(CH$_2$)$_2$P(CH$_3$)$_2$[(*R*)-9]. A 50-mL flask with a Teflon inlet valve was charged with (*R*)-Me$_2$SiCp″-[(+)-neomenthylCp]Lu(μ-Cl)$_2$Li(ether)$_2$ (0.503 g, 0.643 mmol) and Li(CH$_2$)$_2$P(CH$_3$)$_2$ (0.064 g, 0.660 mmol). Diethyl ether (40 mL) was syringed into the reaction flask under argon flush. The colorless suspension was stirred at ambient temperature for 12 h. The solvent was then removed *in vacuo*, and the colorless solid residue was dried under high vacuum for 2 h. Pentane (30 mL) was condensed into the reaction flask *in vacuo* at –78 °C. The mixture was then warmed to room temperature and filtered. The colorless precipitate (LiCl) was extracted once with pentane (5 mL). The combined colorless filtrate was concentrated *in vacuo* to ca. 10 mL and then slowly cooled to –78 °C. A colorless microcrystalline solid was isolated by cold filtration. The precipitate consisted of 0.139 g (34% yield) of an approximately equimolar amounts of (*R*)- and (*S*)-Me$_2$SiCp″[(+)-neomenthylCp]Lu(CH$_2$)$_2$P(CH$_3$)$_2$. Solvent was removed *in vacuo* from the filtrate, affording a colorless microcrystalline solid consisting of the diastereomerically pure (*R*)-isomer. Recrystallization of the crude product from cold (–78 °C) pentane yielded 0.253 g (61% yield) of (*R*)-Me$_2$SiCp″[(+)-neomenthylCp]Lu(CH$_2$)$_2$P(CH$_3$)$_2$ as colorless microcrystals.

^{1}H NMR (benzene-d_6): δ 6.30 (t, 1H), 6.19 (t, 1H), 5.73 (t, 1H), 3.25 (br s, 1H), 2.33 (s, 3H), 2.16 (br d, 1H), 2.08 (m, 1H), 1.96 (s, 3H), 1.94 (s, 3H), 1.92 (s, 3H), 1.84 (br d, 1H), 1.63–1.25 (m, 6H), 1.04 (d, 3H), 1.02 (d, $^2J_{P-H}$ = 12 Hz, 3H), 0.96 (d, 3H), 0.93 (s, 3H), 0.90 (d, $^2J_{P-H}$ = 12 Hz, 3H), 0.76 (s, 3H), 0.74 (d, 3H), 0.17 (td, 1H), –0.11 (dd, 1H), –0.13 (br d, 1H), –0.32 (br t, 1H). ^{13}C NMR (benzene-d_6): δ 135.5, 123.6, 121.1, 119.7, 118.8, 115.9, 112.6, 112.0, 111.5, 103.0, 49.5, 42.1, 38.0, 35.9, 29.6, 29.0, 24.4, 23.4, 22.8, 20.8 (d, J_{P-C} = 30 Hz), 19.7 (d, J_{P-C} = 27 Hz), 16.9 (d, J_{P-C} = 50 Hz), 14.5 (d, J_{P-C} = 43 Hz), 14.4, 12.0, 11.9, 1.8, –0.17. ^{31}P NMR (benzene-d_6): δ 1.69 (m, $^2J_{P-H}$ = 12.3 Hz). CD (heptane), λ_{max} ([θ]): 314 (–4570), 252 (+40 200) nm. Anal. Calcd for $C_{30}H_{50}LuPSi$: C, 55.88; H, 7.82. Found: C, 55.87; H, 7.84.

Reaction of (*R,S*)-Me$_2$SiCp″[(+)-neomenthylCp]YCH(SiMe$_3$)$_2$ with H$_2$. A 5 mm J. Young NMR tube was charged with 10 mg of Me$_2$SiCp″[(+)-neomenthylCp]YCH(SiMe$_3$)$_2$ in the glovebox. On the vacuum line, benzene-d_6 (0.6 mL) was condensed *in vacuo* into the tube at –78 °C, and the tube was then back-filled with hydrogen or deuterium. The sample was warmed to ambient temperature and shaken to dissolve the solids. The ^{1}H and ^{2}H NMR spectra were then recorded at ambient temperature. The only assignable peaks in the NMR spectra were of the Y hydride/deuteride and CH$_2$(TMS)$_2$ or CHD(TMS)$_2$.

^{1}H NMR (benzene-d_6): δ 4.28 (t, 2H, $^1J_{Y-H}$ = 32 Hz), 0.7 (s, 18H), –0.05 (s, 2H). ^{2}H NMR (benzene-d_6): δ 4.3 (br s, ~2D), –0.045 (br s, ~1D).

Epimerization of Me$_2$SiCp″[(–)-phenylmenthylCp]Y(NHPr)(NH$_2$Pr). A 5 mm J. Young NMR tube was charged with 10 mg (0.014 mmol) of (*R,S*)-Me$_2$SiCp″[(–)-phenylmenthylCp]YN(SiMe$_3$)$_2$ in the glovebox. On the vacuum line, toluene (0.6 mL) and *n*-propylamine (40–50 equiv) were condensed *in vacuo* into the tube at –78 °C, and the tube was then back-filled with argon. The sample was immediately inserted into the thermostated probe (25 °C ± 0.4 °C) of the Varian XL-400, and an initial spectrum was recorded. Protonolysis of the Ln–N bond of **7h** was complete within minutes at room temperature, and the only solution species which was observed could be assigned to an (*R,S*)-Me$_2$SiCp″-[(–)-phenylmenthylCp]Y(NHPr)–(NH$_2$Pr) mixture. The time evolution of the integrals of the cyclopentadienyl protons at δ 6.39 ppm(*S*) and 5.40 ppm (*R*) were monitored at 25 °C; the relative concentrations of the (*R*)- and (*S*)-epimers were determined from the relative areas of the integrals. The sample was then allowed to relax to equilibrium, and after 24 h a final spectrum was recorded. The data were fit by linear least-squares analysis to the rate expression for the approach to equilibrium, eq 2. The

$$\ln[(S_e - S_0)/(S_e - S)] = (k + k')t \qquad (2)$$

Scheme 1. Synthesis of Chiral Ancillary Ligands

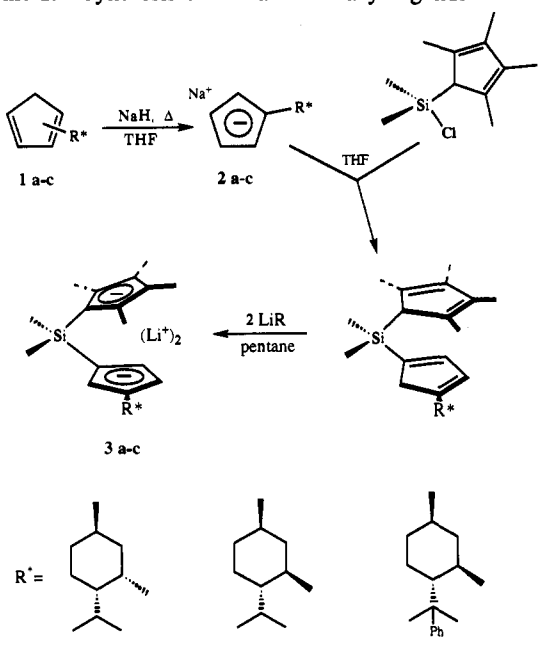

plot of $\ln[(S_e - S_0)/(S_e - S)]$, where S and S_e are the mole fractions of S at time, t, and at equilibrium, respectively, versus time, afforded $(k + k')$ from the line slope.[33] The forward (k) and reverse (k') constants for the epimerization could be determined from the slope of the line and the equilibrium expression, $K = k/k'$.

Results

We begin with a discussion of the synthesis of chiral ancillary ligands and the subsequent preparation of the organolanthanide chloro complexes. The absolute configuration of a representative chloro complex is established by single crystal X-ray diffraction. The solution chiroptical properties of the chloro complexes are then discussed in relation to their relative configurations. The configurational stability and selective epimerization of the chloro complexes in donor solvents is next presented, followed by the course and stereoselectivity of alkylation and amidation reactions. The absolute configurations of the resulting hydrocarbyl and amido complexes follow from solution chiroptical properties and single crystal X-ray diffraction. Finally, the reactivity of the chiral hydrocarbyl and amido complexes is discussed as a prelude to the catalytic chemistry.[20] It will be seen that establishment of the absolute configuration of these complexes by CD spectroscopy used in tandem with X-ray diffraction studies is essential to understanding diastereoselectivity and absolute configuration in the initial complexation reaction as well as in subsequent alkylation and amidation reactions. Importantly, selective epimerization of the chloro complexes allows enrichment in either antipode, with diastereomerically pure complexes usually obtained after a single recrystallization. The configurational stability and structural features of the hydrocarbyl and amide precatalysts under catalytic conditions provide additional understanding of observed catalytic[20] behavior.

Ligand Synthesis. A general, large-scale synthesis of the $Me_2Si(Cp''H)(R^*CpH)$ ancillary ligands and the corresponding dilithium derivatives is outlined in Scheme 1. This procedure permits convenient variation of the chiral auxiliary (R*) for probing structure/reactivity relationships. Chiral cyclopentadienes **1a–c** are metalated with NaH in refluxing THF to afford the corresponding sodium salts **2a–c** as crystalline, highly air- and moisture-sensitive solids in high yields (~95%). These reagents undergo rapid and quantitative condensation with $Me_2Si(Cp''H)Cl$ to yield the diprotio $Me_2Si(Cp''H)(R^*CpH)$ ligands with exclusively 1,3-regiospecific substitution of the chiral Cp moiety. The diprotio ligands are not isolated but are converted immediately to the corresponding dilithium derivatives **3a–c** by treatment with 2 equiv of $LiCH_2SiMe_3$. These anionic reagents are obtained as solvent-free, air- and moisture-sensitive microcrystalline solids in virtually quantitative (97%) isolated yields from this one-pot synthesis. The sodium salts **2a–c** are recrystallized, the organosilane is distilled, and $LiCH_2SiMe_3$ is sublimed immediately prior to the synthesis. Conventional analytical techniques confirm the high purity of **3a–c**. Alternatively, the chiral cyclopentadienes can be metalated directly with $LiCH_2SiMe_3$ and the lithium salt utilized *in situ* for the remainder of the procedure.

Chiral Organolanthanide Chloro Precursors. The chiral $Me_2SiCp''(R^*Cp)Ln(\mu\text{-}Cl)_2Li(ether)_2$ complexes were synthesized in good yield and analytical purity by transmetalation of **3a–c** with the appropriate lanthanide trichloride (eq 3). The formation

$$\underset{\mathbf{3}}{Me_2SiCp''(R^*Cp)Li_2} + LnCl_3 \xrightarrow[2.\ Et_2O]{1.\ THF} \underset{\mathbf{4}}{Me_2SiCp''(R^*Cp)Ln(\mu\text{-}Cl)_2Li(ether)_2} + LiCl \quad (3)$$

R* = (+)-neomenthyl	Ln = La (**4a**), Nd (**4b**), Sm (**4c**), Y (**4d**), Lu (**4e**)
R* = (–)-menthyl	Ln = Sm (**4f**), Y (**4g**), Lu (**4h**)
R* = (–)-phenylmenthyl	Ln = Y (**4i**)

of the bis(diethyl ether)LiCl adducts corresponds exactly to the behavior of the achiral $Cp'_2Ln(\mu\text{-}Cl)_2Li(ether)_2$,[2] $Me_2SiCp''_2Ln(\mu\text{-}Cl)_2Li(ether)_2$,[4] and $Me_2SiCp''CpLn(\mu\text{-}Cl)_2Li(ether)_2$ congeners.[19] In the isoleptic series **4a–e** and **4f–h**, all complexes except **4a** are highly soluble in diethyl ether and are obtained as crystalline solids by slow cooling of the solutions. Complex **4a** is unstable toward salt elimination in diethyl ether solution at ambient temperature, presumably with concomitant dimer/oligomer formation analogous to $Cp'_2La(\mu\text{-}Cl)_2Li(ether)_2$.[2b] This characteristic necessitates a low-temperature (<–20 °C) workup. Similar behavior has been observed for other salt adducts of Cp' complexes of the larger, early lanthanides.[2a,4] Alternatively, the mono-DME adducts can be prepared (eq 4), however these exhibit

$$\underset{\mathbf{3}}{Me_2SiCp''(R^*Cp)Li_2} + LnCl_3 \xrightarrow[3.\ Et_2O]{1.\ THF\ 2.\ DME} \underset{\mathbf{5}}{Me_2SiCp''(R^*Cp)Ln(\mu\text{-}Cl)_2Li(DME)} + LiCl \quad (4)$$

R* = (–)-menthyl	Ln = Sm (**5a**), Lu (**5b**)
R* = (+)-neomenthyl	Ln = Sm (**5c**)

a marked decrease in ether solubility. In addition, 12-crown-4 adducts may be prepared by addition of excess 12-crown-4 to an ethereal solution of $Me_2SiCp''(R^*Cp)Ln(\mu\text{-}Cl)_2Li(ether)$. The crown adducts are only sparingly soluble in ether and precipitate as microcrystalline solids.

The readily interpretable ^1H and ^{13}C NMR spectra of diamagnetic complexes **4a**, **4d**, **4e**, **4g**, **4h**, **4i**, and **5b** indicate high diastereoselection (>80% de) in the complexation reaction (eqs 3 and 4). Diastereomers produced are epimeric with respect to the orientation of the chiral auxiliary on the Cp group relative

(33) Moore, J. W.; Pearson, R. G. *Kinetics and Mechanism*, 3rd ed.; Wiley: New York, 1981; Chapters 2 and 3.

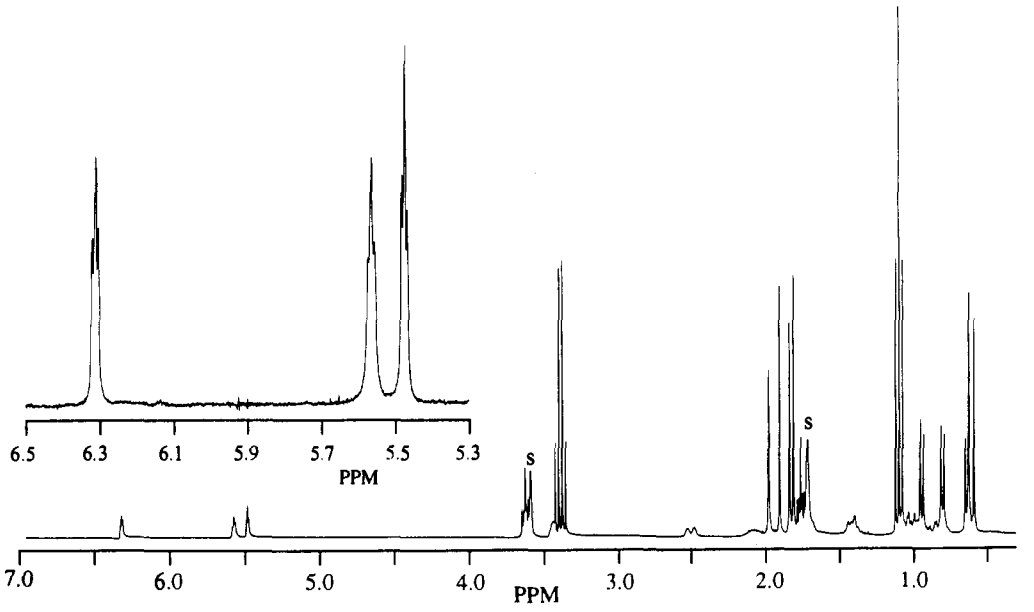

Figure 1. ^{1}H NMR spectrum (400 MHz) of $Me_2SiCp''[(+)$-neomenthylCp]$Lu(\mu$-$Cl)_2Li(ether)_2$ (**4e**) as a solution in diethyl ether-d_{10}.

to thelanthanide center (**G**, **H**). The (*S*)- and (*R*)-planar chiral

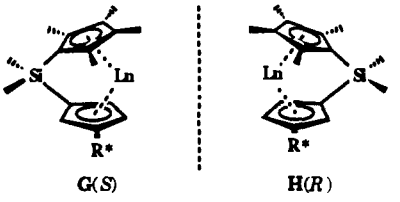

configurational nomenclature is based on an application of the Cahn–Ingold–Prelog convention to inorganic and organometallic complexes.[34] A single recrystallization from diethyl ether is sufficient to obtain single diastereomers of **4** and **5** in essentially complete optical purity (>95% by ^{1}H NMR) except for **4a**, which, due to its limited solubility, cannot be effectively enriched beyond the initial diastereoselection. The ^{1}H NMR spectrum of **4e**, particularly in the diagnostic cyclopentadienyl proton region, exemplifies this class of complexes: only one set of ancillary ligand resonances is observed for the complex, in agreement with the presence of a single diastereomer (Figure 1). Within the isoleptic diamagnetic series $Me_2SiCp''[(+)$-neomenthylCp]Ln-$(\mu$-$Cl)_2Li(ether)_2$ (Ln = La, Y, Lu) and $Me_2SiCp''[(-)$-menthylCp]$Ln(\mu$-$Cl)_2Li(ether)_2$ (Ln = Y, Lu), the dispersion of the chemical shifts in the ^{1}H NMR spectra, especially in the cyclopentadienyl region, indicates a similar planar chiral configuration of the predominant epimer for each complex and, by analogy, across the entire lanthanide series.

Molecular Structure of (*R*)-$Me_2SiCp''[(+)$-neomenthylCp]Lu-$(\mu$-$Cl)_2Li(ether)_2$ [(*R*)-4e]. Single crystal X-ray diffraction analysis of optically pure **4e** reveals a single planar chiral configuration of the diastereotopic, chirally-substituted Cp group, the (*R*)-configuration, in the molecular structure (Figure 2). Data collection information and selected bond lengths and bond angles with estimated standard deviations are summarized in Tables 1 and 2. The complex adopts the pseudotetrahedral, bent metallocene motif commonly observed for $Cp_2LnX_2^-$ complexes.[35,36]

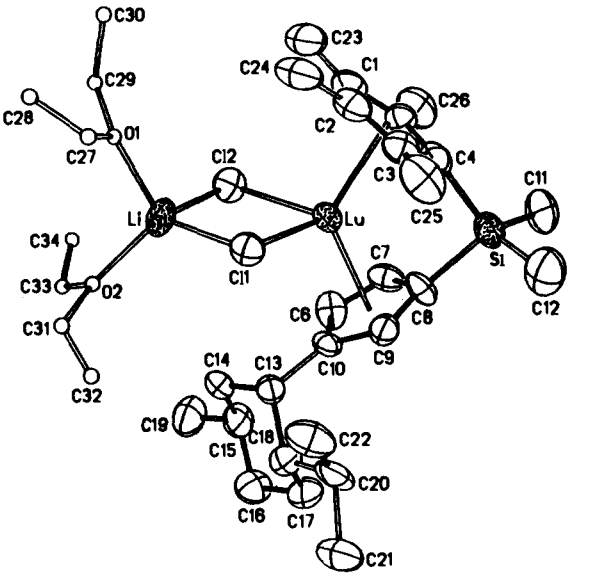

Figure 2. Perspective ORTEP drawing of the molecular structure of (*R*)-$Me_2SiCp''[(+)$-neomenthylCp]$Lu(\mu$-$Cl)_2Li(ether)_2$ [(*R*)-**4e**]. All non-hydrogen atoms are represented by thermal ellipsoids drawn to encompass 50% probability.

All non-hydrogen atoms were refined anisotropically except for the atoms of the diethyl ether molecules, which were disordered. The bond distances and angles of the $Lu(\mu$-$Cl)_2Li(ether)_2$ coordination group compare well with the corresponding features of analogous, achiral $Cp'_2Yb(\mu$-$Cl)_2Li(ether)_2$.[35a] In addition, the ring centroid–Ln–ring centroid angle in (*R*)-**4e**, ∠Cg(1)–Lu–Cg(2) (125.4°), undergoes a typical[2,35] contraction compared to those of standard Cp'_2LnX complexes (134–140°). This, no doubt, is due to the enforced link between the two Cp ligands in the present complexes. The Lu–C_{ring} bond distances display the dispersion pattern observed in other ring-bridged organolanthanide complexes, with longer Lu–C_{ring} distances for carbon atoms (C(1), C(2), C(6), C(10)) distal to the Me_2Si bridge vs proximal carbon atoms (C(4), C(8)). The Lu–C_{ring} distances, ∠C(4)–Si–C(8) (97.8(7)°), and ∠Cg(1)–Lu–Cg(2) (125.4°) are, within experi-

(34) (a) Sloan, T. E. *Top. Stereochem.* **1981**, *12*, 1–36. (b) Stanley, K.; Baird, M. C. *J. Am. Chem. Soc.* **1975**, *97*, 6598–6599. (c) Krow, G. *Top. Stereochem.* **1970**, *5*, 31–68.

(35) (a) Watson, P. L.; Whitney, J. F.; Harlow, R. L. *Inorg. Chem.* **1981**, *20*, 3271–3278. (b) Schumann, H.; Albrecht, I.; Loebel, J.; Hahn, E.; Hossain, M. B.; Van der Helm, D. *Organometallics* **1986**, *5*, 1296–1304. (c) Rausch, M. D.; Moriarty, K. J.; Atwood, J. L.; Weeks, J. A.; Hunter, W. E.; Brittain, H. G. *Organometallics* **1986**, *5*, 1281–1283. (d) Tilley, T. D.; Andersen, R. A. *Inorg. Chem.* **1981**, *20*, 3267–3271. (e) Wayda, A. L.; Evans, W. E. *Inorg. Chem.* **1980**, *19*, 2190–2191.

(36) (a) Lappert, M. F.; Singh, A.; Atwood, J. L.; Hunter, W. E. *J. Chem. Soc., Chem. Commun.* **1981**, 1191–1192. (b) Lappert, M. F.; Singh, A.; Atwood, J. L.; Hunter, W. E.; Zhang, H. M. *J. Chem. Soc., Chem. Commun.* **1983**, 69–70. (c) Atwood, J. L.; Hunter, W. E.; Rogers, R. D.; Holton, J.; McMeeking, J.; Pearce, R.; Lappert, M. F. *J. Chem. Soc., Chem. Commun.* **1978**, 140–142.

Table 1. X-ray Diffraction Data Collection Parameters for Chiral Organolanthanide Complexes

	(*R*)-**4e**	(*R*,*S*)-**6c**	(*R*,*S*)-**6d**	(*R*)-**6f**	(*R*)-**6g**	(*S*)-**7b**	(*S*)-**7e**	(*R*)-**7f**
formula	$C_{34}H_{60}Cl_2LiLuO_2Si$	$C_{33}H_{59}Si_3Sm$	$C_{33}H_{59}Si_3Y$	$C_{33}H_{59}Si_3Sm$	$C_{33}H_{59}Si_3Y$	$C_{32}H_{58}NSi_3Sm$	$C_{32}H_{58}NSi_3Sm$	$C_{64}H_{116}N_2Si_6Y_2$
M	781.8	690.48	629.0	1380.97	1257.98	691.47	691.47	1259.96
cryst size, mm	0.41 × 0.36 × 0.40	0.35 × 0.42 × 0.45	0.37 × 0.32 × 0.24	0.5 × 0.3 × 0.1	0.3 × 0.3 × 0.25	0.2 × 0.2 × 0.3	0.39 × 0.38 × 0.14	0.42 × 0.45 × 0.12
color, habit	colorless, plates	yellow, platelets	colorless, plates	yellow, platelets	colorless, plates	orange, plates	orange, platelets	colorless, plates
cryst system	orthorhombic	monoclinic	monoclinic	triclinic	monoclinic	monoclinic	orthorhombic	triclinic
space group	$P2_12_12_1$	$P2_1$	$P2_1$	$P\bar{1}$	$P2_1$	$P2_1$	$P2_12_12_1$	$P\bar{1}$
a, Å	12.240(2)	18.334(6)	19.178(4)	8.993(3)	12.319(3)	9.122(2)	10.217(3)	8.937(3)
b, Å	12.876(2)	8.723(3)	8.736(1)	12.738(2)	15.707(4)	10.112(3)	19.103(6)	12.397(6)
c, Å	24.387(5)	21.398(8)	21.391(5)	16.549(4)	18.693(5)	18.478(3)	19.456(7)	16.673(7)
α, deg	90	90	90	86.04(2)	90	90	90	85.53(2)
β, deg	90	97.64(3)	97.62(2)	82.81(2)	91.59(2)	90.58(2)	90	82.17(2)
γ, deg	90	90	90	72.91(2)	90	90	90	74.78(2)
V, Å^3	3843.6(1.4)	3392(4)	3552(2)	1797(2)	3616(3)	1704(1)	3797(4)	1764(2)
Z	4	4	4	2	4	2	4	2
d(calcd), g cm^{-3}	1.35	1.352	1.18	1.276	1.155	1.35	1.276	1.186
diffractometer	Nicolet R3m/μ	*a*	*a*	*a*	*a*	*a*	*a*	*a*
temp, °C	24	−120	−120	−120	−120	−120	−120	−120
radiation	*b*	*b*	*b*	*b*	*b*	*b*	*b*	*b*
scan type	Wyckoff	$2\theta/\omega$	ω	ω/θ	$\theta/2\theta$	ω/θ	ω/θ	ω/θ
2θ range, deg	4–48	4–48	4–50	2–48	2–48	2–54	2–50	2–48
no. of unique data	3401	4350	6707	8327	5234	3930	3584	8208
no. of obs reflctns	2640	3099	3514	4959	3001	3356	2621	6204
	($F_o > 5\sigma(F_o)$)	($I > 3\sigma(I)$)	($I > 3\sigma(I)$)	($I > 3\sigma(I)$)	($I > 3\sigma(I)$)	($I > 2.58\sigma(I)$)	($I > 3\sigma(I)$)	($I > 3\sigma(I)$)
no. of params	197	296	348	665	336	334	334	344
$R(F)$	0.0509	0.068	0.071	0.026	0.054	0.029	0.044	0.065
$R_w(F)$	0.0514	0.086	0.082	0.030	0.058	0.032	0.047	0.066
GOF	1.332	2.84	2.02	0.47	0.63	1.07	0.99	1.26

[a] Enraf-Nonius CAD4. [b] Graphite-monochromated Mo Kα (λ = 0.7107 Å).

Table 2. Selected Bond Lengths (Å) and Angles (deg) in Coordination Groups of (*R*)-Me_2SiCp''[(+)-neomenthylCp]Lu(μ-Cl)$_2$Li(ether)$_2$ [(*R*)-**4e**]

Lu–Cl(1)	2.569(4)	Si–C(8)	1.906(15)	Lu–C(7)	2.545(16)
Lu–C(2)	2.652(16)	Si–C(12)	1.890(22)	Lu–C(9)	2.584(15)
Lu–C(4)	2.518(16)	Li–O(2)	2.001(31)	Cl(1)–Li	2.354(26)
Lu–C(6)	2.670(15)	Lu–Cl(2)	2.571(4)	Si–C(4)	1.869(18)
Lu–C(8)	2.533(16)	Lu–C(1)	2.681(15)	Si–C(11)	1.855(19)
Lu–C(10)	2.696(13)	Lu–C(3)	2.572(15)	Li–O(1)	2.011(27)
Cl(2)–Li	2.409(25)	Lu–C(5)	2.569(13)		
Cl(1)–Lu–Cl(2)	86.9(1)		Cl(1)–Lu–Li	42.8(4)	
Cl(2)–Lu–Li	44.1(4)		Cl(1)–Li–Cl(2)	95.8(9)	
Cl(1)–Li–O(1)	108.1(12)		Cl(1)–Li–O(2)	118.1(12)	
Cl(2)–Li–O(1)	110.3(11)		Cl(2)–Li–O(2)	118.5(13)	
O(1)–Li–O(2)	105.5(12)		C(11)–Si–C(12)	106.8(9)	
C(4)–Si–C(8)	97.8(7)		Lu–C(1)–C(23)	124.7(12)	
Lu–C(10)–C(13)	119.7(9)		Lu–C(3)–C(25)	119.2(10)	
Lu–C(2)–C(24)	120.8(16)		Lu–C(5)–C(26)	120.0(11)	

mental error, identical to those of $Me_2SiCp''CpLuCH(SiMe_3)_2$, e.g., $\angle$Cg(1)–Si–Cg(2) = 125.2°, with similar but achiral ancillary ligation.[19]

The (+)-neomenthyl auxiliary is located on a single side of the asymmetric complex. The cyclohexyl group of the chiral auxiliary adopts a chair conformation in which only the Cp substituent occupies an axial position. Identical conformations are observed in the structures of Mo[37] and Ru[38] (+)-neomenthylCp complexes. The Lu–C(10)–C(13) angle, 119.7(9)°, does not differ significantly from the Lu–C_{ring}–C_{methyl} angles, 124.7(12)°, 121.5(11)°, 119.2(10)°, and 120.0(11)°, of other ring substituents on the Cp″ group, suggesting that no gross structural distortions arise from the steric bulk of the R* group. In the (*R*)-configuration of the planar chiral Cp ligand, the adjacent chiral auxiliary adopts a conformation about the C(10)–C(13) bond axis in which the bulky equatorial isopropyl group of the auxiliary is oriented *syn* to the Me_2Si bridge. In the structural determinations of related hydrocarbyl and amide complexes, both *syn* and *anti* conformations of the isopropyl group are observed (*vide infra*). The selective interactions between these two orientations of the chiral auxiliary and the appended achiral portion of the molecule appear to play a major role in the relative stabilities of the (*R*)- and (*S*)-epimers (*vide infra*). Additionally, the analogous samarium complex **4c** was determined to be isostructural with (*R*)-**4e**.

Circular Dichroism Spectroscopy of Me_2SiCp''[R*Cp]Ln(μ-Cl)$_2$Li(S)$_x$ Complexes. Correlations of metal configuration among the series of chloro complexes **4** and **5** can be inferred from solution chiroptical properties. Two characteristic absorption maxima are observed for all the chloro complexes. The higher energy absorption typically displays a greater Cotton effect. In principle, three types of transitions are possible for lanthanide cyclopentadienyl complexes: generally weak, metal-based f–f transitions (4f–4f or 4f–4f^{n-1}5d), ligand-to-metal charge-transfer transitions (LMCT; ligand π–metal 4f or ligand π–metal 5d), and ligand-based transitions (π–π^*).[39] Since the present optical transitions have relatively high oscillator strength and are observed for the closed-shell La^{3+}, Y^{3+}, and Lu^{3+} complexes and since the CD features of **4** and **5** exhibit slight, metal-dependent shifts in accord with optical electronegativity considerations,[40] we tentatively associate these features with LMCT excitations. No strong transitions are detected in the CD spectra of the parent dilithio ligands **3** in the region from 250 to 500 nm. This suggests that the CD absorptions of **4** and **5** are largely due to planar asymmetry induced by the bidentate, chelating arrangement of the chiral ligand.

Within the series of isoleptic complexes Me_2SiCp''[(+)-neomenthylCp]Ln(μ-Cl)$_2$Li(ether)$_2$ (Ln = Sm, Y, Lu), the CD

(37) (a) Faller, J. W.; John, J. A.; Mazzieri, M. R. *Tetrahedron Lett.* **1989**, *30*, 1769–1772. (b) Faller, J. W.; Chao, K.-H. *Organometallics* **1984**, *3*, 927–932. (c) Faller, J. W.; Chao, K.-H. *J. Am. Chem. Soc.* **1983**, *105*, 3893–3898. (d) Faller, J. W.; Shvo, Y. *J. Am. Chem. Soc.* **1980**, *102*, 5396–5398. (e) Faller, J. W.; Linebarrier, D. L. *J. Am. Chem. Soc.* **1989**, *111*, 1937–1939.

(38) (a) Cesarotti, E.; Chiesa, A.; Ciani, G. F.; Sironi, A.; Vefghi, R.; White, C. *J. Chem. Soc., Dalton Trans.* **1984**, 653–661. (b) Cesarotti, E.; Ciani, G. F.; Sironi, A. *J. Organomet. Chem.* **1981**, *216*, 87–95. (c) Cesarotti, E.; Angoletta, M.; Walker, N. P. C.; Hursthouse, M. B.; Vefghi, R.; Schofield, P. A.; White, C. *J. Organomet. Chem.* **1985**, *286*, 343–360. (d) Lindsay, C.; Cesarotti, E.; Adams, S. H.; Bailey, N. A.; White, C. *Organometallics* **1990**, *9*, 2594–2602.

(39) (a) Edelstein, N. In *Fundamental and Technological Aspects of Organo-f-Element Chemistry*; Marks, T. J., Fragala, I. L., Eds.; Reidel: Dordrecht, 1985; Chapter 7. (b) Carnall, W. T. In *Organometallics of the f-Elements*; Marks, T. J., Fischer, R. D., Eds.; Reidel: Dordrecht, 1978; Chapter 9. (c) Marks, T. J. *Prog. Inorg. Chem.* **1978**, *24*, 51–107.

(40) Jørgensen, C. K. *Modern Aspects of Ligand Field Theory*; North Holland: Amsterdam, 1971; Chapter 28.

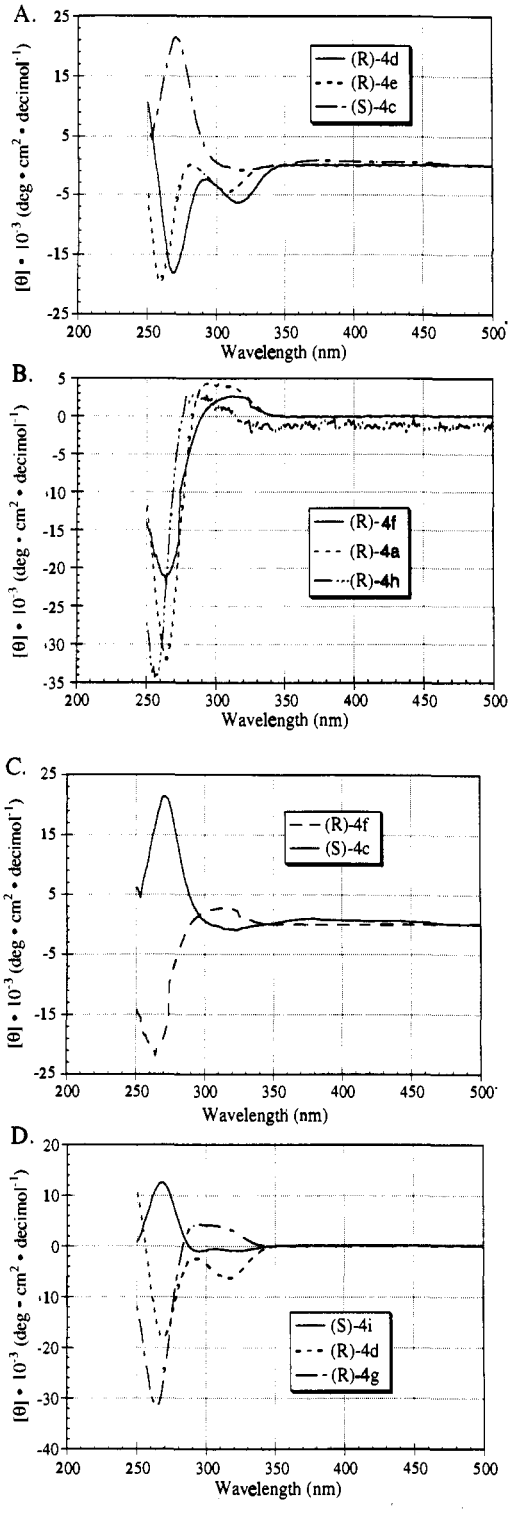

Figure 3. Circular dichroism spectra as solutions in diethyl ether in the 250–500 nm wavelength range. (A) $Me_2SiCp''[(+)$-neomenthylCp]Sm-$(\mu$-Cl)$_2$Li(ether)$_2$ (**4c**), $Me_2SiCp''[(+)$-neomenthylCp]Y$(\mu$-Cl)$_2$Li-(ether)$_2$ (**4d**), and $Me_2SiCp''[(+)$-neomenthylCp]Lu$(\mu$-Cl)$_2$Li(ether)$_2$ (**4e**). (B) $Me_2SiCp''[(-)$-menthylCp]Sm$(\mu$-Cl)$_2$Li(ether)$_2$ (**4f**), Me_2-$SiCp''[(-)$-menthylCp]Y$(\mu$-Cl)$_2$Li(ether)$_2$ (**4g**), and $Me_2SiCp''[(-)$-menthylCp]Lu$(\mu$-Cl)$_2$Li(ether)$_2$ (**4h**). (C) $Me_2SiCp''[(+)$-neomenthylCp]-Sm$(\mu$-Cl)$_2$Li(ether)$_2$ (**4c**), and $Me_2SiCp''[(-)$-menthylCp]Sm$(\mu$-Cl)$_2$-Li(ether)$_2$ (**4f**). (D) $Me_2SiCp''[(+)$-neomenthylCp]Y$(\mu$-Cl)$_2$Li(ether)$_2$ (**4d**), $Me_2SiCp''[(-)$-menthylCp]Y$(\mu$-Cl)$_2$Li(ether)$_2$ (**4g**), and Me_2SiCp''-$[(-)$-phenylmenthylCp]Y$(\mu$-Cl)$_2$Li(ether)$_2$ (**4i**).

traces (Figure 3A) have identical morphologies; however, the sign of the Cotton effect of the more intense absorption is positive for the Sm complex and negative for the Y and Lu complexes. The (*R*)-configuration is assigned to **4d** and **4e** on the basis of

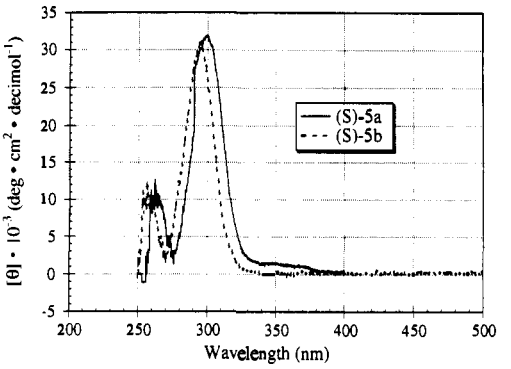

Figure 4. Circular dichroism spectra of $Me_2SiCp''[(-)$-menthylCp]Sm-$(\mu$-Cl)$_2$Li(DME) (**5a**) and $Me_2SiCp''[(-)$-menthylCp]Lu$(\mu$-Cl)$_2$Li-(DME) (**5b**) as solutions in diethyl ether in the 250–500 nm wavelength range.

the (*R*)-**4e** X-ray results and the similarity of the CD spectra of the two complexes. Although not shown, the La and Nd complexes are also assigned the (*R*)-configuration on the basis of similar CD spectroscopic features. The positive Cotton effect of the more intense absorption in the CD spectrum of **4c**, especially in relation to crystallographically characterized **4e**, necessitates an (*S*)-configurational assignment. The anomalous behavior of the Sm complex in the (+)-neomenthyl series may be attributed to the relative solubility and configurational stability of this complex (*vide infra*). Interestingly, within the series of isoleptic Me_2-$SiCp''[(-)$-menthylCp]Ln$(\mu$-Cl)$_2$Li(ether)$_2$ complexes (Ln = Sm, Y, Lu), the CD traces (Figure 3B) have identical morphologies and all exhibit a negative Cotton effect for the more intense absorption. Accordingly, the (*R*)-configuration is assigned to **4f–h**.

Among analogous complexes having different chiral ancillary ligands, i.e., $Me_2SiCp''(R^*Cp)Sm(\mu$-Cl)$_2$Li(ether)$_2$ (R* = (+)-neomenthyl, (–)-menthyl) and $Me_2SiCp''(R^*Cp)Y(\mu$-Cl)$_2$Li-(ether)$_2$ (R* = (+)-neomenthyl, (–)-menthyl, (–)-phenylmenthyl), the CD spectra reveal an interesting dependence of the planar chiral configurations on the nature of the chiral auxiliary. Sm complexes **4c** and **4f** display a pseudoenantiomeric relationship based on their CD spectra (Figure 3C). This observation argues for opposite planar chiral configurations, i.e., opposite cyclopentadienyl diastereoface selection: (*S*)- and (*R*)-configurations, respectively. In contrast, the analogous Y complexes **4d** and **4g** have similar CD spectra, particularly with respect to the sign of the higher energy absorption (Figure 3D). The (*R*)-configuration is assigned to both complexes based on correlation of the CD spectra with the spectrum of structurally characterized (*R*)-**4e**. In addition, the (*R*)-configuration of **4g** is supported by the CD spectroscopy and X-ray structure determinations on hydrocarbyl ($CH(SiMe_3)_2$) and amide ($N(SiMe_3)_2$) derivatives (*R*)-**6g** and (*R*)-**7f**, respectively (*vide infra*). The CD spectra in Figure 3D clearly indicate a pseudoenantiomorphic relationship between the optically-pure reaction products **4d** and **4g** versus **4i**, since similar morphologies but opposite Cotton effects are observed. This observation leads to the assignment of the (*S*)-configuration to **4i**, particularly in comparison to (*R*)-**4g**, since the relative configurations of all three asymmetric carbon centers of the respective chiral auxiliaries (–)-menthyl and (–)-phenylmenthyl, are equivalent.

The CD traces of the isoleptic complexes $Me_2SiCp''[(-)$-menthylCp]Ln$(\mu$-Cl)$_2$Li(DME) (Ln = Sm, Lu) have identical morphologies and positive Cotton effects for the more intense absorption (Figure 4). The (*S*)-configuration is assigned to these two complexes, while the (*R*)-configuration is assigned to the analogous ether adducts **4f** and **4h** (Figure 3B). The (*S*)-configurational assignment to **5a** is further supported by the subsequent CD spectroscopy and single crystal structural determination for amide derivative (*S*)-**7e** (*vide infra*). Although

Table 3. Solvent-Dependent Equilibrium Epimer Ratios at 25 °C for $Me_2SiCp''[R^*Cp]Ln(\mu\text{-}Cl)_2Li(ether)_2$ Complexes[a]

complex	structure	equilibrium epimer ratio (*R*:*S*)	solvent
4a	neomenthylLaCl	75:25	THF
4b	neomenthylNdCl	74:26	THF
4c	neomenthylSmCl	74:26	THF
4c	neomenthylSmCl	34:66	Et_2O
4d	neomenthylYCl	74:26	THF
4d	neomenthylYCl	46:54	Et_2O
4e	neomenthylLuCl	74:26	THF
4e	neomenthylLuCl	51:49	Et_2O
4f	menthylSmCl	20:80	THF
4f	menthylSmCl	>95:5	Et_2O
4g	menthylYCl	20:80	THF
4g	menthylYCl	90:10	Et_2O
4h	menthylLuCl	20:80	THF
4h	menthylLuCl	85:15	Et_2O
4i	phenylmenthylYCl	6:94	THF
4i	phenylmenthylYCl	83:17	Et_2O

[a] Equilibrium epimer populations determined by ^1H NMR spectroscopy.

(*R*)-**4d** and (*R*)-**4g** have the same planar chiral configuration, the respective CD spectra are not superimposable (Figure 3D). This is not unexpected, since the chiral auxiliaries are epimeric at a single asymmetric carbon center. In summary, the sign of the higher energy, more intense Cotton effect absorbance can be utilized to empirically correlate the planar chiral configurations of the complexes **4**, **5**, **6**, and **7**. A negative sign corresponds to the (*R*)-configuration, while a positive sign corresponds to the (*S*)-configuration. This rule of thumb also satisfactorily correlates the solution chiroptical properties of the hydrocarbyl and amide derivatives of **6** and **7** with the stereochemistry inferred from structure and reactivity studies (*vide infra*).

Epimerization of $Me_2SiCp''[R^*Cp]Ln(\mu\text{-}Cl)_2Li(S)_x$ Complexes. Although chiral chloro complexes **4** and **5** could be isolated and spectroscopically/structurally characterized as optically pure diastereomers of specifically determined absolute configuration, slow rearrangement occurs in donor solvents such as ether to an equilibrium mixture of diastereomers which are epimeric in the planar chiral configuration of the chirally-substituted Cp ligands. The epimerization process requires the formal dissociation of the chiral Cp ligand group from the lanthanide center and subsequent recoordination of the metal to the opposite diastereoface (eq 5).

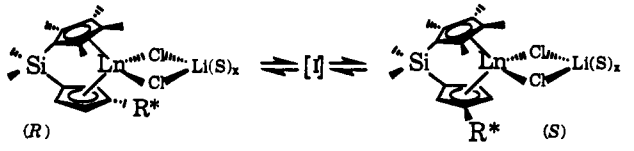

(5)

The extent of the epimerization depends on the donor solvent, the lanthanide ion, R*, and the temperature. Equilibrium epimer ratios in THF and diethyl ether were determined by ^1H NMR and are summarized in Table 3. Interestingly, the epimerization can be completely inhibited by the addition of exogenous ligands which are capable of strongly coordinating Li^+ to solutions of **4** and **5**. For example, the initial (*R*)-configuration of **4d** is preserved for days in the presence of 1 equiv of 12-crown-4 in THF-d_8 at ambient temperature. Under identical conditions, in the absence of the lithium-selective crown ether, (*R*)-**4d** rearranges within 1 h to an equilibrium mixture of epimers.

Within the isoleptic series $Me_2SiCp''[(+)\text{-neomenthylCp}]Ln(\mu\text{-}Cl)_2Li(ether)_2$, the equilibrium population of the (*R*)-epimer increases in diethyl ether as the Ln^{3+} ionic radius decreases, although in THF, the equilibrium epimer ratio remains essentially constant across the lanthanide series. Although the **4d** and **4e** (*R*)-epimers are the initial synthetic reaction products, extensive

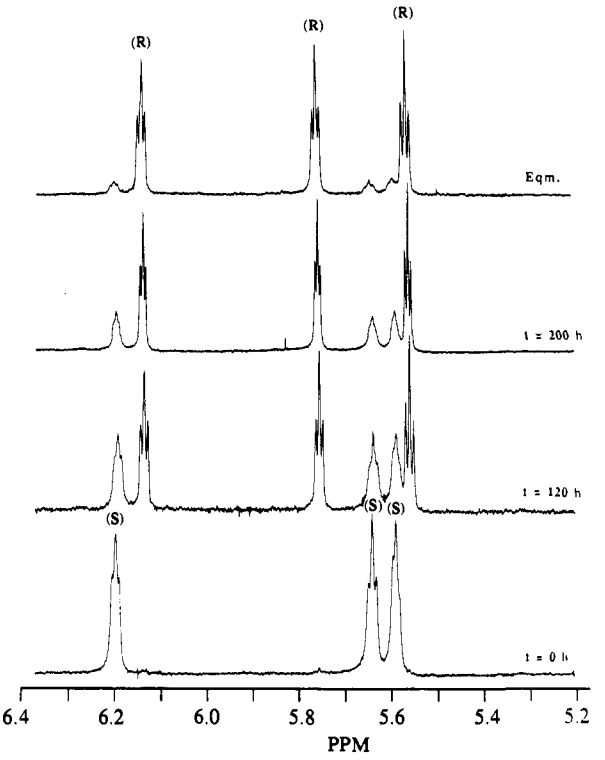

Figure 5. Time evolution of the cyclopentadienyl proton region of the ^1H NMR spectrum for the epimerization of (*S*)-$Me_2SiCp''[(-)\text{-phenylmenthylCp}]Y(\mu\text{-}Cl)_2Li(ether)_2$ [(*S*)-**4i**] in diethyl ether-d_{10} in 25 °C.

epimerization occurs in diethyl ether solution at ambient temperature, culminating in essentially complete loss of stereochemical integrity. The isolation on synthetic workup of diastereomerically pure (*R*)-**4d** and (*R*)-**4e** probably reflects their relatively slow epimerization rates in diethyl ether such that the initial high diastereoselections for the (*R*)-epimer in the synthesis solvent, THF, are preserved in the products and high yields of the crystalline (*R*)-epimers are obtained. In contrast to the (+)-neomenthyl chlorides, the epimer equilibria for the (–)-menthyl and (–)-phenylmenthyl complexes favor the opposite (*S*)-epimer complexes in THF under identical conditions. This is likely a consequence of the opposite configuration of the cyclopentadienyl-substituted asymmetric carbon center in the (–)-menthyl, (–)-phenylmenthyl auxiliaries versus the (+)-neomenthyl group. In diethyl ether, the (*R*)-configuration is strongly preferred under normal ambient temperature workup conditions. The (*R*)-epimers of **4f–h** are isolated in high yield, implying both facile and selective epimerization.

In diethyl ether, the epimerizations of (*S*)-**4i** and (*S*)-**5b** are relatively slow at ambient temperature, and the epimerization kinetics can be monitored by ^1H NMR. As an example, the change in the cyclopentadienyl region of the (*S*)-**4i** spectrum with time is shown in Figure 5. Slow evolution of the (*R*)-epimer resonances is detected with a concomitant decrease in the relative intensity of the (*S*)-epimer resonances. Integration of the Cp ^1H resonances at δ 6.20 and 6.14 ppm assignable to the (*S*)- and (*R*)-epimers, respectively, affords kinetic data. A first-order rate law (eq 6, Figure 6A) obtains with a derived rate constant $k' = 1.62(2) \times 10^{-6}$ s^{-1} ($t_{1/2}$ = 118 h). Similarly, integration of the

$$n = k'[(S)\text{-}4i] \qquad (6)$$

Cp resonances at δ 6.09 and 6.00 ppm assignable to the (*S*)- and (*R*)-epimers of **5b**, respectively, affords equilibration kinetic data for this complex in Et_2O at 25 °C. The derived first-order rate constant is $k' = 6.7(1) \times 10^{-5}$ s^{-1} ($t_{1/2}$ = 2.8 h). Finally, the kinetics of epimerization of the series (*R*)-**4f–h** to (*S*)-**4f–h** in THF at 25 °C were similarly determined. Interestingly, the

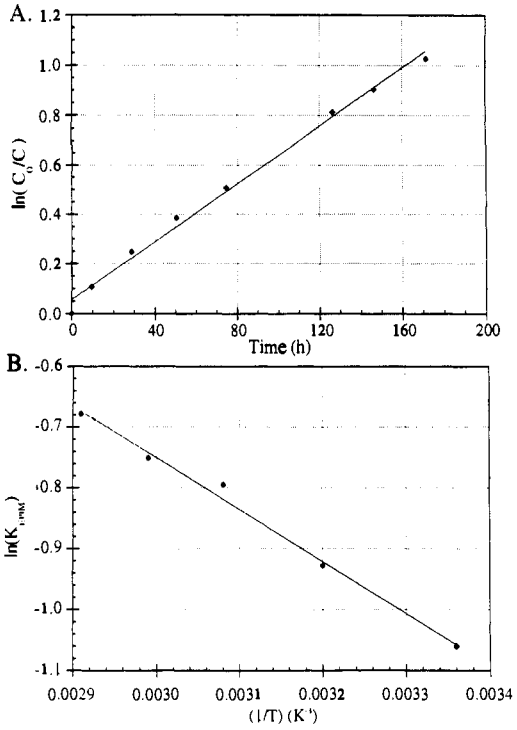

Figure 6. (A) Kinetic plot for the epimerization of (*S*)-Me_2SiCp''-[(–)-phenylmenthylCp]$Y(\mu\text{-}Cl)_2Li(ether)_2$ [(*S*)-**4i**] in diethyl ether-d_{10} at 25 °C. (B) Van't Hoff plot for the epimerization of (*R*)-Me_2SiCp''-[(+)-neomenthylCp]$Lu(\mu\text{-}Cl)_2Li(ether)_2$ [(*R*)-**4e**] in THF-d_8.

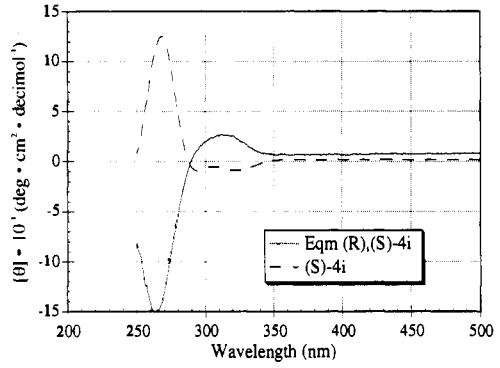

Figure 7. Circular dichroism spectra of (*S*)-Me_2SiCp''[(–)-phenylmenthylCp]$Y(\mu\text{-}Cl)_2Li(ether)_2$ [(*S*)-**4i**] and its equilibrium epimer distribution (83:17, *R*:*S*) as solutions in diethyl ether in the 250–500 nm range.

epimerization kinetics exhibit negligible Ln dependence, with the derived first-order rate constants being identical within experimental error, $k' = 2.2(3) \times 10^{-5}$ s^{-1} ($t_{1/2}$ = 8.8 h).

The CD spectra of (*S*)-**4i** and the 83:17 (*R*):(*S*) equilibrium epimer population of **4i** in diethyl ether (Figure 7) clearly display a pseudoenantiomorphic relationship. This suggests opposite planar chiral configurations for the two complexes since the chiral auxiliaries are identical and unchanged throughout the epimerization process. Additionally, the CD spectrum of (*R*)-**4i** is essentially superimposable upon that of (*R*)-**4g**, independently confirming the validity of planar chiral configurational correlation within the (+)-neomenthyl, (–)-menthyl, and (–)-phenylmenthyl series of complexes. This result is further supported by the chiroptical properties of the corresponding hydrocarbyls and amides (*vide infra*).

The temperature dependence of the epimerization process was examined for complexes (*R*)-**4e** and (*R*)-**4f** in THF. The equilibrium constants for epimerization more closely approach unity as the temperature is increased, although the change in the equilibrium isomer population is slight (ca. 50%) over a 50 °C range. The (*R*) ⇌ (*S*) equilibria obey a simple van't Hoff dependence on the temperature (Figure 6B), with ΔH = 1.7 ± 0.3 and 4.8 ± 0.5 kcal/mol and ΔS = 3.6 ± 0.8 and 13.4 ± 0.5 eu being extracted by least-squares. These parameters are, as expected, relatively small, indicating that the two epimers have similar bonding energetics and steric interactions, and account for the sensitivity of the equilibria to solvation effects observed on changing from THF to diethyl ether. *Importantly, by choice of recrystallization solvent and temperature, it is possible to isolate chloro complexes of either the (S)- or the (R)-configuration.* This selective epimerization and isolation of diastereomerically pure organolanthanide chloro complexes is a crucial prerequisite for the preparation of hydrocarbyl/amide precatalysts of desired configuration.

Synthesis of Chiral Organolanthanide Hydrocarbyls and Amides. Next on the pathway to chiral catalysts is the preparation of chiral hydrocarbyl and amide complexes. These complexes will serve as efficient precatalysts in asymmetric catalytic studies.[20] As with the chloro complexes, there are two possible planar chiral configurations possible for the hydrocarbyl and amide complexes. These configurational isomers are diastereomerically related and, *a priori*, are expected to exhibit differing catalytic activity and selectivity. Therefore, it is desirable to develop systematic routes to both antipodes of the precatalysts. CD spectroscopy and X-ray diffraction studies are used in tandem to establish the absolute configuration of this new class of C_1-symmetric complexes.

The reaction between the diastereomerically pure Me_2SiCp''-(R*Cp)$Ln(\mu\text{-}Cl)_2Li(ether)_2$ complexes **4** and 1 equiv of $LiCH(SiMe_3)_2$ or $MN(SiMe_3)_2$ (M = Na, K) in toluene affords Me_2SiCp''(R*Cp)$LnCH(SiMe_3)_2$ (eq 7) and Me_2SiCp''(R*Cp)-$LnN(SiMe_3)_2$ (eq 8) complexes, respectively, in generally high yield and constitutional purity. This reactivity closely corresponds

$$\underset{\mathbf{4}}{Me_2SiCp''(R^*Cp)Ln(\mu\text{-}Cl)_2Li(S)_2} + LiCH(TMS)_2 \xrightarrow[\text{2. pentane}]{\text{1. toluene}} \underset{\mathbf{6}}{Me_2SiCp''(R^*Cp)LnCH(TMS)_2} + 2LiCl \quad (7)$$

R* = (+)-neomenthyl Ln = La (**6a**), Nd (**6b**), Sm (**6c**), Y (**6d**), Lu (**6e**)
R* = (–)-menthyl Ln = Sm (**6f**), Y (**6g**), Lu (**6h**)
R* = (–)-phenylmenthyl Ln = Y (**6i**)

$$\underset{\mathbf{4,5}}{Me_2SiCp''(R^*Cp)Ln(\mu\text{-}Cl)_2Li(S)} + MN(TMS)_2 \xrightarrow[\text{2. pentane}]{\text{1. toluene}} \underset{\mathbf{7}}{Me_2SiCp''(R^*Cp)LnN(TMS)_2} + MCl + LiCl \quad (8)$$

R* = (+)-neomenthyl Ln = La (**7a**), Sm (**7b**), Y (**7c**), Lu (**7d**)
R* = (–)-menthyl Ln = Sm (**7e**). Y (**7f**), Lu (**7g**)
R* = (–)-phenylmenthyl Ln = Y (**7h**)

to the behavior of the achiral Cp'_2LnR, $Me_2SiCp''_2LnR$, and $Me_2SiCp''CpLnR$ analogs (R = $CH(SiMe_3)_2$, $N(SiMe_3)_2$).[2,4,19,41] Additionally, the reaction between the diastereomerically pure Me_2SiCp''(R*Cp)$Ln(\mu\text{-}Cl)_2Li$(DME) complexes **5** and 1 equiv of $MN(SiMe_3)_2$ (M = Na, K) in toluene affords the Me_2SiCp''-(R*Cp)$LnN(SiMe_3)_2$ complexes (eq 8). All products gave satisfactory analytical data except **6a**, the synthesis of which did not proceed to completion even after 48 h at ambient temperature in either toluene or diethyl ether.

The stereochemical course of eqs 7 and 8 is not straightforward, and epimerization of the Ln center can occur, with the degree of epimerization strongly dependent on the reaction conditions, identity of R*, nature of S, and the initial configuration of the

(41) Evans, W. J.; Keyer, R. A.; Ziller, J. W. *Organometallics* **1993**, *12*, 2618–2633.

chloro complex. The homochiral (+)-neomenthyl chloro complexes (*R*)-**4a–e** undergo extensive epimerization under the above alkylation/amidation conditions with the extent of epimerization increasing with decreasing Ln ionic radius. *In situ* ^{1}H NMR indicates formation of essentially equimolar quantities of (*R*)- and (*S*)-**6e** from the reaction of (*R*)-**4e** and $LiCH(SiMe_3)_2$ in toluene, although only 30% epimerization occurs upon reaction of (*R*)-**4e** with 1 equiv of $MN(SiMe_3)_2$ (M = Na, K). In addition, the epimer mixture (*R,S*)-Me_2SiCp''[(+)-neomenthylCp]LnR (R = $CH(SiMe_3)_2$, $N(SiMe_3)_2$), in which both epimers are present in the same unit cell (*vide infra*), preferentially crystallizes from the reaction mixture. This precludes the separation of hydrocarbyl epimers **6d** and **6e**, since an approximately equimolar mixture of epimers is initially obtained as the product. This also limits the yield of the diastereomerically pure (*R*) Sm hydrocarbyl complex **6c** and the $N(TMS)_2$ (*R*)-epimers **7a–d**, which can be isolated by fractional crystallization of the less soluble (*R,S*)-mixture. The ^{1}H NMR spectra of the crystalline (+)-neomenthyl epimer mixtures exhibit twice the number of expected resonances. For example, in the cyclopentadienyl proton region of (*R,S*)-**6d** and (*R,S*)-**7c**, six major resonances (two are partially overlapped) of equal intensity are observed (Figure 8), indicating the presence of equimolar amounts of (*R*)- and (*S*)-epimers. The spectroscopic data thus support solution structures **I**, **J** and **K**, **L** for the pairs of hydrocarbyl and amido complexes, respectively. The asymmetry introduced by the chiral ancillary ligand renders the two $SiMe_3$ groups magnetically inequivalent, unlike the symmetric $Cp'_2LnE(SiMe_3)_2$ (E = CH, N) complexes and ring-bridged congeners.[2,4,19,41] In addition, the ^{1}H NMR spectra of (+)-neomenthyl hydrocarbyl complexes (*R,S*)-**6d,e** display minor resonances in the cyclopentadienyl region (Figure 8), corresponding to two additional discrete complexes, each associated with a single (*R*)- or (*S*)-epimer of the major product. The presence of two minor isomers which do not readily undergo exchange with each other or with the corresponding major isomer at ambient temperature is evident throughout the NMR spectroscopy of the $CH(TMS)_2$ complexes. In contrast, minor isomers are not observed in the ^{1}H spectra of the analogous $N(TMS)_2$ complexes (*R,S*)-**7c,d**, which should have an essential planar arrangement of the $LnNSi_2$ group. These solution species are probably associated with conformational isomers of the diastereotopic $CH(TMS)_2$ moiety arising from hindered rotation about the Ln–Cα σ bond. Similar hindered rotation about a M–Cα bond of a $CH(TMS)_2$ group and interconversion of pairs of conformational isomers has been observed for $Cp_2Zr(R)CH(SiMe_3)_2$ and $Cp^*_2Zr(Cl)CH(SiMe_3)_2$ complexes ($Cp^* = C_5H_4(SiMe_3)$).[42]

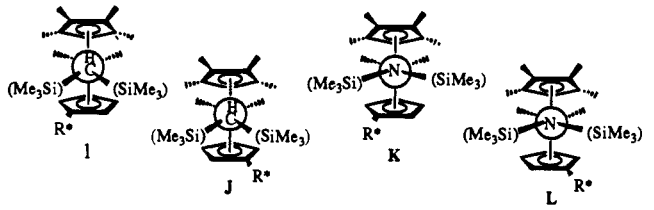

In marked contrast to the (*R*)-(+)-neomenthyl chlorides discussed above, the (–)-menthyl chlorides (*R*)-**4f–h** do not undergo significant epimerization under alkylation or amidation reaction conditions, e.g., retention of the initial (*R*)-configuration occurs predominantly for **6f–h** and **7e–g**. The CD spectra of **6f–h** (Figure 9A) all exhibit identical curve morphologies and negative Cotton effects. Accordingly, the (*R*)-configuration, which has been confirmed in the crystal structure determination for **6g**, is assigned. Although not shown, **7e–g** have similar CD spectra, all exhibiting negative Cotton effects, and therefore are assigned the (*R*)-configuration, confirmed by the X-ray structure determinations for **7e** and **7f** (*vide infra*). Additionally, DME complexes (*S*)-**5a,b** and (*R*)-**5c** undergo amidation with net retention of configuration but do not undergo clean conversion to the respective hydrocarbyl complexes upon reaction with $MCH(SiMe_3)_2$ (M = Li, K). Particularly under forcing conditions (e.g., excess $MCH(SiMe_3)_2$ (M = Li, K) and long reaction times), extensive epimerization occurs. Amidation of (*R*)-**4f,h**, (*S*)-**5a,b**, and (*R*)-**5c** provides a high-yield route to the complementary (*R*)- and (*S*)-configurational epimers of amido complexes **7b,e,g**. Figures 9B and 9C clearly demonstrate the pseudoenantiomorphous relationship between the (*R*)- and (*S*)-amides **7e** and **7g**, respectively. Interestingly, the (–)-phenylmenthyl complex (*S*)-**4i** undergoes almost complete epimerization upon substitution with $LiCH(SiMe_3)_2$ and to a lesser extent with $NaN(SiMe_3)_2$. The epimer ratios of the products **6i** and **7h**, 82:18 and 61:39, respectively, favor the (*R*)-epimer, with a configuration opposite that of the precursor complex. This configurational assignment is based on the similarity of the CD spectrum of the (–)-phenylmenthyl complex **6i** with those of the corresponding (–)-menthyl complexes (*R*)-**6f** and (*R*)-**6g** (Figure 9A). The (*R*)-configuration of **6g** is unambiguously assigned from the diffraction study. Apparently, diastereoselection in eqs 7 and 8 reflects the relative stability of the epimers of precursor complexes **4** and **5** in diethyl ether (*vide supra*), although similar stereochemical outcomes are observed in weakly coordinating toluene.

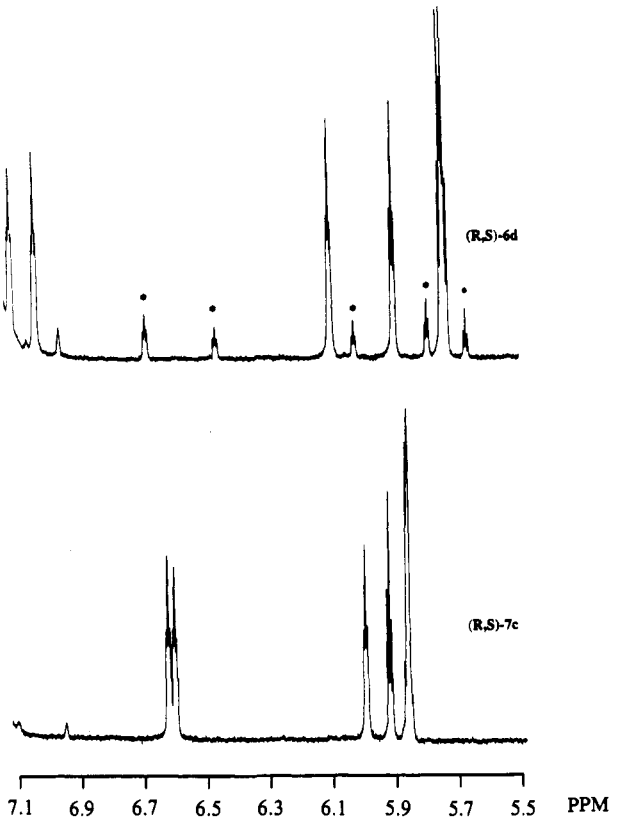

Figure 8. ^{1}H NMR spectra (400 MHz) of (*R,S*)-Me_2SiCp''[(+)-neomenthylCp]$YCH(TMS)_2$ [(*R,S*)-**6d**] and (*R,S*)-Me_2SiCp''[(+)-neomenthylCp]$YN(TMS)_2$ [(*R,S*)-**7c**] in the cyclopentadienyl region as C_6D_6 solutions. Minor isomers of (*R,S*)-**6d** are indicated by asterisks.

The extent of epimerization attending eqs 7 and 8 also depends strongly on the cation of the metal alkyl or amide reagent. *In situ* ^{1}H NMR spectroscopic experiments indicate that alkali metal exchange between $MN(SiMe_3)_2$ (M = Na, K) and LiCl (from chloro precursors **4** and **5**) occurs under the reaction conditions of eq 8 and that the formation of $LiN(SiMe_3)_2$ may account for partial epimerization in the formation of (*R*)-(+)-neomenthyl amides **7a–d**. NMR scale reactions between either (*R*)-**4d** or (*R*)-**4e** and 1 equiv of $LiN(SiMe_3)_2$ lead to formation of essentially

(42) (a) Lappert, M. F.; Riley, P. I.; Yarrow, P. I. W.; Atwood, J. L.; Hunter, W. E.; Zaworotko, M. J. *J. Chem. Soc., Dalton Trans.* **1981**, 814–821. (b) Jeffery, J.; Lappert, M. J.; Luong-Thi, N. T.; Atwood, J. L.; Hunter, W. E. *J. Chem. Soc., Chem. Commun.* **1978**, 1081–1083.

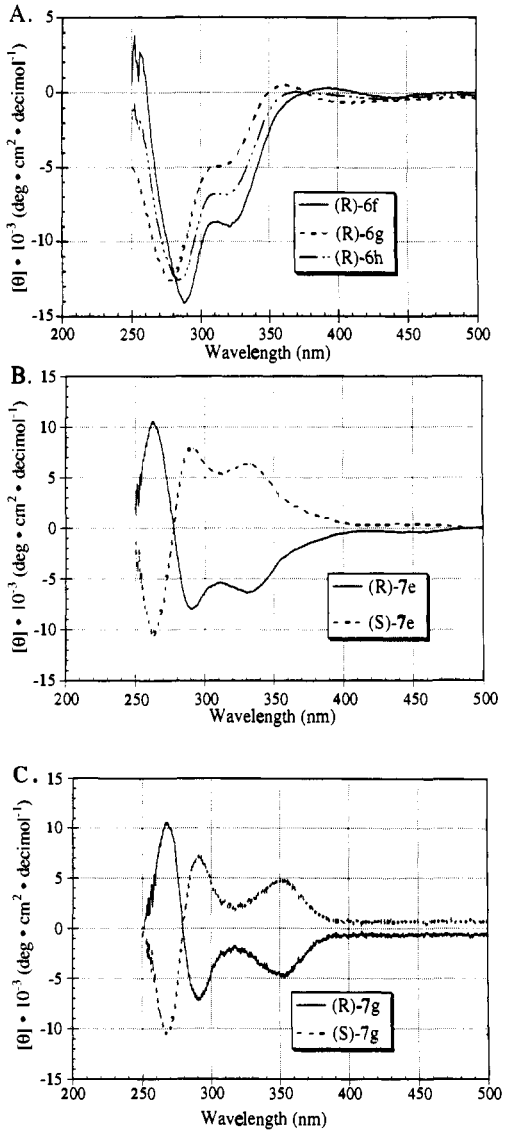

Figure 9. Circular dichroism spectra as solutions in heptane in the 250–500 nm wavelength range. (A) (*R*)-Me_2SiCp''[(–)-menthylCp]SmCH(TMS)$_2$ [(*R*)-**6f**], (*R*)-Me_2SiCp''[(–)-menthylCp]YCH(TMS)$_2$ [(*R*)-**6g**], and (*R*)-Me_2SiCp''[(–)-menthylCp]LuCH(TMS)$_2$ [(*R*)-**6h**]. (B) (*R*)-Me_2SiCp''[(–)-menthylCp]SmN(TMS)$_2$ [(*R*)-**7e**] and (*S*)-Me_2SiCp''[(–)-menthylCp]SmN(TMS)$_2$ [(*S*)-**7e**]. (C) (*R*)-Me_2SiCp''[(–)-menthylCp]LuN(TMS)$_2$ [(*R*)-**7g**] and (*S*)-Me_2SiCp''[(–)-menthylCp]LuN(TMS)$_2$ [(*S*)-**7g**].

equimolar amounts of the (*R*)- and (*S*)-epimers of **7c** or **7d**, respectively. However, if *2 equiv* of either KCH(SiMe$_3$)$_2$ or MN(SiMe$_3$)$_2$ (M = Na, K) are employed with the (*R*)-(+)-neomenthyl chlorides (eq 9), only a single hydrocarbyl or amide complex, **6** or **7**, respectively, is observed.

$$Me_2SiCp''(R^*Cp)Ln(\mu\text{-}Cl)_2Li(S)_x + 2ME(TMS)_2 \xrightarrow[2.\ \text{pentane}]{1.\ \text{toluene}} Me_2SiCp''(R^*Cp)LnE(TMS)_2 + 2MCl + LiCl \quad (9)$$

E = N, M = Na or K
E = CH, M = K

The equivalent of LiE(SiMe$_3$)$_2$ which remains unreacted after complete consumption of **4** is spectroscopically identifiable. The reaction of MN(SiMe$_3$)$_2$ (M = Na, K) with (*R*)-**4a–e** can be successfully accomplished on a preparative scale, and the (+)-neomenthyl amide complexes **7a–d** can be isolated as optically pure crystalline solids. The similar chemical shift dispersions in the ^{1}H NMR spectra of these diamagnetic complexes (**7a,c,d**),

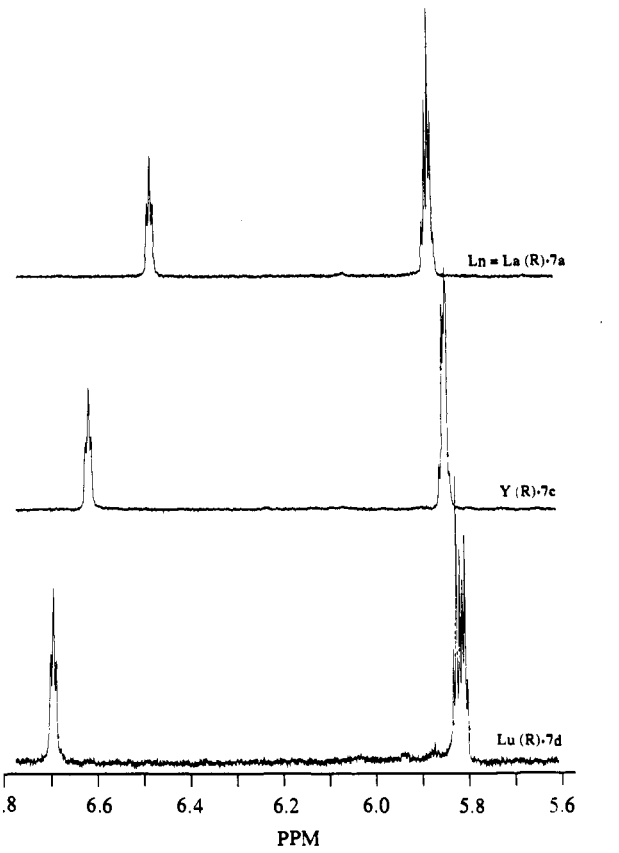

Figure 10. ^{1}H NMR spectra (400 MHz) of (*R*)-Me_2SiCp''[(+)-neomenthylCp]LnN(TMS)$_2$ (Ln = La, Y, Lu) [(*R*)-**7a,c,d**] in the cyclopentadienyl region as solutions in C_6D_6.

particularly in the diagnostic Cp region (Figure 10), suggest a common planar chiral configuration. The (*R*)-configuration is assigned to **7a–d** on the basis of CD spectra (Figure 11A), which display a higher energy absorption with a negative Cotton effect. The CD spectra of corresponding optically-pure (+)-neomenthyl chloro complexes (*R*)-**4b–e** display a similar negative Cotton effect. These complexes are assigned the (*R*)-configuration on the basis of the diffraction-derived molecular structure of (*R*)-**4e** (*vide supra*). The similarity of the CD spectra of the (+)-neomenthyl and (–)-menthyl Y amide complexes (*R*)-**7c** and (*R*)-**7f**, respectively, additionally supports this configurational assignment (Figure 11B). The latter complex is unambiguously assigned the (*R*)-configuration on the basis of a single crystal diffraction study. These observations suggest that the amidation reaction of eq 9 proceeds largely with retention of configuration at the Ln center. Furthermore, short duration preparative scale reactions using *2 equiv* of KCH(SiMe$_3$)$_2$ and (*R*)-**4d** or (*R*)-**4e** in diethyl ether, benzene, or toluene substantially suppress epimerization. However, prolonged reaction times lead to significant epimerization. This may be a consequence of either the greater reactivity or the differing steric demands of the CH(TMS)$_2$ reagent versus the N(TMS)$_2$ reagent.

In contrast to the (*R*)-epimer, (*S*)-Me_2SiCp''[(+)-neomenthylCp]Sm(μ-Cl)$_2$Li(ether)$_2$ (**4c**) does not undergo significant epimerization during the alkylation and amidation reactions (eqs 7 and 8) at ambient temperature. *In situ* ^{1}H NMR of the reaction mixtures indicates the presence of a single epimer of the hydrocarbyl and amide complexes, **6c** and **7b**, respectively. Although the reaction between (*S*)-**4c** and 1 equiv of LiCH(SiMe$_3$)$_2$ at low temperature (–78 °C) does result in considerable epimerization of reaction product **6c**, the ambient temperature reaction can be successfully accomplished on a preparative scale with only a single equivalent of alkylating or amidating reagent. Products **6c** and **7b** are isolated as crystalline, homochiral

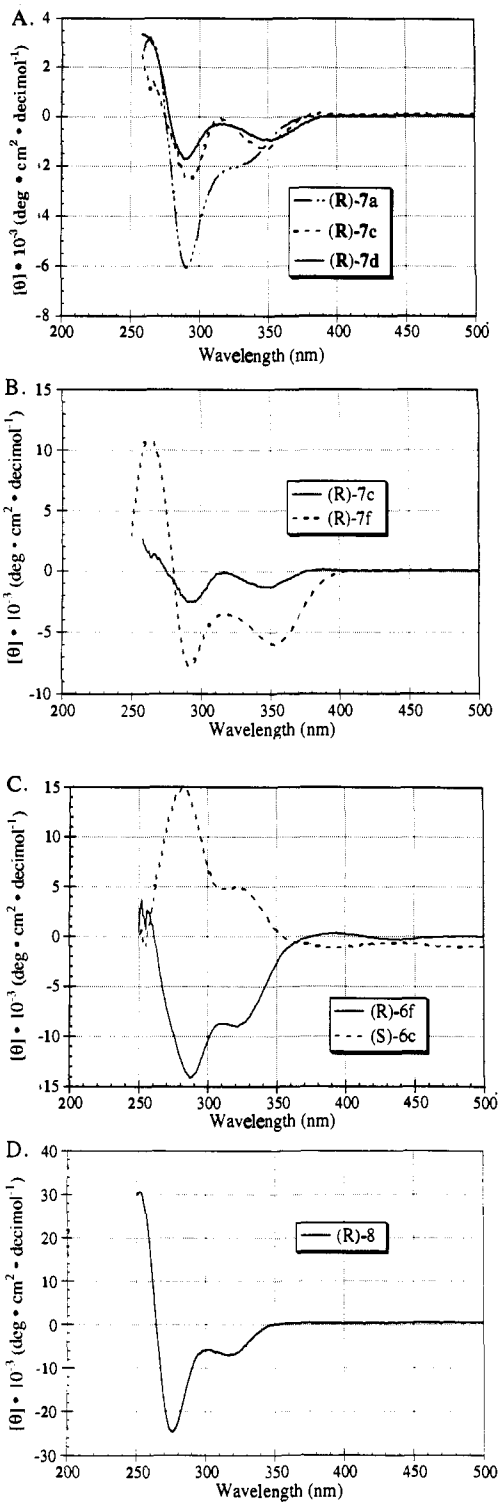

Figure 11. Circular dichroism spectra as solutions in heptane in the 250–500 nm wavelength range. (A) (*R*)-Me_2SiCp''[(+)-neomenthylCp]-LnN(TMS)$_2$ (Ln = La, Y, Lu) [(*R*)-**7a,c,d**]. (B) (*R*)-Me_2SiCp''[(+)-neomenthylCp]YN(TMS)$_2$ [(*R*)-**7c**] and (*R*)-Me_2SiCp''[(−)-menthylCp]-YN(TMS)$_2$ [(*R*)-**7f**]. (C) (*R*)-Me_2SiCp''[(−)-menthylCp]SmCH(TMS)$_2$ [(*R*)-**6f**] and (*S*)-Me_2SiCp''[(+)-neomenthylCp]SmCH(TMS)$_2$ [(*S*)-**6c**]. (D) Me_2SiCp''[(+)-neomenthylCp]Lu(η^2-2-$Me_2NCH_2C_6H_4$) (**8**).

complexes, which are assigned the (*S*)-configuration on the basis of CD spectra. The CD absorptions of (*S*)-**6c** display opposite, positive Cotton effects in comparison to the corresponding (−)-menthylsamarium complex **6g** (Figure 11C), which has been unambiguously assigned the (*R*)-configuration from a single crystal diffraction study (*vide infra*). The (*S*) assignment in the (+)-neomenthylsamarium complex **7b** is confirmed by a single crystal diffraction study of (*S*)-**7b**.

The reaction between (*R*)-**4e** and other alkylating reagents was also investigated. Both Me_2SiCp''[(+)-neomenthylCp]Lu-(η^2-2-$C_6H_4CH_2NMe_2$) (**8**) and Me_2SiCp''[(+)-neomenthylCp]-Lu(η^2-$(CH_2)_2PMe_2$) (**9**) were synthesized in this manner from Li(2-$C_6H_4CH_2NMe_2$) (eq 10) or Li$(CH_2)_2P(CH_3)_2$ (eq 11), respectively.

$$Me_2SiCp''[(+)\text{-neomenthylCp}]Lu(\mu\text{-Cl})_2Li(ether)_2 + \underset{\textbf{4e}}{}$$
$$Li(2\text{-}C_6H_4CH_2NMe_2) \xrightarrow[2.\ pentane]{1.\ toluene} Me_2SiCp''[(+)\text{-neomenthylCp}]Lu(\eta^2\text{-}2\text{-}C_6H_4CH_2NMe_2) + \underset{\textbf{8}}{} LiCl \quad (10)$$

$$Me_2SiCp''[(+)\text{-neomenthylCp}]Lu(\mu\text{-Cl})_2Li(ether)_2 + \underset{\textbf{4e}}{}$$
$$Li(CH_2)_2PMe_2 \xrightarrow[2.\ pentane]{1.\ toluene} Me_2SiCp''[(+)\text{-neomenthylCp}]Lu(\eta^2\text{-}(CH_2)PMe_2) + \underset{\textbf{9}}{} LiCl \quad (11)$$

In situ ^{1}H NMR indicates that a single product (**8**) is formed in eq 10. The product is assigned the (*R*)-configuration on the basis of this observation and the similarity of the CD spectrum (Figure 11D) to those of homochiral complexes (*R*)-**6g** and (*R*)-**6i**. A chelating, η^2-bonding mode of the hydrocarbyl group is expected on the basis of analogous $Cp_2Y(\eta^2\text{-}2\text{-}Me_2NCH_2C_6H_4)$.[43] However, for **8**, two hydrocarbyl group chelating arrangements (**M**, **N**) are *a priori* possible for the (*R*)-epimer due to the asymmetry of the chiral ligand. A single set of resonances in the

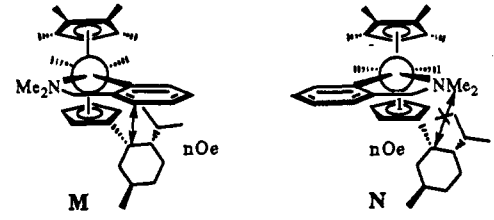

^{1}H NMR spectrum of **8** indicates that one arrangement must be strongly preferred. Difference NOE experiments suggest close proximity of the hydrocarbyl ligand phenyl group to R* as in **M**. Complex **9** is formed in good stereoselectivity (>80%), and the predominant epimer can be isolated optically pure via fractional crystallization. ^{1}H, ^{13}C, and ^{31}P NMR suggest structure **O** in analogy to $Cp'_2Lu(\eta^2\text{-}(CH_2)_2PMe_2)$.[44] The (*R*)-configuration is based on the similarity of the CD spectrum to (*R*)-**8** (*vide infra*). All four methylene protons of the ylide bridge are inequivalent in the NMR due to the asymmetry of the ancillary ligand. The

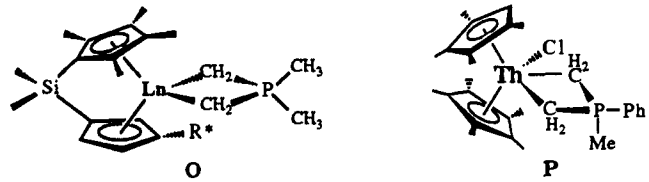

coupling patterns strongly resemble those of the four inequivalent methylene protons observed in the slow exchange limit for Cp'_2-Th(Cl)[η^2-$(CH_2)_2P(CH_3)(Ph)$] (**P**).[45] The yttrium analogue to (*R*)-**9** can be similarly prepared with less epimerization upon substitution. The inequivalent ylide methylene protons undergo rapid interconversion at 25 °C, similar to complex **P**.[45]

Table 4. Selected Metrical Parameters for Chiral Organolanthanide Hydrocarbyl Complexes

(*R*)-**6d**		(*S*)-**6d**		(*R*)-**6f Sm1**		(*R*)-**6f Sm2**		(*R*)-**6g Y1**		(*R*)-**6g Y2**	
					Bond Distances (Å)						
Y1–C1	2.68(1)	Y2–C34	2.45(2)	Sm–C10	2.634(6)	Sm–C50	2.636(5)	Y–C1	2.57(2)	Y–C34	2.59(1)
Y1–C2	2.65(1)	Y2–C35	2.74(2)	Sm–C11	2.737(6)	Sm–C51	2.694(6)	Y–C2	2.66(1)	Y–C35	2.71(1)
Y1–C3	2.78(2)	Y2–C36	2.84(1)	Sm–C12	2.681(6)	Sm–C52	2.862(6)	Y–C3	2.74(1)	Y–C36	2.77(1)
Y1–C4	2.71(1)	Y2–C37	2.75(2)	Sm–C13	2.738(6)	Sm–C53	2.815(6)	Y–C4	2.67(2)	Y–C37	2.66(1)
Y1–C5	2.60(2)	Y2–C38	2.56(2)	Sm–C14	2.613(6)	Sm–C54	2.677(6)	Y–C5	2.57(1)	Y–C38	2.53(1)
Y1–C6	2.64(1)	Y2–C49	2.49(2)	Sm–C1	2.616(9)	Sm–C41	2.609(8)	Y–C6	2.55(1)	Y–C49	2.55(1)
Y1–C7	2.68(1)	Y2–C53	2.53(2)	Sm–C2	2.658(9)	Sm–C45	2.719(9)	Y–C10	2.63(1)	Y–C50	2.60(1)
Y1–C8	2.75(2)	Y2–C52	2.66(2)	Sm–C3	2.761(8)	Sm–C44	2.841(8)	Y–C9	2.69(2)	Y–C51	2.71(2)
Y1–C9	2.85(1)	Y2–C51	2.60(2)	Sm–C4	2.783(8)	Sm–C43	2.822(8)	Y–C8	2.71(2)	Y–C52	2.73(2)
Y1–C10	2.67(2)	Y2–C50	2.61(1)	Sm–C5	2.683(8)	Sm–C42	2.637(8)	Y–C7	2.59(1)	Y–C53	2.62(2)
Y1–C25	2.49(1)	Y2–C58	2.36(1)	Sm–C33	2.504(7)	Sm–C73	2.487(7)	Y–C25	2.40(1)	Y–C58	2.41(1)
Y1–C29	2.86(2)	Y2–C59	2.77(2)	Sm–C30	2.865(7)	Sm–C68	2.998(6)	Y–C27	2.75(2)	Y–C63	2.73(2)
Y1–Si3	3.238(6)	Y2–Si5	3.204(7)	Sm–Si3	3.285(2)	Sm–Si5	3.312(2)	Y–Si2	3.171(5)	Y–Si6	3.153(5)
Si1–C1	1.83(1)	Si4–C34	1.93(2)	Si1–C10	1.863(6)	Si4–C50	1.862(6)	Si1–C1	1.88(1)	Si4–C34	1.86(1)
Si1–C6	1.89(1)	Si4–C49	1.91(2)	Si1–C1	1.876(8)	Si4–C41	1.880(8)	Si1–C6	1.89(2)	Si4–C49	1.87(1)
Si1–C33	1.88(2)	Si4–C65	1.84(2)	Si1–C25	1.848(8)	Si4–C66	1.868(7)	Si1–C33	1.87(2)	Si4–C66	1.88(2)
Si1–C32	1.78(2)	Si4–C66	1.93(2)	Si1–C26	1.861(7)	Si4–C65	1.866(7)	Si1–C32	1.88(2)	Si4–C65	1.82(2)
					Bond Angles (deg)						
Cg1–Y1–Cg2[a]	125.5	Cg1–Y2–Cg2[a]	130.0	Cg1–Sm–Cg2[a]	120.6	Cg1–Sm–Cg2[a]	121.1	Cg1–Y–Cg2[a]	124.3	Cg1–Y–Cg2[a]	123.5
C1–Si1–C6	103.9(6)	C34–Y2–C49	93.3(9)	C10–Si1–C1	98.7(3)	C50–Si4–C41	99.8(3)	C1–Si1–C6	99.2(6)	C34–Si4–C49	99.1(6)
C33–Si1–C32	103.4(9)	C65–Y2–C66	112.1(8)	C25–Si1–C26	107.5(4)	C66–Si4–C65	108.7(3)	C33–Si1–C32	107.4(7)	C66–Si4–C65	107.7(7)
Y1–C25–Si2	131.5(9)	Y2–C58–Si6	126.3(8)	Sm–C33–Si2	126.7(4)	Sm–C73–Si6	98.9(3)	Y–C25–Si3	134.5(9)	Y–C58–Si5	133.3(7)
Y1–C25–Si3	92.2(6)	Y2–C58–Si5	101.6(7)	Sm–C33–Si3	97.9(3)	Sm–C33–Si5	127.1(3)	Y–C25–Si2	95.3(6)	Y–C58–Si6	95.2(6)
Y1–C7–C11	110.9(9)	Y2–C50–C54	122(1)	Sm–C2–C6	113.4(6)	Sm–C45–C46	117.3(6)	Y–C10–C14	116(1)	Y–C50–C54	115(1)
Y1–C8–C12	125(1)	Y2–C51–C55	124(1)	Sm–C3–C7	122.7(6)	Sm–C44–C49	127.5(6)	Y–C9–C13	129(1)	Y–C51–C55	127(1)
Y1–C9–C13	117(1)	Y2–C52–C56	135(1)	Sm–C4–C8	125.4(6)	Sm–C43–C48	125.4(5)	Y–C8–C12	128(1)	Y–C52–C56	124(1)
Y1–C10–C14	119(1)	Y2–C53–C57	120(1)	Sm–C5–C9	120.7(5)	Sm–C42–C47	118.9(5)	Y–C7–C11	119(1)	Y–C53–C57	117(1)
Y1–C3–C15	134(1)	Y2–C36–C39	125(1)	Sm–C12–C15	128.7(4)	Sm–C52–C55	124.5(4)	Y–C3–C15	124(1)	Y–C36–C39	125.6(9)

[a] Cg, ring centroid.

Molecular Structures of Chiral Organolanthanide Hydrocarbyl and Amide Complexes

General Features. Low-temperature single crystal X-ray structural determinations were carried out on selected chiral hydrocarbyl (E = CH) and amide (E = N) complexes to unambiguously establish absolute configuration (**Q** (*S*) and **R** (*R*)) as well as to systematically investigate structural features.

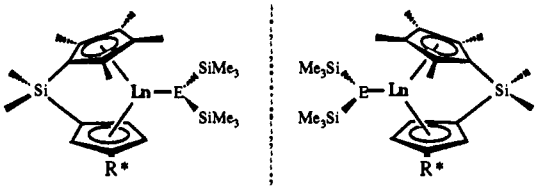

Q(*S*) **R**(*R*)

For ease of comparison, key metrical parameters for the hydrocarbyl and amide complexes are listed in Tables 4 and 5, respectively. The molecular structures of the chiral hydrocarbyl complexes will be discussed first, beginning with (*R*,*S*)-Me_2SiCp''-[(+)-neomenthylCp]YCH$(SiMe_3)_2$ (*R*,*S*)-**6d**. This complex typifies the (+)-neomenthyl hydrocarbyl complexes in that (*R*)- and (*S*)-planar chiral configurations crystallize in *the same unit cell*. This not entirely improbable crystallization phenomenon[46] allows a detailed comparison between the (*R*)- and (*S*)-configurations of this complex. Furthermore, the analogous Sm complex **6c** was determined to be isostructural in a preliminary X-ray study. The structures of (*R*)-**6g** and (*R*)-**6f** are then discussed. In particular, a detailed comparison is made between (*R*)-**6g** and the (*R*)-molecule in (*R*,*S*)-**6d**. These complexes possess the same planar configuration, Ln^{3+} ion, and E, but have different chiral auxiliaries. Additionally, (*R*)-**6f** and (*R*)-**6g** are compared, with these complexes possessing the same planar configuration, chiral auxiliary, and E, but differing in Ln^{3+} ion. This series of related hydrocarbyl complexes allows a detailed examination of the various structural factors which determine the spatial disposition of the (+)-neomenthyl and (–)-menthyl ancillary ligands. Next, the structures of three representative amide complexes ((*S*)-**7b**, (*S*)-**7e**, and (*R*)-**7f**) are discussed, with comparisons being made between complexes that differ by a single structural feature. Additionally, comparisons between similar hydrocarbyl and amide complexes are made. Of interest in all cases is the disposition of the chiral ancillary ligation and, in particular, the spatial orientation of the chiral auxiliary, namely the orientation of the *i*-Pr group (*syn* or *anti*) to the Me_2Si bridge. The orientation of the chiral auxiliary is significant because it serves as a primary stereochemical basis for asymmetric induction.[20]

In all the structures, a single trimethylsilyl substituent of the hydrocarbyl or amide ligand approaches the Ln^{3+} center at an acute ∠Ln–Cα–Siβ (S), a pattern observed previously in $Cp'_2LnE(SiMe_3)_2$ (E = CH, N) derivatives.[2,4,19] This geometry has been attributed in recent theoretical studies,[47] supported by corroboratory PES evidence,[48] to an interaction between the electron-deficient Ln^{3+} center and the electron density of the Si–C bond. The present close contacts between Ln–Siβ, (3.153(5)–3.238(6) Å), formally nonbonding in the classical sense, suggest an appreciable interaction in the solid state. Indeed, the Ln–Cγ contacts (2.73(2)–2.998(6) Å) are indistinguishable from the upper limit of the range of the formally interacting Ln–C_{ring} distances (2.63(4)–2.78(2) Å). Consequently, the Ln–Cα bond does not lie in the Ln,Cg(1),Cg(2) plane (for symmetric complexes such as $Cp'_2LnCH(SiMe_3)_2$ and $Me_2SiCp''_2LnCH(SiMe_3)_2$, a mirror plane bisects the π ancillary ligand–Ln framework) and instead is skewed in the equatorial girdle toward one side of the

(43) Rausch, M. D.; Foust, D. F.; Rogers, R. D.; Atwood, J. L. *J. Organomet. Chem.* **1984**, *265*, 241–248.
(44) (a) Schumann, H.; Albrecht, I.; Reier, F.-W.; Hahn, E. *Angew. Chem., Int. Ed. Engl.* **1984**, *23*, 522–523. (b) Manzer, L. *Inorg. Chem.* **1976**, *14*, 2567–2569.
(45) Cramer, R. E.; Roth, S.; Edelmann, F.; Bruck, M. A.; Cohn, K. C.; Gilje, J. W. *Organometallics* **1989**, *8*, 1192–1199.
(46) Brock, C. P.; Schweizer, W. B.; Dunitz, J. D. *J. Am. Chem. Soc.* **1991**, *113*, 9811–9820 and references therein.
(47) (a) Tatsumi, K.; Nakamura, A. *J. Am. Chem. Soc.* **1987**, *109*, 3195–3206. (b) Bursten, B. E.; Fang, A. *Inorg. Chim. Acta* **1985**, *110*, 153–160. (c) Koga, N.; Morokuma, K. *J. Am. Chem. Soc.* **1988**, *110*, 108–112.
(48) Fragalá, I. L. *Abstracts of Papers*; 197th National Meeting of the American Chemical Society, Dallas, TX, April 9–14, 1989; American Chemical Society: Washington, DC, 1989; INOR39.

Table 5. Selected Metrical Parameters for Chiral Organolanthanide Amide Complexes

(S)-7b		(S)-7e		(R)-7f Y1		(R)-7f Y2	
			Bond Distances (Å)				
Sm–C12	2.644(6)	Sm–C10	2.67(1)	Y–C10	2.603(8)	Y–C50	2.59(1)
Sm–C13	2.651(7)	Sm–C14	2.74(1)	Y–C11	2.675(9)	Y–C51	2.66(1)
Sm–C14	2.771(7)	Sm–C13	2.93(1)	Y–C12	2.79(1)	Y–C52	2.81(1)
Sm–C15	2.881(6)	Sm–C12	2.89(1)	Y–C13	2.69(1)	Y–C53	2.747(9)
Sm–C11	2.738(7)	Sm–C11	2.69(1)	Y–C14	2.590(9)	Y–C54	2.61(1)
Sm–C16	2.670(7)	Sm–C1	2.73(1)	Y–C1	2.59(1)	Y–C41	2.57(1)
Sm–C20	2.705(6)	Sm–C5	2.71(1)	Y–C2	2.61(1)	Y–C42	2.61(1)
Sm–C19	2.767(7)	Sm–C4	2.85(1)	Y–C3	2.69(1)	Y–C45	2.669(9)
Sm–C18	2.763(7)	Sm–C3	2.94(1)	Y–C4	2.70(1)	Y–C44	2.76(1)
Sm–C17	2.685(5)	Sm–C2	2.81(1)	Y–C5	2.64(1)	Y–C43	2.71(1)
Sm–N	2.300(5)	Sm–N	2.302(9)	Y–N	2.281(8)	Y–N	2.211(8)
Sm–C29	3.077(7)	Sm–C29	3.03(1)	Y–C30	2.875(4)	Y–C72	2.983(6)
Sm–Si2	3.320(2)	Sm–Si2	3.316(2)	Y–Si2	3.174(6)	Y–Si6	3.199(7)
Si3–C12	1.861(7)	Si1–C10	1.92(1)	Si1–C10	1.87(1)	Si4–C50	1.86(1)
Si3–C16	1.868(7)	Si1–C1	1.89(2)	Si1–C1	1.87(1)	Si4–C41	1.85(1)
Si3–C31	1.862(8)	Si1–C25	1.86(2)	Si1–C25	1.85(1)	Si4–C66	1.85(1)
Si3–C32	1.866(8)	Si1–C26	1.87(1)	Si1–C26	1.86(1)	Si4–C65	1.87(1)
			Bond Angles (deg)				
Cg1–Sm–Cg2[a]	119.3	Cg1–Sm–Cg2[a]	121.3	Cg1–Y–Cg2[a]	122.1	Cg1–Y–Cg2[a]	122.4
C12–Si3–C16	99.6(3)	C10–Si1–C1	101.9(6)	C10–Si1–C1	98.1(4)	C50–Si4–C41	98.4(4)
C31–Si3–C32	106.9(4)	C25–Si1–C26	106.7(7)	C25–Si1–C26	109.7(5)	C65–Si4–C66	108.5(5)
Sm–N–Si1	115.1(3)	Sm–N–Si2	109.0(5)	Y–N–Si3	123.4(4)	Y–N–Si5	109.4(3)
Sm–N–Si2	111.4(3)	Sm–N–Si3	121.5(4)	Y–N–Si2	105.9(4)	Y–N–Si6	125.9(5)
Sm–C20–C24	122.7(6)	Sm–C5–C9	114.1(9)	Y–C2–C6	116.8(7)	Y–C42–C47	119.5(6)
Sm–C19–C23	124.1(5)	Sm–C4–C8	119.7(9)	Y–C3–C7	125.9(7)	Y–C45–C46	119.9(7)
Sm–C18–C22	121.3(5)	Sm–C3–C7	126.5(9)	Y–C4–C8	125.2(8)	Y–C44–C49	130.0(8)
Sm–C17–C21	119.2(4)	Sm–C2–C6	118.1(8)	Y–C5–C9	121.2(8)	Y–C43–C48	124.7(7)
Sm–C15–C2	127.2(4)	Sm–C12–C15	123.7(8)	Y–C12–C15	128.7(5)	Y–C52–C55	130.9(6)

[a] Cg, ring centroid.

molecule (S). For the present laterally dissymmetric complexes,

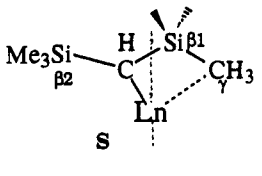

S

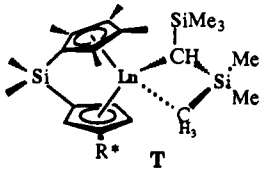

T

the anomalous Me_3Si substituent approaches, counterintuitively, the more sterically crowded site of the organolanthanide, i.e., that appended to the bulky R* chiral auxiliary. This is observed in *all* of the present hydrocarbyl complexes, with the two Ln–Cα–Siβ angles ranging from 92.2(6)° to 101.6(4)° for ∠Ln–Cα–Siβ1 and from 126.3(8)° to 134.5(9)° for ∠Ln–Cα–Siβ2. This phenomenon is also observed, although to a lesser degree, in all but one of the amide complexes, with the two Ln–Cα–Siβ angles ranging from 105.9(4)° to 109.4(3)° for ∠Ln–Cα–Siβ1 and from 121.5(5)° to 125.9(5)° for ∠Ln–Cα–Siβ2. If this close approach is constructed as incipient metallacyclobutane formation, which it indeed geometrically resembles, then the more highly substituted half of the quasimetallacycle, i.e., that with the noninteracting trimethylsilyl substituent, orients *anti* to the sterically-demanding chiral auxiliary as in T. The fact that $Cp'_2LnCH(SiMe_3)_2$ and $Me_2SiCp''_2LnCH(SiMe_3)_2$ undergo facile cyclometalation[4] supports this structural analogy to an incipient metallacycle.[4a] However, in the $N(TMS)_2$ complex (S)-**7b**, the TMS substituent approaches the Sm center on the less sterically crowded side of the complex—the side distal to the chiral auxiliary. This complex exhibits similar ∠Ln–Cα–Siβ1 and ∠Ln–Cα–Siβ2 angles, 111.4(3)° and 115.1(3)°, respectively. The small difference in the ∠Ln–Cα–Siβ angles (<4°) may be a result of adventitious packing forces and not of any interaction between the Sm center and the Siβ–Cγ bond. The long Sm–Siβ1 contact (3.384(2) Å) supports the latter assertion. Indeed, this distance is very similar to the distances observed in achiral $Cp'_2SmN(TMS)_2$[41] (3.387(1) and 3.416(1) Å), which does not exhibit agostic interactions between the Siβ–Cγ bond and the Sm center.

Molecular Structures of Chiral Hydrocarbyl Complexes. X-ray structure analysis of **6d** reveals that the unit cell contains two crystallographically independent molecules with opposite planar chiral configurations of the chirally-substituted cyclopentadienyl ligand. The structures of (R)-Me_2SiCp''[(+)-neomenthylCp]-$YCH(SiMe_3)_2$ and (S)-Me_2SiCp[(+)-neomenthylCp]$YCH(SiMe_3)_2$ (Figures 12A and 12B, respectively) clearly demonstrate this epimeric relationship. A preliminary structure determination for **6c** indicates an identical molecular arrangement in the asymmetric unit. In contrast, X-ray analysis of homochiral (R)-**6g** and (R)-**6f** indicates that each unit cell contains two symmetry-related sets of two independent molecules, with each adopting only a single planar chiral configuration, the (R)-configuration. These observations confirm the configurational assignments of (R)-**6g** and (R)-**6f** from CD spectra (*vide supra*). The molecular structures (R)- and (S)-**6d**, (R)-**6g**, and (R)-**6f** adopt the bent metallocene arrangement typical of Cp'_2LnR complexes[2,41] and ring-linked analogues;[4,19] the structures are unremarkable in this respect. Also, one Me_3Si group approaches the Ln^{3+} center at an acute ∠Ln–Cα–Siβ similar to those of other Me_3Si groups (*vide supra*). Of interest in the present complexes are the spatial disposition of the π-ancillary ligands, the $CH(TMS)_2$ fragment, and the chiral auxiliary.

The presence of both epimers in the unit cell of **6d** permits detailed comparison of the respective (R) and (S) molecular structures (Figure 12). For most features, no significant differences in metrical data are observed between (R)- and (S)-**6d**. However, some disparities appear with respect to the disposition of the hydrocarbyl and π-ancillary ligands. For the $CH(TMS)_2$ group, significant metrical differences are observed between the (R)- and (S)-epimers which suggest greater steric crowding at the Y^{3+} ion in (R)-**6d**. Thus, the Y–Cα bond distance is *significantly longer* in the (R)-epimer (2.49(1) Å) than in the (S)-epimer (2.36(1) Å). In more sterically crowded $Cp'_2YCH(SiMe_3)_2$,[2c] Y–Cα = 2.47(1) Å, closely approaching tht of (R)-**6d**. However, the Y–Cα bond distance in (S)-**6d** is very short, approaching the corresponding Lu–Cα bond distance (2.365(7) Å) in even less crowded $Me_2SiCp''CpLuCH(SiMe_3)_2$.[19] This is

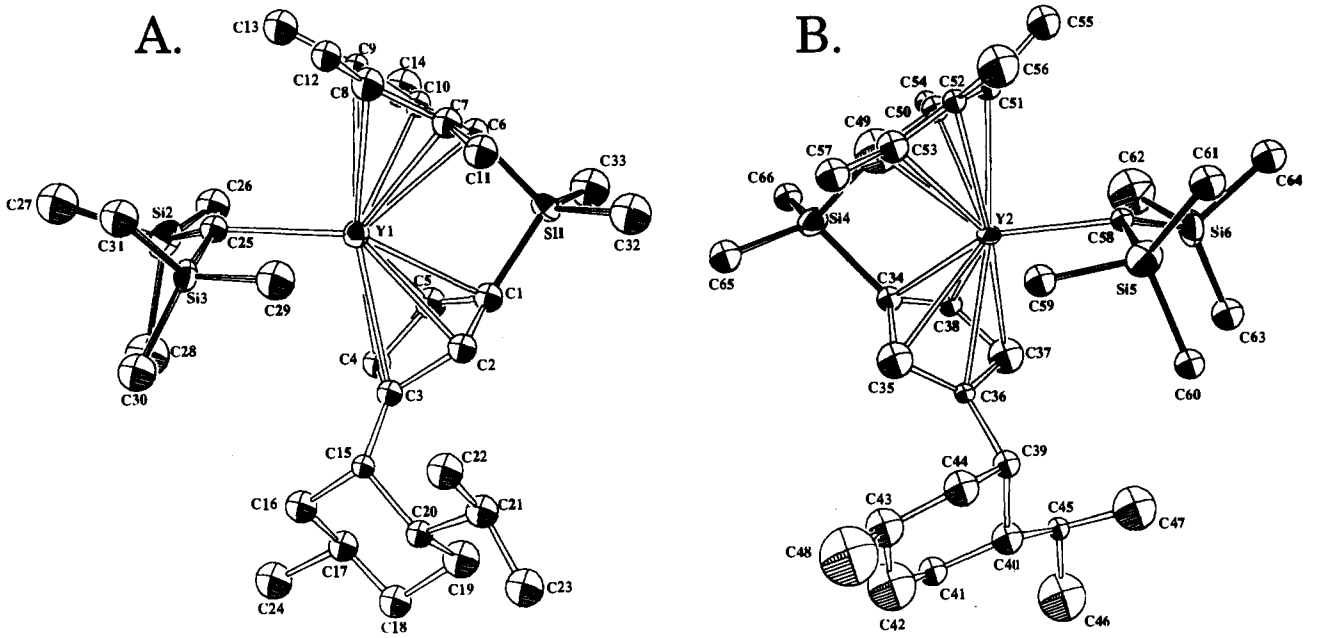

Figure 12. Perspective ORTEP drawing of the molecular structures of (A) (*R*)-$Me_2SiCp''[(+)$-neomenthylCp]YCH$(TMS)_2$ [(*R*)-**6d**] and (B) (*S*)-$Me_2SiCp''[(+)$-neomenthylCp]YCH$(TMS)_2$ [(*S*)-**6d**].

especially significant considering the smaller eight-coordinate ionic radius of Lu^{3+} (0.977 Å) versus that of Y^{3+} (1.019 Å).[49] Additionally, ∠Y–Cα–Siβ is rather acute in (*R*)-**6d** (92.2(6)°) in comparison to those of (*S*)-**6d** (101.6(7)°) and other Cp'_2-$LnCH(SiMe_3)_2$ complexes.[2,4,19] This may be in partial compensation for the longer Y–Cα contact in (*R*)-**6d**. Analogously, a significant decrease in ∠Y–Cα–Siβ is observed in (*R*)-**6d**, which has a longer Y–Cα bond in comparison to that of (*S*)-**6d**, with a shorter Y–Cα contact. Structural differences in the geometry of the π-ancillary ligand are also observed between the two epimers of **6d**. Thus, the C(1)–Si(1)–C(6) angle of 103.9(6)° in (*R*)-**6d** is larger than the corresponding angle C(34)–Si(4)–C(49), 93.3-(9)°) observed in (*S*)-**6d**. Furthermore, the Y1–C(3)–C(15) angle (134(1)°) is greater in (*R*)-**6d** than the corresponding angle (Y2–C(36)–C(39), 125(1)° in (*S*)-**6d**, which also suggests a greater steric crowding at the yttrium center in (*R*)-**6d**. In addition, the Cg(1)–Y–Cg(2) angle decreases from 130.0° (*S*) to 125.5° (*R*), with a concomitant increase in the dihedral angle of the Cp mean planes from 112.1° (*S*) to 114.0° (*R*).

The origin of the aforementioned structural differences most likely resides in nonbonded interactions between the sterically-demanding chiral auxiliary and the cyclopentadienyl and/or CH-$(TMS)_2$ ligands. The different (*R*), (*S*) planar chiral configurations in **6d** require distinctly different spatial orientations of the (+)-neomenthyl chiral auxiliary in the two epimers, presumably for steric reasons. The (*R*)-epimer adopts a *syn* orientation of the *i*-Pr substituent of the neomenthyl group with respect to the Me_2Si bridge of the ancillary ligand (Figure 12A, *i*-Pr "back"), while the (*S*)-epimer adopts an opposite *anti* orientation (Figure 12B, *i*-Pr "forward"). Note that the *i*-Pr group is equatorially disposed and the Cp group axially as in (+)-neomenthyl (*R*)-**4e** (Figure 2). In general, the disposition of the short nonbonded contacts and consequently their effect on the structure of the complex depend on this orientation (*syn* vs *anti*) of R* for a given epimer. Short nonbonded contacts (less than the sum of the van der Waals radii for methyl–methyl, methylene (4.0 Å), or cyclopentadienyl–methyl, methylene interactions (3.7 Å))[50] are observed in the molecular structures of both (*R*)- and (*S*)-**6d** (Table 6). The (*R*)-epimer has multiple short nonbonded interactions between the *i*-Pr group and the proximal carbons C(2), C(3), and C(11) of the Cp ligand (Figure 12A), while

(49) Shannon, R. E. *Acta Crystallogr.* **1976**, *A32*, 751–760.
(50) Bondi, A. *J. Chem. Phys.* **1964**, *68*, 441.

Table 6. Nonbonded Contacts between Nonadjacent Carbon Atoms Less than the Sum of the van der Waals Radii for (*R*)-$Me_2SiCp''[(+)$-neomenthylCp]YCH$(SiMe_3)_2$ [(*R*)-**6d**] and (*S*)-$Me_2SiCp''[(+)$-neomenthylCp]YCH$(SiMe_3)_2$ [(*S*)-**6d**]

(*R*)-**6d**		(*S*)-**6d**	
C(2)–C(19)	3.62(2)	C(35)–C(44)	2.92(2)
C(2)–C(20)	3.28(2)	C(35)–C(43)	3.17(2)
C(2)–C(21)	3.31(2)	C(36)–C(43)	3.28(2)
C(2)–C(23)	3.63(2)	C(36)–C(41)	3.18(2)
C(3)–C(17)	3.12(2)	C(36)–C(40)	2.63(2)
C(3)–C(19)	3.18(2)	C(36)–C(45)	3.28(2)
C(3)–C(20)	2.64(2)	C(37)–C(40)	3.37(2)
C(3)–C(21)	3.34(2)	C(37)–C(45)	3.21(2)
C(4)–C(16)	2.92(2)	C(37)–C(47)	3.55(3)
C(4)–C(17)	3.24(2)	C(37)–C(58)	3.66(2)
C(11)–C(22)	3.86(2)	C(52)–C(59)	3.65(2)
C(12)–C(29)	3.75(2)	C(51)–C(58)	3.34(2)
C(13)–C(25)	3.59(2)	C(55)–C(59)	3.68(3)
C(13)–C(26)	3.70(3)	C(56)–C(58)	3.78(2)
C(15)–C(29)	3.89(3)	C(39)–C(60)	3.88(2)
C(16)–C(29)	3.88(2)	C(47)–C(63)	3.83(3)

lesser interactions are observed between *i*-Pr and C(36), C(37) of the CpR* ring in the (*S*)-epimer (Figure 12B). These interactions are plausible on the basis of the aforementioned *syn* and *anti* orientations of the *i*-Pr groups for the (*R*)- and (*S*)-epimers, respectively. Additionally, short contacts are observed between C(39), C(44), and C(40) of the chiral auxiliary and C(58), C(63), C(59), and C(60) of the hydrocarbyl ligand in the (*S*)-epimer, while no significant interactions of this type are observed in the (*R*)-epimer. As a consequence of these interactions, the contacts between the Cp'' rings and the $CH(TMS)_2$ ligand are shorter and more numerous in (*S*)-**6d** than in (*R*)-**6d** since the *i*-Pr group forces the $CH(TMS)_2$ group "upward" into the Cp'' ring in the former case.

The differences in the short nonbonded contacts between the (*R*)- and (*S*)-epimers arising from differences in the orientation of the chiral auxiliary account well for the gross differences in the molecular structures of (*R*)- and (*S*)-**6d**. Close contacts between the *i*-Pr R* substituent and C(63), C(59), and C(60) of the $CH(TMS)_2$ ligand should destabilize the aforementioned metal–β-(Si–C) agostic interaction normally observed in the molecular structures of $Cp'_2LnCH(SiMe_3)_2$ complexes.[2,4,19] Indeed, the Y–C(58)–Si(5) angle in (*S*)-**6d** opens considerably, and a shorter than expected Y–C(58) distance is observed,

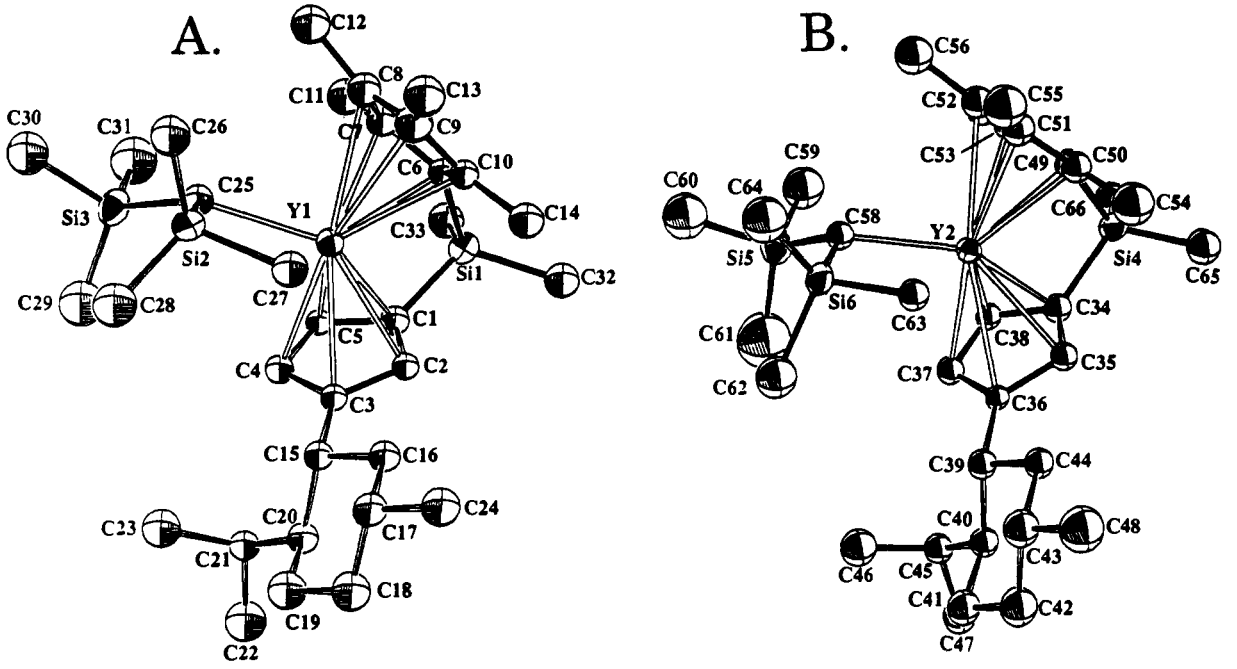

Figure 13. Perspective ORTEP drawing of the molecular structure of (*R*)-Me_2SiCp''[(–)-menthylCp]YCH$(TMS)_2$ [(*R*)-**6g**]. (A) Molecule **Y1**. (B) Molecule **Y2**. All non-hydrogen atoms are represented by thermal ellipsoids drawn to encompass 50% probability.

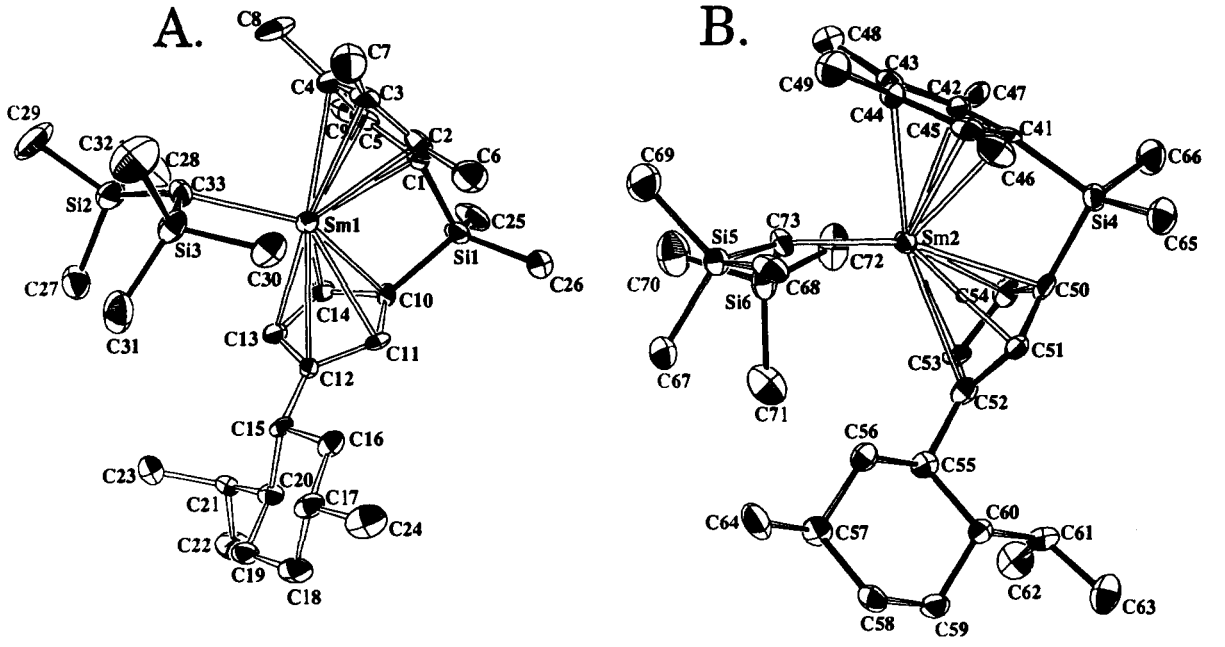

Figure 14. Perspective ORTEP drawing of the molecular structure of (*R*)-Me_2SiCp''[(–)-menthylCp]SmCH$(TMS)_2$ [(*R*)-**6f**]. (A) Molecule **Sm1**. (B) Molecule **Sm2**. All non-hydrogen atoms are represented by thermall ellipsoids drawn to encompass 50% probability.

presumably as a consequence of the lessened agostic interaction. The frontal interactions between the chiral auxiliary, the CH$(SiMe_3)_2$ group, and the Cp'' methyl groups in (*S*)-**6d** also appear to force the Y atom deeper into the Cp_2Y "clamshell", as evidenced by shorter Cg–Y contacts and the opening of ∠Cg(1)–Y–Cg(2) (130.0°). This latter value is larger than typically observed in ring-bridged, bis(cyclopentadienyl)lanthanide complexes (118–126°).[4,19] In contrast, the structure of (*R*)-**6d** suggests that the Y^{3+} is displaced out of the clamshell, as evidenced by relatively long contacts between Y^{3+} and C(1) and C(6), the cyclopentadienyl carbon atoms attached to the Me_2Si bridge. These Y–C(1), C(6) distances approach the Y–C_{ring} distances of intermediate ring carbons C(2), C(5), C(7), and C(10). Consequently, the Y–Cg distances are longer and ∠Cg(1)–Y–Cg(2) (125.5°) more acute in (*R*)-**6d** than the corresponding parameters in (*S*)-**6d**. The anomalously long Y–C(25) contact (2.49 Å) in (*R*)-**6d** remains difficult to account for. However, even with the relatively long Y–C(25) contact and the acute ∠Y–C(25)–C(3), significant nonbonded interactions arise between the methyl groups of CH$(SiMe_3)_2$ and Cp'' in (*R*)-**6d**. This suggests that closer contact between Y and C(25) would give rise to even greater, hence more energetically-demanding, nonbonded repulsions.

X-ray analyses of (–)-menthyl complexes **6g** and **6f** reveal that each unit cell contains two crystallographically independent molecules (**Ln1** and **Ln2**) with the same planar chiral (*R*)-configurations. The structures of the Y and Sm derivatives, **6g** and **6f**, are shown in Figures 13A and B and Figures 14A and B, respectively. A detailed comparison between each of the (*R*)-molecules of menthyl-based (*R*)-**6g** and the (*R*)-molecule of (+)-neomenthyl-based (*R,S*)-**6d** is followed by a comparison of the two (–)-menthyl-based complexes **6g** and **6f**. **Y1** and **Y2** of (*R*)-**6g** and the (*R*)-molecule of (+)-neomenthyl (*R,S*)-**6d** have similar

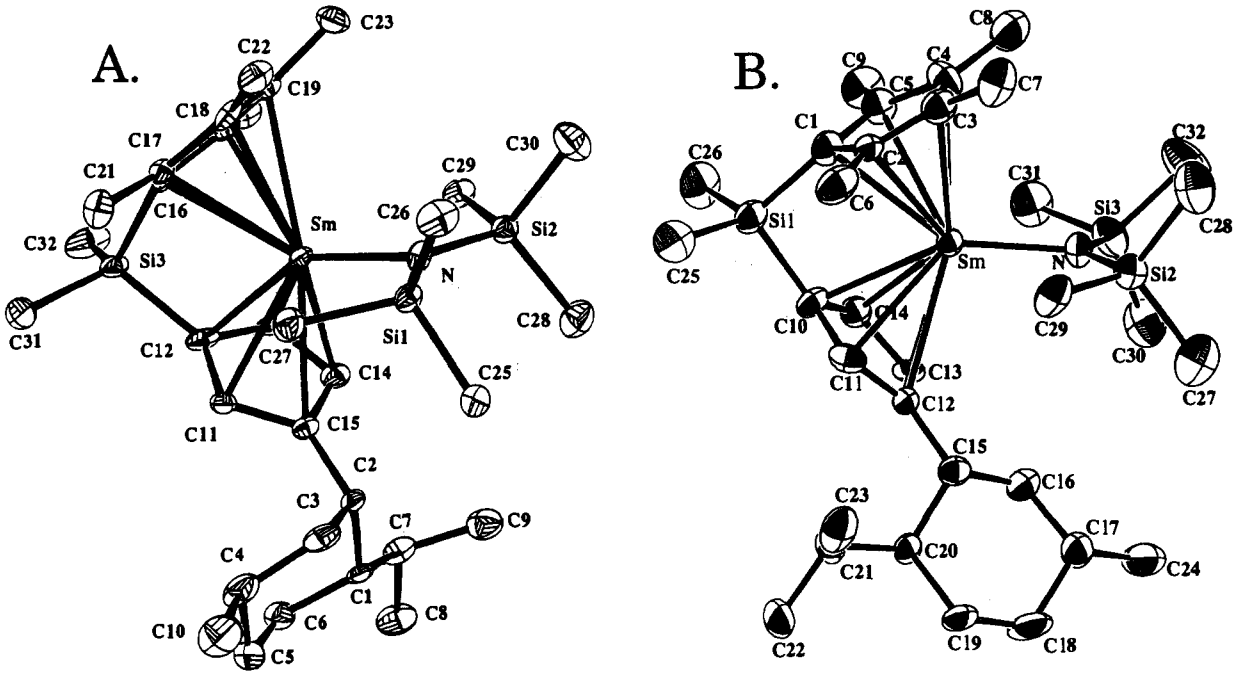

Figure 15. Perspective ORTEP drawing of the molecular structure of (A) (*S*)-Me_2SiCp''[(+)-neomenthylCp]SmN(TMS)$_2$ [(*S*)-**7b**] and (B) (*S*)-Me_2SiCp''[(−)-menthylCp]SmN(TMS)$_2$ [(*S*)-**7e**]. All non-hydrogen atoms are represented by thermal ellipsoids drawn to encompass 50% probability.

metrical parameters. However, there are also significant differences. The *i*-Pr groups of the chiral auxiliaries in **Y1** and **Y2** of (*R*)-**6g** orient *anti* to the Me_2Si bridge (*i*-Pr "forward"), in contrast to the *syn* orientation observed in the (*R*)-molecule of (*R,S*)-**6d** (Figure 12A, *i*-Pr "back"). These constitutionally identical molecules differ only in one stereocenter, that of the sp^3 carbon α to the Cp ring bearing the chiral auxiliary, e.g., 1*S* for (+)-neomenthyl (*and axial Cp*) vs 1*R* for (−)-menthyl (*and equatorial Cp*). This difference manifests itself in several marked structural dissimilarities. The Y–E distances in **Y1** and **Y2** are 2.40(1) and 2.41(1) Å, respectively. However, for (*R*)-**6d**, this distance increases to 2.49(1) Å. Consequently, the Ln–E–Siβ1 angle is more acute (92.2(6)°) in (*R*)-**6d** than in either **Y1** (95.3(6)°) or **Y2** (95.2(6)°) of (*R*)-**6g**. This inverse relationship between the Ln–E–Siβ1 angle and the Ln–E distance is also exhibited in the enantiomerically related (*R*)- and (*S*)-**6d** pair (*vide supra*). Additionally, the Y1–C3–C15 and Y2–C36–C39 angles, 124(1)° and 125.6(9)°, respectively, are substantially more acute in (*R*)-**6g** than ∠Y–C3–C15 (134(1)°) in (*R*)-**6d**. These observations suggest greater steric crowding in the (*R*)-molecule of **6d** than in either **Y1** or **Y2** of (*R*)-**6g**. Additionally, there are several close nonbonded contacts between R* of the (*R*)-molecule of **6d** which are not observed in either **Y1** or **Y2** of (*R*)-**6g**. It thus appears that the *syn* orientation of the *i*-Pr group in the (*R*)-molecule of **6d** results in unfavorable steric interactions between R* and the $CH(TMS)_2$ moiety, resulting in significant distortion of the π ancillary ligands and the $CH(TMS)_2$ fragment.

Molecules **Sm1** and **Sm2** of (*R*)-**6f** differ from the isoleptic Y structure (*R*)-**6g** with respect to orientation of the R* *i*-Pr group (Figure 13). **Y1** and **Y2** of (*R*)-**6g** adopt the *anti* configuration of the *i*-Pr group, while **Sm1** and **Sm2** of (*R*)-**6f** adopt the *anti* and *syn* configurations, respectively. Despite the difference in the orientation of the chiral auxiliary, **Sm1** and **Sm2** have very similar metrical parameters. The Sm–Cα distance in **Sm1** (2.504(7) Å) is slightly longer than that in **Sm2** (2.487(7) Å), with the Sm–Cα–Siβ1 angle of **Sm1** (97.9(3)°) being more acute than that in **Sm2** (98.9(3)°). However, there are substantial differences in the respective Sm–Cγ contacts (2.865(7) versus 2.998(6) Å). The Cg–Sm–Cg angles (120.6° and 121.1°) for **Sm1** and **Sm2**, respectively, are more acute than those observed in either the (*R*)- or (*S*)-molecules of **6d** (125.5° and 130.0°, respectively) or **Y1** and **Y2** of (*R*)-**6g** (124.3° and 123.5°). This most likely results from the greater ionic radius of Sm^{3+}, which forces Sm^{3+} farther out of the Cp_2 "clamshell".

Molecular Structures of Chiral Amide Complexes. Diffraction analyses of (+)-neomenthyl **7b** and (−)-menthyl **7e** indicate the (*S*)-configuration in both complexes (Figures 15A and B, respectively), while analysis of (−)-menthyl **7f** indicates the (*R*)-configuration in the two independent molecules **Y1** and **Y2** (Figures 16A and B, respectively). The complexes display the bent metallocene geometry typically observed in Cp'_2LnR structures.[2,4,19,41] The Cg(1)–Ln–Cg(2) angles (119.3°, 121.3°, 122.1°, and 122.4°) in (*S*)-**7b**, (*S*)-**7e**, and **Y1**, **Y2** of (*R*)-**7f**, respectively, closely agree with the corresponding parameters for early Ln, ring-bridged complexes: $(Me_2SiCp''_2CeCl)_2$ (118.9°),[4b] $(Me_2SiCp''_2NdCl)_2ClLi(THF)_2^+$ (121.3°),[4a] and $Me_2SiCp''_2$-$NdCH(SiMe_3)_2$ (121.6°).[4a] The Ln–C_{ring} distances display the usual dispersion pattern observed in ring-bridged complexes, and the average Ln–C ring distances compare well with Cp'_2LnR complexes.[2c,41,51] No significant distortions of the π ancillary ligation are observed in (*S*)-**7b** or (*S*)-**7e**, in contrast to the (*S*)-molecule of **6d**, which may reflect the different steric requirements of $N(TMS)_2$ *vis-à-vis* $CH(TMS)_2$ and/or the larger ionic radius of Sm^{3+} versus Y^{3+}. However, **Y1** and **Y2** exhibit some distortions in the ancillary ligands. The chiral auxiliary is bent out of the Cp mean plane with Sm–C_{ring}–Cα angles of 128.7(5)° and 130.9(6)°, respectively. These angles approach that observed in the (*R*)-molecule of **6d** (134(1)°), which exhibits significant close contacts between the chiral ancillary ligands and the $CH(TMS)_2$ fragment. Note that the Cp fragment is axially disposed in the (+)-neomenthyl amide structure (**7b**) and equatorially disposed in the (−)-menthyl amides (**7e,f**). As in all structures examined in this study, the *i*-Pr group remains equatorial.

The $N(TMS)_2$ ligand in (*S*)-**7b** is displaced laterally in the equatorial girdle away from the chiral auxiliary, in contrast to all of the other structurally characterized complexes. This complex displays the smallest difference between Ln–Cα–Siβ1 and Ln–Cα–Siβ2 angles of only 3.7°, with the other crystallographically characterized amides having differences in the range of 12.5–17.5°. The Sm–N bond distances (2.300(5) and 2.302(9) Å) in (*S*)-**7b** and (*S*)-**7e**, respectively, correlate well with the corresponding distances for $Cp'_2SmN(SiMe_3)_2$ (Sm–N = 2.301(3)

(51) Evans, W. E.; Ulibarri, T. A. *J. Am. Chem. Soc.* **1987**, *109*, 4292–4297.

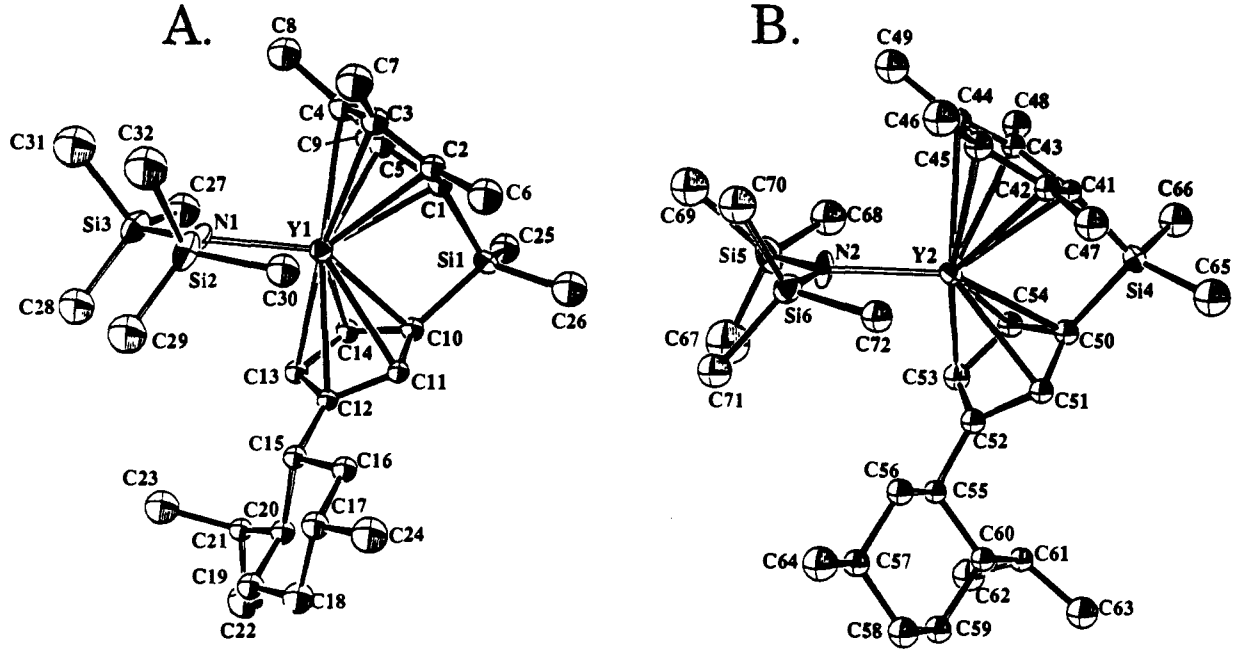

Figure 16. Perspective ORTEP drawing of the molecular structure of (*R*)-Me_2SiCp''[(–)-menthylCp]YN(TMS)$_2$ [(*R*)-**7f**]. (A) Molecule **Y1**. (B) Molecule **Y2**. All non-hydrogen atoms are represented by thermall ellipsoids drawn to encompass 50% probability.

Table 7. Summary of Preferred Chiral Auxiliary Conformations in the Solid State

complex	structure	Cp	*i*-Pr vs Me_2Si
(*R*)-**4e**	(*R*)-neomenthylLuCl	axial	*syn*
(*R*)-**6d**	(*R*)-neomenthylYCH(TMS)$_2$	axial	*syn*
(*S*)-**6d**	(*S*)-neomenthylYCH(TMS)$_2$	axial	*anti*
(*R*)-**6g**	(*R*)-menthylYCH(TMS)$_2$	equatorial	*anti*
(*R*)-**6g**	(*R*)-menthylYCH(TMS)$_2$	equatorial	*anti*
(*R*)-**6f**	(*R*)-menthylSmCH(TMS)$_2$	equatorial	*anti*
(*R*)-**6f**	(*R*)-menthylSmCH(TMS)$_2$	equatorial	*syn*
(*S*)-**7b**	(*S*)-neomenthylSmN(TMS)$_2$	axial	*anti*
(*S*)-**7e**	(*S*)-menthylSmN(TMS)$_2$	equatorial	*syn*
(*R*)-**7f**	(*R*)-menthylYN(TMS)$_2$	equatorial	*anti*
(*R*)-**7f**	(*R*)-menthylYN(TMS)$_2$	equatorial	*syn*

Å),[41] $Cp'_2YN(SiMe_3)_2$ (Y–N = 2.274(5) Å),[2c] and (*R*)-Me_2SiCp''[(–)-menthylCp]YN(SiMe$_3$)$_2$ (Y–N = 2.28 Å) after correction for the difference in eight-coordinate ionic radii between Sm^{3+} and Y^{3+} (0.06 Å)[56] for the latter two complexes. The corresponding N(TMS)$_2$ and CH(TMS)$_2$ complexes exhibit similar structural features but display some significant differences. The shorter Ln–N distances compared to the Ln–Cα distances appear to decrease the agostic interactions between the Ln^{3+} and the Siβ–Cγ bond. Additionally, the planar arrangement of the N(TMS)$_2$ moiety appears to decrease unfavorable steric interactions between R* and the N(TMS)$_2$ fragment compared to the corresponding CH(TMS)$_2$ complexes.

Table 7 summarizes the R* conformations observed in these structural studies. In all cases, the *i*-Pr substituent remains equatorial, while the Cp substituent is axial in (+)-neomenthyl structures and equatorial in (–)-menthyl structures. In all cases where R* = (+)-neomenthyl, the *i*-Pr group is oriented *syn* in the (*R*)-configuration and *anti* in the (*S*)-configuration (four cases). For R* = (–)-menthyl, the *i*-Pr group is oriented *anti* in four out of six (*R*) structures and *syn* in the other two (*R*) structures. In the one (*S*)-(–)-menthyl structure, the orientation is *syn*. The preponderance of these results indicates that, among other structural features, (*R*)- and (*S*)-epimers differ substantially in the orientation of the *i*-Pr substituent.[52]

(52) Efforts to confirm these conformational preferences in solution by ^{1}H NOE studies have so far yielded ambiguous results.

Chiral Organolanthanide Hydrocarbyls and Amides. Stoichiometric Reactivity Patterns

In contrast to chiral chloro complexes **4** and **5**, the hydrocarbyl and amide complexes do not undergo epimerization in solution after isolation. Solutions of (*R*,*S*)-**6c** and (*R*)-**7c** are configurationally stable even after 48 h at 60 °C in C_6D_6. As a prelude to the catalytic studies, it was of interest to study the reactivity of the chiral hydrocarbyl and amide complexes toward primary amines and hydrogen. These reagents were chosen because they are involved in two distinctive organolanthanide-catalyzed olefin transformations, hydroamination/cyclization and hydrogenation, respectively.[20]

Reaction of Complexes 6–9 with Alkylamines. The hydrocarbyl and amide groups of **6–9** are rapidly protonolyzed by simple proton sources such as alkylamines, presumably forming organolanthanide amide–amine adducts (eq 12) in analogy to well-characterized $Cp'_2Ln(NHR)(NH_2R)$ complexes.[8c,53a,b] ^{1}H NMR

$$Me_2SiCp''(R^*Cp)LnR + 2H_2NR' \rightarrow Me_2SiCp''(R^*Cp)Ln(NHR')(NH_2R') + RH \quad (12)$$

spectroscopic experiments indicate that protonolysis of the Ln–R bond occurs with retention of the initial planar chiral configuration, although the incipient amide–amine adducts slowly undergo epimerization in the presence of excess amine, even in weak donor solvents such as toluene. The equilibrium ratios observed for several (+)-neomenthyl complexes in the presence of 40–50-fold excess of *n*-propylamine indicate preponderance of the (*R*)-epimers (Table 8). In contrast, the equilibrium ratios for the (–)-menthyl complexes greatly favor the (*S*)-epimer, with the (*R*)-epimer resonances below ^{1}H NMR detection limits. The equilibrium ratios are independent of the initial optical purity of the precursor complexes, i.e., the pairs (*R*,*S*)-**6e**/(*R*)-**8**, (*R*,*S*)-**6c**/(*S*)-**7b**, and (*R*)-**7e**/(*S*)-**7e** each afford identical equilibrium epimer populations under identical conditions. This observation implies the generation and epimerization of a common molecular species, e.g., $Me_2SiCp''(R^*Cp)Ln(NHPr)(NH_2Pr)$, from either complex under the reaction conditions. Significantly, the prefer-

(53) (a) Heeres, H. J.; Renkema, J.; Booji, M.; Meetsma, A.; Teuben, J. H. *Organometallics* **1988**, *7*, 2495–2502. (b) Bercaw, J. E.; Davies, D. L.; Wolczanski, P. T. *Organometallics* **1986**, *5*, 443–450. (c) Coughlin, E. B.; Bercaw, J. E. *J. Am. Chem. Soc.* **1992**, *114*, 7606–7607.

Table 8. Equilibrium Epimer Populations for Me_2SiCp''[(+)-neomenthylCp]Ln(NH-*n*-Pr)(NH_2-*n*-Pr) at 25 °C in Toluene Solution[a]

initial complex	initial structure	epimer ratio (*R*:*S*)
(*R*,*S*)-**6c**	(*R*,*S*)-neomenthylSmCH(TMS)$_2$	80:20
(*R*,*S*)-**7b**	(*R*,*S*)-neomenthylSmN(TMS)$_2$	81:19
(*R*,*S*)-**6d**	(*R*,*S*)-neomenthylYCH(TMS)$_2$	76:24
(*R*,*S*)-**6e**	(*R*,*S*)-neomenthylLuCH(TMS)$_2$	82:18
(*R*)-**8**	(*R*)-neomenthylLu(η^2-2-$C_6H_4CH_2NMe_2$)	80:20

[a] Determined by ^{1}H NMR spectroscopy.

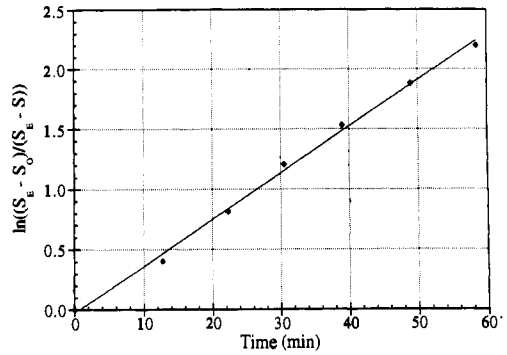

Figure 17. Kinetic plot of the relaxation to equilibrium of (*R*,*S*)-Me_2SiCp''[(–)-phenylmenthylCp]YN(TMS)$_2$ [(*R*,*S*)-**7h**] with excess propylamine in toluene at 25 °C.

ence for the (*R*)-planar chiral configuration of the organolanthanide amine–amido adduct remains approximately constant in the (+)-neomenthyl series as the Ln^{3+} ionic radius contracts, similar to the trend for epimerization of (+)-neomenthyl chloro complexes **4** in THF (*vide supra*). Similarly, the (*S*)-epimer of the (–)-menthyl and (–)-phenylmenthyl amine–amido adducts is selectively formed under identical conditions, just as (*S*)-epimers are preferred in THF under equilibrium conditions.

For (–)-phenylmenthyl complex **7h**, the relaxation to equilibrium of the assumed amine–amido adduct, Me_2SiCp''[(–)-phenylmenthylCp]Y(NHPr)(NH_2Pr), from the initial (61(*R*):39(*S*)) epimer ratio was monitored by ^{1}H NMR. The epimerization process obeys a strict, first-order, two-site equilibrium rate expression (eq 2). The forward (k = 5.74(4) × 10^{-4} s^{-1}; $t_{1/2}$ = 0.34 h) and reverse (k' = 7.1(1) × 10^{-5} s^{-1}; $t_{1/2}$ = 2.7 h) rate constants and the equilibrium constant, K_{eq} = 8.1 ± 0.8, can be extracted from least-squares fitting of the data to eq 2 (Figure 17) for the (*S*) → (*R*) epimerization.

Reaction of Complexes 6–9 with Hydrogen. Among **6–9**, only the CH(TMS)$_2$ complexes **6** undergo significant hydrogenolysis of the E(TMS)$_2$ group at 1 atm of H_2, 25 °C, affording $CH_2(SiMe_3)_2$ and an organolanthanide hydrido complex (eq 13).The

$$2Me_2SiCp''(R^*Cp)LnCH(SiMe_3)_2 + 2H_2 \rightarrow [Me_2SiCp''(R^*Cp)LnH]_2 + 2CH_2(SiMe_3)_2 \quad (13)$$

hydrogenolysis is very rapid as evidenced by ^{1}H NMR and the immediate color change of the Sm solution from red-orange to yellow (characteristic colors of $Cp'_2SmCH(TMS)_2$ and -H complexes, respectively). *In situ* ^{1}H NMR indicates clean and quantitative conversion of the hydrocarbyl complex to a new species. The presence of a stoichiometric amount of $CH_2(TMS)_2$ and a characteristic triplet[19] at δ 4.28 ppm ($^1J_{^{89}Y-^1H}$ = 32 Hz) support the formation of a Y(μ-H)Y structure. As expected, substituting D_2 for H_2 yields $CHD(SiMe_3)_2$ and a Y deuteride in equimolar quantities as evidenced by ^{2}H NMR. However, unlike achiral $(Cp'_2LnH)_2$[2] and $(Me_2SiCp''_2LnH)_2$,[4] the present chiral hydrido species are thermally unstable in solution at ambient temperature, with several unassignable resonances appearing in the ^{1}H spectra within several hours. A dimeric formulation for the initial hydrogenolysis product is in analogy to the well-characterized $(Cp'_2LnH)_2$[2] and $(Me_2SiCp''_2LnH)_2$[4] complexes. *In situ* ^{1}H NMR of the hydrogenolysis products derived from the homochiral (*S*)-**6c** indicates the clean and immediate formation of a single hydride complex with no concomitant epimerization. Two C_2-symmetric dimer structures, U and V, are most plausible.

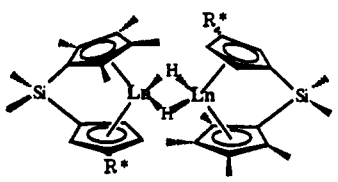

U

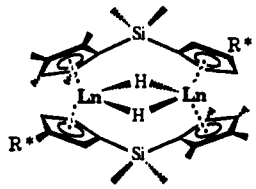

V

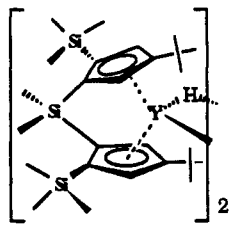

W

Each structure corresponds to a well-characterized organolanthanide motif, either $(Me_2SiCp''_2LnH)_2$ (U)[2b] or $(Et_2SiCp''LuH)_2$ (V)[19] (only the (*S*,*S*)-dimer structure is shown in each case). The ancillary ligation of the chiral complexes more closely resembles the latter complex in the degree of ring substitution. However, the reactivity for the hydrogenation of hindered olefins reported in the following contribution[20] argues for more classical structure U. The ligand redistribution U → V is doubtlessly controlled by the sterics and electronics of the ancillary ligation. The C_2-symmetric complex $[(Me_2Si(1\text{-}TMS\text{-}3\text{-}t\text{-}BuCp)_2YH]_2$ has the structure **W**,[53c] suggesting that sufficient steric bulk may prevent ligand redistribution reactions in even less substituted Cp systems.

Discussion

The organolanthanides Cp'_2LnR and $Me_2SiCp''_2LnR$ (R = $CH(SiMe_3)_2$, H) serve as precatalysts for a variety of interesting and potentially useful olefin transformations.[5-12] These well-defined complexes are readily amenable to kinetic and mechanistic investigations such that molecular level catalyst–substrate interactions can be correlated with macroscopic reactivity/selectivity patterns. Rational modification of the ancillary ligation has now afforded a series of C_1-symmetric Me_2SiCp''[R*Cp]LnR, complexes in which an asymmetric environment is created around the Ln^{3+} center. Structure/reactivity relationships within this chiral series and between it and the parent achiral organolanthanides form the basis for this discussion.

Configurational Stability and Epimerization. Chiral chloro complexes **4** and **5** are obtained as crystalline, optically-pure diastereomers from a single diethyl ether recrystallization of the initial synthetic products. However, they undergo epimerization in donor solvents, with equilibrium populations strongly dependent upon Ln^{3+}, R*, temperature, and solvent. The stereochemistries of homochiral products **4** and **5** actually isolated from the synthesis are determined by the epimerization rate of the complex in a given solvent. For complexes of smaller lanthanides bearing the (+)-neomenthyl and (–)-phenylmenthyl auxiliaries (**4d**, **4e**, **4i**), the (*R*)- and (*S*)-isomers, respectively, are isolated from ambient temperature workup. For **4i**, the epimerization process is relatively slow ($t_{1/2}$ = 119 h). For (+)-neomenthyl complexes of the early lanthanides (**4b**, **4c**) and all of the (–)-menthyl complexes (**4f**, **4g**,

4i), epimerization is more facile at ambient temperature, and consequently, the more stable epimers, (*S*)-**4b**, (*S*)-**4c**, (*R*)-**4f**, (*R*)-**4g**, and (*R*)-**4h**, are isolated in the standard workup. In workup at low temperatures, a mixture of epimers enriched in the opposite epimer is obtained. This mixture closely corresponds to the equilibrium ratio in THF. The (*R*)-epimers of **4b** and **4c** can be isolated optically pure via low-temperature workup, but complexes **4a** and **4f–h** cannot be effectively enriched beyond the THF equilibrium ratio. However, DME adducts of **5** exhibit significantly depressed epimerization rates in the workup solvent (diethyl ether), permitting the less stable (*S*)- and (*R*)-isomers of the (–)-menthyl and early (+)-neomenthyl series to be isolated. DME adducts exhibit poor ether solubility, which facilitates successful fractional crystallization.

The relative stabilities of the **4** and **5** series chloro epimers appear to reflect a complex interplay of steric and solvation (Li^+ ligand) effects. Interestingly, K_{epim} in *THF* is nearly invariant across the Ln^{3+} series within R* = (+)-neomenthyl or R* = (–)-menthyl classes (Table 3). However, K_{epim} in *ether* is sensitive to Ln for R* = (+)-neomenthyl yet insensitive for R* = (–)-menthyl. Variable temperature (*R*) ⇌ (*S*) equilibration studies on **4e** and **4f** (*vide supra*) indicate that ΔH and ΔS differences between epimers are, in this case, small. Some understanding of these and other stereochemical preferences can be found in intramolecular nonbonded repulsions between the chiral auxiliary and the $Me_2SiCp''CpLn$ as well as μ-$Cl_2Li(S)_2/CH(TMS)_2/N(TMS)_2$ fragments of the molecules.

From the diffraction structural studies (Table 7) and substituted cyclohexane conformational considerations, it is not surprising that the *i*-Pr substituent occupies an equatorial position, thus forcing the $Me_2SiCp''CpLnCl_2Li(S)_2$ unit into equatorial or axial dispositions in the (–)-menthyl or (+)-neomenthyl structures, respectively. Examination of the structures and space-filling models indicates that for R* = (–)-menthyl and (–)-phenylmenthyl, nonbonded repulsions between the substituted cyclohexane and the $Me_2SiCp''CpLn$ portion of the complex are minimized when the (*S*)-epimer adopts a *syn* (**X**, *i*-Pr "back") orientation of R* and when the (*R*)-epimer adopts an *anti* (**Y**, *i*-Pr "forward") orientation (eq 14). Indeed, this is the general

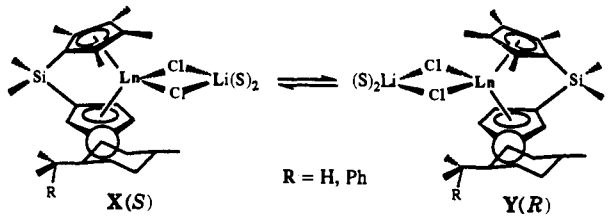

X(*S*) **Y**(*R*)

(14)

pattern observed in the seven crystal structures (Table 7). Note, however, that conformation **Y** (*R*) introduces the greatest nonbonded interactions between the bulky *i*-Pr/Me_2PhC R* substituents and the $Ln(\mu\text{-}Cl)_2Li(S)_2$ group. This result appears consistent, then, with the (*S*)-epimers being the most stable (–)-menthyl/(–)-phenylmenthyl structures in THF (**4f–i**, Table 3). That the (–)-menthyl (*R*)-epimers are more stable in ether solution suggests diminished *i*-Pr/Me_2PhC-$Ln(\mu\text{-}Cl)_2Li(S)_2$ steric interactions, perhaps due to weaker ether coordination of Li^+.

The $R^*Me_2SiCp''CpLnCl_2Li(S)_2/CH(TMS)_2/N(TMS)_2$ relationships change considerably for R* = (+)-neomenthyl, with the Cp unit now in an axial disposition and (*R*)-epimers favoring a *syn* *i*-Pr orientation and the (*S*)-epimers an *anti* (Table 7, eq 15). The diffraction data and space-filling models suggest that *i*-$PrLn(\mu\text{-}Cl)_2Li(S)_2$ nonbonded interactions are now minimized in the (*R*)-epimer and consistent with the above (–)-menthyl/(–)-phenylmenthyl line of argument—the (*R*)-epimer is now favored in THF solution and the (*S*)-epimer in ether (except for the small Lu^{3+} ion; Table 3).

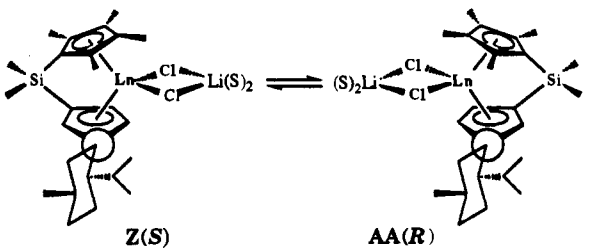

Z(*S*) **AA**(*R*)

(15)

The energetic accessibility of epimer interconversion for **4** has a profound influence on the stereochemical outcome of subsequent alkylation and amidation reactions in ether or toluene. The epimer ratios obtained for **6** generally parallel the equilibrium epimer populations of **4** in ether; (*R*)-**4d** yields (*R*,*S*)-**6d**; (*R*)-**4g** gives (*R*)-**6g**; and (*S*)-**4i** affords predominantly (*R*)-**6i** on reaction with *1 equiv* of $LiCH(SiMe_3)_2$. The $CH(TMS)_2$ ligand apparently prefers an *i*-Pr orientation *anti* to the Me_2Si bridge, i.e., (*S*)-planar chiral for (+)-neomenthyl complexes and (*R*)-planar chiral for (–)-menthyl and (–)-phenylmenthyl. Thus, marked distortions of both the $CH(TMS)_2$ group and the ancillary ligation are seen in the structure of (+)-neomenthyl (*R*)-**6d**, which has a *syn* orientation, versus (+)-neomenthyl (*S*)-**6d**, which has an *anti* orientation (Figure 12). Apparent destabilization of (*R*)-**6d** with respect to (*S*)-**6d** may account for the significant epimerization of (*R*)-**4d** observed on alkylation. Similar distortions of the ancillary ligation are not observed in the molecular structure of (*R*)-**4e** (Figure 2), despite the smaller ionic radius of Lu (0.977 Å)[44] versus Y (1.019 Å),[44] suggesting lesser steric requirements for $Ln(\mu\text{-}Cl)_2Li(S)_2$ versus $CH(TMS)_2$ ligation.

The above observations are also in accord with the result that (+)-neomenthyl chloro complex (*S*)-**4c** selectively yields (*S*)-**6c** or (*S*)-**7b** upon reaction with *1 equiv* of $LiCH(SiMe_3)_2$ or $MN(SiMe_3)_2$ (M = Na, K), respectively. In contrast, the (*R*)-epimers of the (+)-neomenthyl amides can only be prepared stereoselectively by addition of either *1 or 2 equiv* of $MN(SiMe_3)_2$ (M = Na, K) to DME adduct (*R*)-**5** or (*R*)-**4** respectively, which circumvents the epimerization process. Evidently, the *i*-Pr *anti* orientation is strongly preferred in the presence of sterically-demanding σ-ligands such as $CH(TMS)_2$ and $N(TMS)_2$. Thus, preparation of chiral hydrocarbyl and amide complexes with a *syn* orientation of the chiral auxiliary is possible only from the corresponding *syn* chloro complexes when competing epimerization has been completely suppressed.

The actual mechanism for epimerization of the present complexes has not been unambiguously defined. Epimerization must involve permutation of the planar chirality element[55] and thus would require dissociation of the chiral Cp group, rotation about the Si–C(Cp ring) bond, and recoordination to the opposite Cp diastereoface. An intermolecular process involving two organolanthanide molecules seems improbable in view of the observed first-order kinetics for (*S*)-**4i**. A simple mechanism is given in Scheme 2. The participation of a donor molecule, which is equivalent to the solvent for epimerization of **4** in THF or ether, is invoked because in more strongly coordinating THF, the equilibrium is more rapidly established than in more weakly donating diethyl ether. The proposed intermediate (not detected)

(54) (a) Oppolzer, W. *Angew. Chem., Int. Ed. Engl.* **1984**, *23*, 876–889. (b) Oppolzer, W.; Kurth, M.; Reichlin, D.; Moffatt, F. *Tetrahedron Lett.* **1981**, *22*, 2545–2548. (c) Whitesell, J. K.; Bhattacharya, A.; Aguilar, D. A.; Henke, K. *J. Chem. Soc., Chem. Commun.* **1982**, 989–990.

(55) Mislow, K.; Siegel, J. *J. Am. Chem. Soc.* **1984**, *106*, 3319–3328.

is structurally similar to well-known $CpLnX_2 \cdot 3S$ complexes.[56] Reactive nucleophilic reagents such as $LiN(TMS)_2$ and $LiCH(TMS)_2$ can also effect epimerization of **4** at rates much faster than the simple solvent-induced epimerization rates and which appear to be commensurate with the substitution rates. Once formed, the hydrocarbyl and amido complexes are configurationally stable in hydrocarbon solvents (>48 h at 60 °C in benzene).

Epimerization depends additionally on the counterion. In the proposed mechanism, the chiral Cp anion dissociates as an ion pair/complex with Li^+. Formation of this species would provide a low barrier to the proposed intermediate, and, thus, to epimerization. The effective substitution of K^+ or Na^+ for Li^+ by reaction of **4** with 2 equiv of $KCH(SiMe_3)_2$ or $MN(SiMe_3)_2$ ($M^+ = Na^+, K^+$) inhibits epimerization, affording the hydrocarbyl derivatives **6** with net retention of configuration and amide derivatives **7** with complete retention of configuration. Substitution of K^+ or Na^+ for Li^+ should raise the barrier for dissociation since the CpR* group must bear more negative charge due to decreased covalent interaction with the cation. In addition, epimerization of chloro complexes **4** is inhibited in THF by addition of exogenous Li^+ binders such as TMEDA or 12-crown-4. The strongly coordinated Li^+ would not effectively stabilize the dissociation of the cyclopentadienyl anion, due to a lessened Li–Cp interaction—a situation similar to that of the K^+ or Na^+ above. Ion-pair redistribution reactions have been reported for other organolanthanide complexes. Redistribution between $Cp'_2La(OAr)$ and $(Li(OAr)\cdot THF)_2$ (Ar = 2,6-dimethylphenyl) (eq 16) is facile in benzene at 80 °C.[57] Furthermore, conproportionation reactions among cyclopentadienyl Ln species (eq 17) is a common synthetic procedure.[58]

$$Cp'_2La(OAr) + LiOAr \rightleftharpoons Cp'La(OAr)_2 + LiCp' \qquad (16)$$

$$2Cp_3Ln + LnCl_3 \rightleftharpoons 3Cp_2LnCl \qquad (17)$$

Epimerizations of metal atom central chirality have been reported for a number of 18-electron organometallics.[59] These proceed through a dissociative mechanism in which a ligand such as a phosphine is initially lost, resulting in a stereochemically nonrigid, unsaturated intermediate (e.g., eq 18). Recapture of the donor ligand may occur to yield either the (*R*)- or the (*S*)-isomer of the initial complex. In contrast, epimerization of **4** probably occurs via an associative mechanism (Scheme 2), which is in accord with the coordinative unsaturation and kinetic lability of the Ln^{3+} ions.

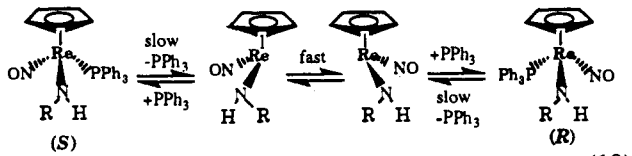

(18)

Scheme 2. Proposed Mechanism for the Epimerization of $Me_2SiCp''[R^*Cp]Ln(\mu\text{-}Cl)_2Li(ether)_2$ Complexes in Donor Solvents

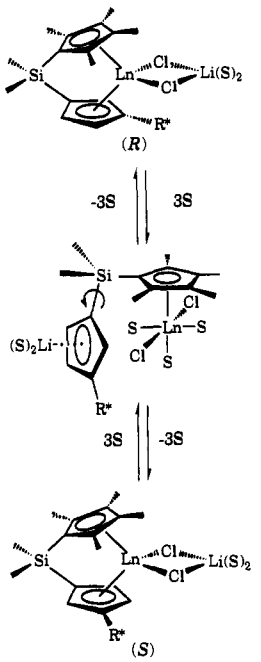

It was also found in this study that both the diastereomerically pure and epimer mixtures of **6** and **7** undergo epimerization in the presence of excess alkyl amine. When homochiral (*S*)-**6c**, (*R*)-**6c**, and (*R*)-**7** are treated with *n*-propylamine at 25 °C, rapid protonolytic cleavage of the $E(TMS)_2$ group occurs, with initial retention of configuration.[60] However, a new set of NMR resonances rapidly evolves which corresponds to one set of resonances observed on the initial addition of *n*-propylamine to the corresponding hydrocarbyl (*R*,*S*)-epimer mixture. Significantly, the corresponding (*R*,*S*)-**6c–e** epimer mixtures also undergo epimerization under these conditions, with a strong preference for a single epimer, (*R*), at equilibrium. The equilibrium epimer populations are independent of the precursor optical purity. Similar epimerization is observed for the (–)-phenylmenthyl complex **7h** under conditions identical to those for the (+)-neomenthyl complexes, except that the opposite (*S*)-epimer of the amine–amido adduct is preferred at equilibrium. The epimerization mechanism for the putative amine–amido adducts is probably similar to Scheme 2 (Scheme 3). However, dissociation of a transiently protonated cyclopentadiene intermediate likely occurs in the former instead of ion-pair dissociation. The epimerization of the amine–amido adducts is facile under these conditions, and the epimerization rate qualitatively depends on the Ln^{3+} ionic radius ($k_{Sm} > k_{Lu}$). The kinetics for **7h** epimerization obey a rate law which is first-order in lanthanide, implying unimolecular organolanthanide participation, and are similar to the aforementioned epimerization kinetics for (*S*)-**4i** in diethyl ether. The rate constant for the (*R*) → (*S*) conversion of **7h** ($k = 5.74(3) \times 10^{-4}$ s^{-1}) is greater than that for the epimerization of (*S*)-**4i** ($k = 1.62(2) \times 10^{-6}$ s^{-1}). These results suggest more facile epimerization under the former conditions, either because of the greater reactivity of *n*-propylamine compared to diethyl ether/THF or because protonolysis of a Ln^{3+} cyclopentadienide is more facile than ion-pair dissociation. The similarity of the equilibrium epimer ratios for the amine–amido complexes under the aforementioned conditions and for **4** and **5**

(56) (a) Hazin, P.; Huffman, J. C.; Bruno, J. W. *Organometallics* **1987**, *6*, 23–27. (b) Day, C. S.; Day, V. W.; Ernst, R. D.; Vollmer, S. H. *Organometallics* **1982**, *1*, 998–1003.

(57) (a) Heeres, H. J.; Teuben, J. H. *Recl. Trav. Chim. Pays-Bas* **1990**, *109*, 226–229. (b) Heeres, H. J.; Meetsma, A.; Teuben, J. H. *Organometallics* **1989**, *8*, 2637–2646. (c) Heeres, H. J.; Meetsma, A.; Teuben, J. H. *J. Chem. Soc., Chem. Commun.* **1988**, 962–963.

(58) (a) Maginn, R. E.; Manastyrskyj, S.; Dubeck, M. *J. Am. Chem. Soc.* **1963**, *85*, 672–676. (b) Manastyrskyj, S.; Maginn, R. E.; Dubeck, M. *Inorg. Chem.* **1963**, *2*, 904–905.

(59) (a) Dewey, M. A.; Gladysz, J. A. *Organometallics* **1990**, *9*, 1351–1353. (b) Martin, G. C.; Boncella, J. M. *Organometallics* **1989**, *8*, 2968–2970. (c) Brunner, H.; Fisch, K.; Jones, P. G.; Salbeck, J. *Angew. Chem., Int. Ed. Engl.* **1989**, *28*, 1521–1523. (d) Brunner, H.; Steger, W. *J. Organomet. Chem.* **1976**, *120*, 239–256. (e) Brunner, H.; Aclasis, J. *J. Organomet. Chem.* **1976**, *104*, 347–362. (f) Brunner, H.; Langer, M. *J. Organomet. Chem.* **1975**, *87*, 223–240. (g) Brunner, H.; Schindler, H.-D. *Z. Naturforsch.* **1971**, *26B*, 1220–1225. (h) Brunner, H.; Aclasis, J.; Langer, M.; Steger, W. *Angew. Chem., Int. Ed. Engl.* **1974**, *13*, 810–811.

(60) Protonolysis reactions of centrally chiral titanocene complexes with hydrogen chloride proceed with retention of the titanium configuration, while nucleophilic substitution occurs with racemization: (a) Leblanc, J. C.; Moise, C.; Tirouflet, J. *J. Organomet. Chem.* **1978**, *148*, 171–178. (b) Leblanc, J. C.; Moise, C.; Tirouflet, J. *Nouv. J. Chim.* **1977**, *1*, 211–215. (c) Moise, C.; Leblanc, J. C.; Tirouflet, J. *J. Am. Chem. Soc.* **1975**, *97*, 6272–6274.

Scheme 3. Proposed Mechanism for the Epimerization of $Me_2SiCp''[R^*Cp]Ln(NHR)(NH_2R)$ Complexes in the Presence of Excess Amine, H_2NR

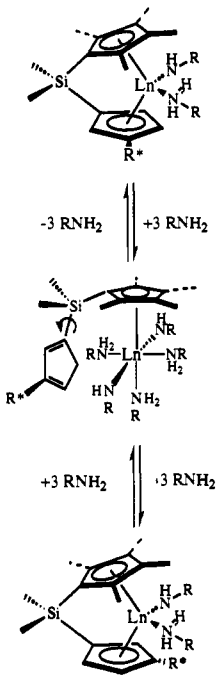

in THF, i.e., the strong preference for the (*R*)-configuration for R* = (+)-neomenthyl and the (*S*)-configuration for R* = (–)-menthyl, implies a similar mode of stereocontrol. This situation presumably also obtains for the amine–amido complexes of other relatively unhindered, linear amines, although the actual microscopic criterion for stereoselection has not been completely elucidated.

Circular Dichroism Spectroscopy and Organolanthanide Configuration. Chiroptical properties of organometallic complexes have been employed to assign relative configurations at the metal center among stereoelectronically similar complexes, and, when used in conjunction with crystal structure determinations, for designation of absolute configuration.[61] For most optically active organometallic complexes, the metal chromophore primarily determines the CD, with the chirality of the ligands usually making a minor contribution. Consequently, the optical rotations of metalloepimers generally have opposite signs. Without exception, the planar chiral configurations of isoleptic homochiral organolanthanide complexes **4**–**9** correlate with the signs of the Cotton effects in the CD. The absolute configurations of chloro complexes **4** and **5**, which serve as precursors for hydrocarbyl and amide derivatives **6** and **7**, respectively, have been established via diffraction and CD spectral correlations. In general, the CD spectra exhibit a higher energy feature in the 260–290 nm range which correlates well with the absolute configuration of the planar chirality element. A negative Cotton effect here indicates (*R*)-configuration, e.g., in **4d** and **4g**, and a positive Cotton effect (*S*)-configuration, as in **4i**. The sign of this feature for **4i** reverses slowly with time, suggesting epimerization at Ln to the (*R*)-configuration (the curve morphology remains essentially invariant). CD spectroscopy is thus a valuable tool not only for the elucidation of organolanthanide configuration but also for studying dynamic processes involving stereochemical changes in the Ln coordination environment.

For homochiral complexes **6** and **7**, CD spectroscopic features are nearly superimposable within a series of isoleptic complexes. However, even (*R*,*S*)-epimer mixtures, e.g., (*R*,*S*)-**6d** and (*R*,*S*)-**7c**, display weak CD features since these complexes, although of opposite configuration, are diastereomers, and hence the CD of the two epimers should not completely cancel. The relationship between the configurations of the (+)-neomenthyl, (–)-menthyl, and (–)-phenylmenthyl complexes, although somewhat complicated by epimerization processes, may be straightforwardly deduced by comparison of CD spectra. Opposite Cotton effects are observed for opposite planar chiral configurations,[61,63] i.e., epimers of the organolanthanide complexes. The observed stereochemistry of these complexes and consequently the molecular chiroptical properties derive from the selective binding of a single Cp diastereoface. For the chiral organolanthanide complexes, the preferential binding of a single Cp diastereoface, i.e., a single planar chiral configuration, corresponds to a single conformation of the chelating asymmetric ancillary ligand due to its rigid, conformationally-restricted chelating arrangement. The selective coordination of the *re*-face of the chiral Cp affords exclusively the (*R*)-epimer of **4**, while selective coordination of the *si*-face yields the (*S*)-epimer. Moreover, the chirality of the R* group ensures that these two configurations are stereochemically distinct and energetically inequivalent; therefore, preferential formation of a single epimer is feasible. Direct correspondence of the structural features of **4** and **5**, and, by analogy, **6** and **7**, to the solution chiroptical properties allows a reasonable prediction of the configuration of novel complexes from the CD spectra.

Conclusions

Chiral organolanthanide complexes of the novel, chelating, asymmetric ancillary ligand $Me_2SiCp''(R^*Cp)^{2-}$ have been synthesized which preferentially adopt a single planar chiral configuration of the asymmetric metal–ligand template. The chloro complexes $Me_2SiCp''(R^*Cp)Ln(\mu\text{-}Cl)_2Li(OEt_2)_2$ can be isolated diastereomerically pure, although epimerization occurs in donor solvents. The slight free energy differences between the two epimers, coupled with the kinetic lability of the Ln^{3+} ion ligation, permits controlled epimerization of the planar chiral configuration. The optical purity and preferred configuration of the derived hydrocarbyl and amide complexes $Me_2SiCp''(R^*Cp)LnE(SiMe_3)_2$ (E = CH or N) depends on the configuration of the chloro precursors, particularly with respect to steric interactions between the R* and the incoming nucleophile during substitution. The present work represents the first study of the synthetic, spectroscopic, and structural properties of chiral organolanthanides. It provides insights into the dynamic processes and configurational stability of these complexes and provides a basis for the rational modification of future metallocene arrays. It also lays the groundwork necessary to understand the catalytic chemistry.[20]

Acknowledgment. We are grateful to for support of this research under NSF GRant CHE9104112. V.P.C. and L.B. thank NSF and Rhône-Poulenc for predoctoral fellowships, respectively. We thank Prof. Paul Loach for access to his CD spectrometer.

Supplementary Material Available: Details of X-ray experimental procedures; tables of positional and anisotropic thermal parameters and full tables of bond distances and angles for (*R*)-**4e**, (*R*,*S*)-**6c**, (*R*,*S*)-**6d**, (*R*)-**6f**, (*R*)-**6g**, (*S*)-**7b**, (*S*)-**7e**, and (*R*)-**7f** (110 pages); tables of observed and calculated structure factors from the final cycle of least-squares refinement (193 pages). This material is contained in many libraries on microfiche, immediately follows this article in the microfilm version of the journal, and can be ordered from the ACS; see any current masthead page for ordering information.

(61) Faller, J. W.; Shvo, Y.; Chao, K.; Murray, H. H. *J. Organomet. Chem.* **1982**, *226*, 251–275.

(62) (a) Falk, H.; Schlögl, K. *Monatsch. Chem.* **1965**, *96*, 1065–1080. (b) Falk, H.; Schlögel, K. *Monatsch. Chem.* **1965**, *96*, 1081–1093.

(63) Cesarotti, E.; Kagan, H. B.; Goddard, R.; Krüger, C. *J. Organomet. Chem.* **1978**, *162*, 297–309.